INFORMATION TO USERS

This manuscript has been reproduced from the microfilm master. UMI films the text directly from the original or copy submitted. Thus, some thesis and dissertation copies are in typewriter face, while others may be from any type of computer printer.

The quality of this reproduction is dependent upon the quality of the copy submitted. Broken or indistinct print, colored or poor quality illustrations and photographs, print bleedthrough, substandard margins, and improper alignment can adversely affect reproduction.

In the unlikely event that the author did not send UMI a complete manuscript and there are missing pages, these will be noted. Also, if unauthorized copyright material had to be removed, a note will indicate the deletion.

Oversize materials (e.g., maps, drawings, charts) are reproduced by sectioning the original, beginning at the upper left-hand corner and continuing from left to right in equal sections with small overlaps.

Photographs included in the original manuscript have been reproduced xerographically in this copy. Higher quality 6" x 9" black and white photographic prints are available for any photographs or illustrations appearing in this copy for an additional charge. Contact UMI directly to order.

UMI®

MODULATION OF L-TYPE Ca^{2+} CURRENT BY FREE INTRACELLULAR Mg^{2+} IN GUINEA PIG VENTRICULAR MYOCYTES

by

Chicuong La

Submitted in partial fulfillment of the requirements
for the degree of Doctor of Philosophy

at

Dalhousie University
Halifax, Nova Scotia, Canada
2001

Canada

DALHOUSIE UNIVERSITY

FACULTY OF GRADUATE STUDIES

The undersigned hereby certify that they have read and recommend to the Faculty of Graduate Studies for acceptance a thesis entitled "Modulation of L-Type Ca^{2+} Current by Free Intracellular Mg^{2+} in Guinea Pig Ventricular Myocytes" by Chicuong La in partial fulfillment of the requirements for the degree of Doctor of Philosophy.

Dated: _____ July 27, 2001 _____

External Examiner:

Research Supervisor:

Examining Committee:

ii
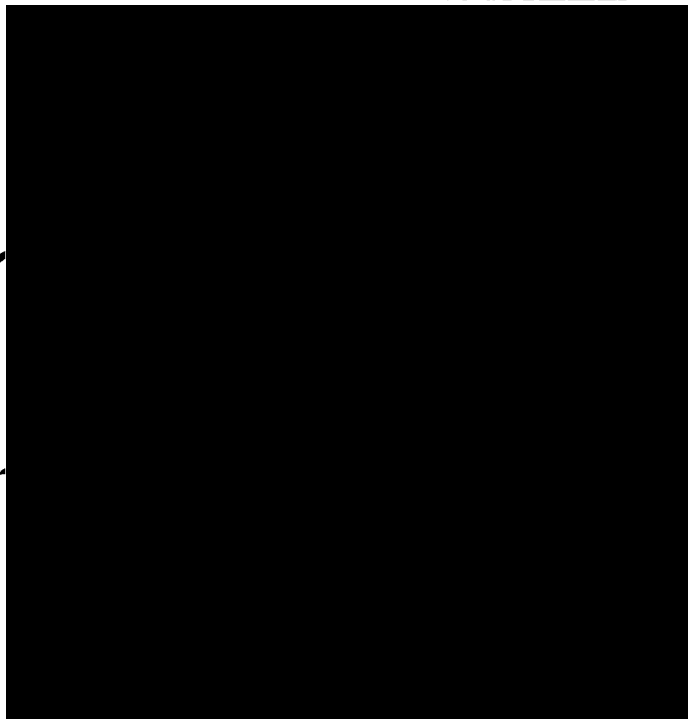
COPYRIGHT AGREEMENT FORM

DALHOUSIE UNIVERSITY

DATE: <u>August 17, 2001</u>

AUTHOR: <u>Chicuong La</u>

TITLE: <u>"Modulation of L-type Ca^{2+} Current by Free Intracellular Mg^{2+} in Guinea Pig Ventricular Myocytes"</u>
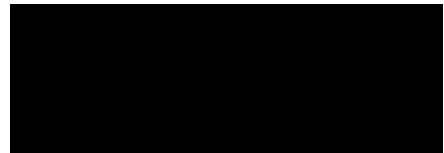
DEPARTMENT: <u>Physiology and Biophysics</u>

DEGREE: <u>Ph.D.</u>　　　CONVOCATION: <u>Fall</u>　　　YEAR: <u>2001</u>

DEDICATION

To my loving wife

and to my family who I have missed dearly during my studies at Dalhousie University.

TABLE OF CONTENTS

ix

LIST OF ILLUSTRATIONS

LIST OF TABLES

ABSTRACT

The effects of cytosolic free magnesium (Mg^{2+}_i) on L-type Ca^{2+} current ($I_{Ca,L}$) were studied in guinea pig ventricular cardiomyocytes. Under basal conditions, the influence of Mg^{2+}_i on $I_{Ca,L}$ was bimodal. Basal $I_{Ca,L}$ density rose with increasing Mg^{2+}_i from 1 μM to 17 μM, while higher Mg^{2+}_i concentrations led to an inhibition of the $I_{Ca,L}$. The stimulation appeared to be caused by an elevated cAMP level, resulting in cAMP dependent protein kinase (PKA) mediated phosphorylation, whereas inhibition appeared to be caused by a reduction in the level of channel phosphorylation. However, this bimodal effect was eliminated, and the current greatly reduced when phosphorylation was suppressed with K252a. On the other hand, preincubation with forskolin (FSK) and 3-isobutyl-1-methylxanthine (IBMX) produced a large stimulation of the $I_{Ca,L}$ and prevented inhibitory effects of the ion at Mg^{2+}_i levels less than 1 mM. In consideration of the results, I postulate that Mg^{2+}_i controls the balance of cAMP dependent phosphorylation of the L-type Ca^{2+} channel. There are four possible sites that Mg^{2+}_i can influence the net production of cAMP: at the receptor, at the G-protein, at the adenylyl cyclase and at the phosphodiesterase. The results from the second set of experiments indicate that Mg^{2+}_i stimulates the activity of all four sites. However, the apparent affinity seems to be higher at the sites that augment the production of cAMP than the sites responsible for its hydrolysis. In addition to Mg^{2+}_i's effect on channel phosphorylation and current amplitude, it has a major influence with $I_{Ca,L}$ inactivation. The results lead me to hypothesize that Mg^{2+}_i inhibits inactivation by competing with Ca^{2+} at the Ca^{2+}-binding sites that are required for Ca^{2+} dependent inactivation.

LIST OF ABBREVIATIONS AND SYMBOLS

A	ampere
ATP	adenosine triphosphate
Ca^{2+}	calcium
Ca^{2+}-Cam	calcium calmodulin complex
cam	calmodulin
cAMP	cyclic adenosine monophosphate
cGMP	cyclic guanosine monophosphate
C_m	cell capacitance
DMSO	dimethyl sulfoxide
DNA	deoxyribose nucleic acid
EC_{50}	concentration of an agonist that produces 50% of the maximal activation
EGTA	ethylene glycol-bis (β-aminoethyl ether)-N,N,N',N'-tetraacetic acid
F	farad
g	gram
G_s	stimulatory G-protein
GTP	guanosine triphosphate
HEPES	N-2-hydroxyethylpiperazine-N'-2-ethanesulfonic acid
Hz	hertz
I	whole-cell current
$I_{Ba,L}$	barium-carried current through L-type Ca^{2+}-channel

IBMX	3-isobutyl-1-methylxanthine
$I_{Ca,L}$	L-type Ca^{2+} current
i.d.	inner diameter
K_m	Michaelis constant
M	moles per liter
m	milli
me^{2+}	divalent metal ion
ms	milli second
mRNA	messenger ribose nucleic acid
n	number of experiments
o.d.	outer diameter
pH	negative logarithm of the hydrogen ion concentration
PKA	cAMP dependent protein kinase
PKI	cAMP dedendent protein kinase inhibitor
p	probability (significance level in a statistical test)
P_f	fraction of available channel
P_o	open state probability
PS	physiological salt solution
R_A	access resistance
RNA	ribose nucleic acid
R_s	series resistance

SEM	standard error of the mean
V	volt
V_{max}	maximum rate of reaction
Vol	cell volume in μm^3
Ω	ohm
τ	time constant
τ_f	fast time component of current inactivation
τ_s	slow time component of current inactivation
μ	micro
~	approximately
<	less than
>	greater than
$\leq$	less than or equal to
$\geq$	greater than or equal to

ACKNOWLEDGEMENTS

I would like to extend my deepest thanks and appreciation to my supervisor Dr. Dieter Pelzer for his guidance, support and friendship throughout the course of my study.

Appreciation is extended to the members of my supervisory committee (Drs. Gregory Ferrier, Roger Croll, Hermann Wolf, and William Moger) and my examining committee (Drs. Peter Backx, Gregory Ferrier, Paul Linsdell, Nik Morgunov, and Douglas Rasmusson) for their time and guidance.

Thanks also go to Dr. Siegried Pelzer for her advice during my studies, Mr. Brian Hoyt for his computer expertise and Mr. Mark Richard for technical support.

I am especially indebted to my friends Dr. You for teaching me the art of patch clamping, and Big D for his most excellent assistance.

Finally I would like to thank my good friends Stephen, Tom, Sergey, Pavel, Gina, and Eddy for enriching my life.

I.   INTRODUCTION

With the advent of the patch clamp method our understanding of cardiac physiology has grown dramatically in the last two decades. This new technique has opened the gateway to the study of transmembrane ion transport and its corresponding pathways. The focus of many of these studies however was on Ca^{2+}, K^+, Na^+ and Cl^- but not Mg^{2+}. Even though Mg^{2+} is the most abundant divalent cation in the cytoplasm, it did not receive the same degree of attention as other ions largely because it lacked any significant transmembrane permeability. Thus, for many years Mg^{2+} was relegated solely as a metabolic co-factor, particularly in reactions involving the transfer of phosphate groups. Although by no means a minor role, other regulatory roles for free internal Mg^{2+} (Mg^{2+}_i) were not considered, mainly because the cytoplasmic concentration was considered too high (3-6 mM) which would be saturating levels for most cellular functions (Flatman, 1984 review). However, by the early 1980's the measurements of internal Mg^{2+} became more accurate and revealed much lower levels of Mg^{2+}_i than previously thought, spawning the idea of Mg^{2+} as a cellular regulator. Since then Mg^{2+}_i has been assigned key roles in the regulation of many 2nd messenger systems (from the receptor level down to the level of the effector), and is implicated in the regulation of both K^+ and Ca^{2+}-channels.

The focus of this present study is on the regulatory roles of Mg^{2+}_i on the L-type Ca^{2+}-channel current ($I_{Ca,L}$) in the guinea pig ventricular myocyte. To establish a foundation for the main thesis, the remainder of this introduction will: (A) review the

1

involvement of $I_{Ca,L}$ and Mg^{2+}_i in excitation contraction coupling (EC-coupling); (B) compare the characteristics of the T-type and L-type cardiac Ca^{2+}-channels; (C) review the structure and function of the cardiac $I_{Ca,L}$; (D) review the regulation of $I_{Ca,L}$; (E) review Mg^{2+}_i homeostasis; (F) review the influence of Mg^{2+}_i on 2nd messenger systems; and (G) review the previous studies involving the effects of Mg^{2+}_i on $I_{Ca,L}$.

SECTION A. ROLE OF $I_{Ca,L}$ AND Mg^{2+}_i IN EC-COUPLING:

Contraction of the heart begins with the depolarization of the cell membrane caused by Na^+ entering the cell through Na^+-channels. Positive membrane potentials promote the opening of Ca^{2+}-channels, resulting in Ca^{2+} entering the cell and down the steep concentration gradient for Ca^{2+}. Ca^{2+}, through L-type Ca^{2+}-channels, contributes to the plateau phase of the ventricular action potential and plays an essential role in coupling cardiac excitability to contraction (New and Trautwein, 1972; Ochi and Trautwein, 1971). The force and speed of contraction are determined by the amplitude and speed of the Ca^{2+} transient. Although Ca^{2+} entering the cell through the $I_{Ca,L}$ directly leads to a transient elevation of the cytoplasmic level of free Ca^{2+}, its predominant role is to trigger the release of Ca^{2+} from the sarcoplasmic reticulum (SR) by binding onto ryanodine sensitive receptor type 2 (RyR2) (Fabiato and Fabiato, 1977; Fabiato, 1985; 1989) (see Figure 1), which is found in the cardiac myocytes (Coronado et al., 1994). In addition, Ca^{2+}-induced Ca^{2+} release (CICR) mechanism, RyR2 has also been suggested to be sensitive to voltage activation in the absence of Ca^{2+} entry from

the extracellular environment (Ferrier and Howlett, 1995; Howlett et al., 1998; Mackiewicz et al., 1999; Ferrier and Howlett, 2001 review).

Mg^{2+} also plays an important role in the excitation-contraction (E-C) coupling of both skeletal and cardiac muscles. When the cells are at rest, physiological Mg^{2+}_i levels exert a powerful inhibitory action on the RyR2 channel. The inhibitory action occurs by the binding of Mg^{2+} to two different modulation sites on the RyR2 channel. At the first site, Ca^{2+} is the agonist whereas Mg^{2+} is the antagonist. The second regulatory site is inhibitory, and both divalent cations Mg^{2+} and Ca^{2+} can bind onto and inhibit the channel (Laver et al., 1997). In the cardiac muscle, the affinity of the Ca^{2+}/Mg^{2+} inhibitory site for divalent cations is very low, (~ 1 mM for both Mg^{2+} and Ca^{2+}), thus it is speculated that in the cardiac muscle, this site plays only a minor inhibitory role during normal cell physiology. In contrast, the binding affinity at the Ca^{2+} dependent activation site is 40-1000-fold stronger for Ca^{2+} than Mg^{2+} (Xu et al., 1996; Laver et al., 1997). Under physiological conditions, most of the channels are inhibited by Mg^{2+} at rest because the Mg^{2+}_i level is ~ 10000-fold higher than the Ca^{2+}_i level (Lui et al., 1998). In order to facilitate Ca^{2+} release from the sarcoplasmic reticulum, the inhibition by Mg^{2+} must be removed. In cardiac cells, Ca^{2+} influx from the outside causes a local rise in the Ca^{2+} level at the sarcoplasmic reticulum; this increase in Ca^{2+} out-competes and displaces Mg^{2+} from the Ca^{2+} dependent activation site and effectively removes the Mg^{2+} inhibition. The activation of the RyR2 channel releases Ca^{2+} into the cytoplasm and reinforces the initial effect of Ca^{2+} from the outside by stimulating nearby channels leading to an amplification of the intracellular calcium level. The rise in internal free

Ca^{2+} activates the contractile filaments leading to the generation of force; Ca^{2+} is subsequently pumped back into the SR by a Ca^{2+}-ATPase pump and extruded from the cell by Na^{+}/Ca^{2+} -exchangers and Ca^{2+}-ATPase pumps (Negretti et al., 1993). For a more complete discussion of E-C coupling see Hobai and Levi (1999), Weir and Balke (1999), and Ferrier and Howlett (2001).
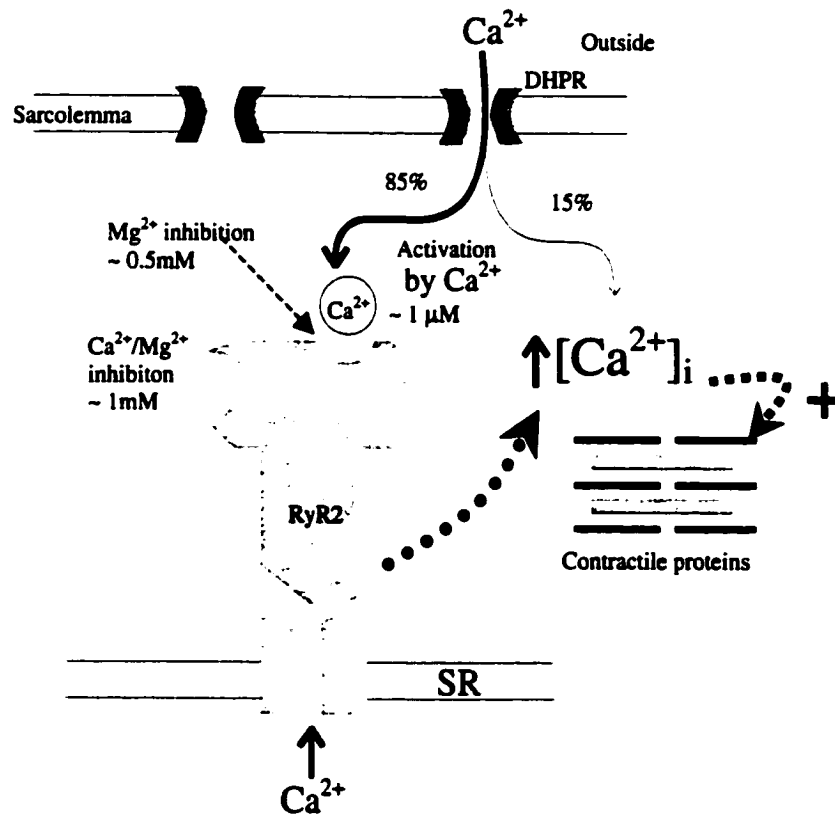
Figure 1: Schematic diagram illustrating CICR in cardiac myocytes. The extracellular Ca^{2+} flowing into the cell binds to and activates the ryanodine receptor type 2 (RyR2) channel in the sarcoplasmic reticulum (SR). The activation of the RyR2 channel amplifies Ca^{2+} influx from the outside through L-type Ca^{2+}-channels by releasing Ca^{2+} from the SR into the cytoplasm. This transient increase in cytoplasmic Ca^{2+} activates the contractile proteins, producing force. The RyR2 channel is inhibited by Mg^{2+} at two different sites: one is at the Ca^{2+} activation site in which Mg^{2+} is a competitive inhibitor, and the other is a non-specific divalent cation Ca^{2+}/Mg^{2+}-binding site, which has a half maximal inhibition constant of ~1mM for both Ca^{2+} and Mg^{2+}.

SECTION B. TYPES OF Ca^{2+}-CHANNELS:

There are essentially five different groups of voltage dependent Ca^{2+}-channels classified according to their electrophysiological and pharmacological properties. They are termed: N, P/Q, R, T, and L. The N, P/Q, and R channels are most prominent in neurons and are involved in the process of vesicle exocytosis; although a complete discussion of their properties is not within the scope of this study, these references offer a background for further review: Vajna et al. 2001; Albillos et al. 2000; Catterall 2000. The dominant form of Ca^{2+}-channels found in cardiac ventricular myocytes are T-type and L-type channels. Clear identification of the two types of channels was first obtained by Nilius and colleagues (1985) on guinea pig ventricular myocytes and by Bean (1985) on canine atrial cells. In guinea pig ventricular myocytes it is estimated that the T-type current amplitude at the voltage eliciting the largest current (V_{peak}) is generally less than 10% of L-type current at V_{peak} (Nilius et al., 1986; Zygmunt and Maylie 1990). Correspondingly channel density for T-type is approximately 0.1 to 0.3 per μm^2 or 1 for every 3 to 10 μm^2 (Droogmans and Nilius 1989), whereas the density for L-type channels is 10 to 20 times higher for guinea pig ventricular myocytes (McDonald et al., 1986; Pelzer et al., 1986; Rose et al., 1992) and other ventricular myocytes such as canine (Bean 1985; Hirano et al, 1989), frog (Bean, 1984), and rabbit (Lew et al., 1991). Table 1 shows a comparison of functional properties and regulation between the T-type and L-type Ca^{2+}-channel. Since the L-type Ca^{2+}-channel has the dominant role in delivering Ca^{2+} for myocyte contraction, it is the focus of my study.

6

Table 1: Physiological Properties of T-type and L-type channels in guinea pig cardiomyocytes. WC = whole cell, SC = single channel, V of I_{max} = potential which elicits the maximum current. (table modified from Pelzer et al., 1989 in Isolated adult cardiomyocytes vol II).

Parameter	charge carrier (mM)	Voltage clamp	T-type channel current	L-type channel current	Reference:
Activation range	10 mM Ca	WC	positive to -50 mV	positive to -40 mV	Mitra and Morad 1986
	110 mM Ba	SC	positive to -50 mV	positive to -20 mV	Nilius et al., 1986
$V_{1/2}$ activation	110 mM Ba	SC	-11 mM	+25 mV	Nilius et al., 1986
Inactivation range	110 mM Ba	SC	-70 to -40 mV	-50 to -10 mV	Nilius et al., 1986
$V_{1/2}$ inactivation	110 mM Ba	SC	-54 mV	-25 mV	Nilius et al., 1986
Inactivation rate	50 mM Ba	SC	t ~ 38.5 msec at -30 mV	---	Nilius et al., 1986
	90 mM Ba	SC	---	t ~ 85 to 1400 msec at +25mV (mean 293 msec)	Cavalie et al., 1986
V of I_{max}	10 Ca	WC	-10 mV	+20 mV	Mitra and Morad 1986
Single channel conductance	110 Ba	SC	~ 8 pS	18-25 pS	Nilius et al., 1985; 1986
relative conductance	110 Ca 110 Ba	SC	Ba = Ca	Ba > Ca	Nilius et al., 1985; 1986
Single channel kinetics	50 Ca/110Ba	SC	Brief clusters of bursts	long clusters of bursts	Nilius et al., 1985; 1986, Cavalie et al., 1986
Isoproterenol	15 Ca	WC	No effect (10 nM) 25-100% increase (1 □M)	large increase (10 nM) large increase (1 □M)	Mitra and Morad 1986
Dihydropyridine blockers	Ca or Ba	WC	0 to slight effect	40% to 80% block	Nilius et al., 1985; Mitra and Morad 1986
Dihydropyridine openers	Ca or Ba	WC	0 to slight effect	large, up to fivefold increase	Nilius et al., 1985;

SECTION C. CARDIAC L-TYPE Ca^{2+}-CHANNEL STRUCTURE AND FUNCTION:

Molecular biology has greatly advanced our understanding of the structure and function of the L-type Ca^{2+}-channel. As shown on Figure 2, the cardiac L-type channel is an oligomeric protein with at least 4 different subunits: α_{1c}, β_2, α_2, δ, and possibly a fifth γ. The main unit, the α_{1c} is approximately 2000 amino acids in size and serves as both the channel pore and voltage sensor. The α_{1c}, which is structurally similar to the voltage dependent Na^+-channel α subunit (Kayano et al., 1988), is comprised of four domains called repeats that are internally homologous to each other and to voltage dependent K^+-channels (Baumann et at., 1987; 1988, Catterall 1993). Each repeat has six transmembrane α helices (S1-S6) and a pore loop (Tanabe et al., 1987). The voltage sensor located in the fourth transmembrane segment (S4) contains a series of residues in which every third one is positively charged. This region is thought to move outward with membrane depolarization, although it is unclear how this leads to channel opening (Catterall, 1988). The S3 region is highly conserved and may play a role in charge-charge interaction with the S4 region. The pore of the channel appears to be formed by the pore loop between the S5 and S6 region. The S1 and S2 segments are poorly conserved, and are believed to interface the lipid of the sarcolemma (Walker and De Waard 1998 review). The carboxyl tail of the α_{1c} contains a sequence that is homologous to the Ca^{2+}-binding EF-hand motif, and this region is postulated to be involved in Ca^{2+} dependent inactivation (de Leon et al., 1995). The cytoplasmic loop

between domains I and II forms the α_1-interaction domain (AID), this region interacts directly with the β-subunit to modify channel inactivation (Castellano et al., 1993; Singer et al., 1991). Although still unconfirmed in cardiac L-type Ca^{2+}-channels, the cytoplasmic loop between domains II and III is important for excitation coupling in skeletal muscle, especially as a direct link for voltage transfer to the ryanodine receptor (Tanabe et al., 1990a; 1990b).

The δ subunit is a proteolytic fragment encoded by the α_2 gene (De Jongh et al., 1990; Jay et al., 1991), and possesses a single hydrophobic segment anchored to the membrane. Meanwhile the α_2 subunit is located on the extracellular surface of the membrane, and is tethered to the δ subunit via a disulfide bond (Gurnett et al., 1996). Coexpression of α_{1c} together with $\alpha_2\delta$ shows a 2-fold increase in the expression of dihydropyridine binding sites, and an upregulation of both gating and ionic currents (Wei et al., 1995; Singer et al., 1991; and Bangalore et al., 1996). These studies suggest the $\alpha_2\delta$ subunit plays an important role in the formation of a functional channel at the membrane surface.

The expression of the γ gene seems to be restricted to skeletal muscle (Jay et al., 1990). However, its co-expression with α_{1c} subunit revealed some minor changes to dihydropyridine binding and channel inactivation (Singer et al., 1991).

The β_2 isoform is the predominant form of the β subunit express in the heart (Hullin et al., 1992). The β_2 subunit located on the cytoplasmic side of the membrane plays several roles. Studies have shown it can directly alter the biophysical properties of the channel, it affects the assembly of the channel complex, and might be involved in

protein kinase regulation of the channel. In addition to an augmentation of the number of high affinity dihydropyridine binding sites (Perez-Reyes et al., 1992), coexpression studies of β_2 and α_{1C} subunits observed a 10-fold increase in current amplitude (Shistik et al., 1995; Castellano et al., 1993a; 1993b), acceleration of both activation and inactivation kinetics (Lacerda et al., 1991; Castellano et al., 1993a), and a negative shift in the activation potential (Castellano et al., 1993a; Tomlinson et al., 1993). A study by Haase and his group (1993) suggests these biophysical effects might be mediated through phosphorylation of the β_2 subunit. In support of this hypothesis, Puri and colleagues (1997) showed the cloned β_2 subunit contains consensus sites for PKA and PKC phosphorylation.

One of the key regulators of the L-type Ca^{2+}-channel is the β-adrenergic system. The binding of β-agonists to the receptor activates the receptor coupled to the stimulatory G-protein (Gs), which dissociates and activates the adenylyl cyclase. Activation of the adenylyl cyclase increases the level of cellular cAMP which binds to the regulatory subunits of cAMP dependent protein kinase (PKA), liberating the catalytic subunits to phosphorylate their substrates on specific serine and threonine residues. Some of the studies that lend support for this pathway are reviewed in Section D of the introduction.

Initial biochemical evidence for the existence of PKA phosphorylation sites occurred in early 1990's. Both the α_{1C} and β_1 subunits were identified as substrates for phosphorylation by PKA in vitro (Yoshida et al., 1992; Hell et al., 1993; Puri et al., 1997). More recently, direct evidence was provided by studies involving neuronal

Ca^{2+}-channels. These studies identified two forms of the α_{1C} subunit, a full length version and a shorter proteolytically truncated form (Hell et al., 1993) which is catalyzed by the Ca^{2+} dependent protease calpain (Hell et al., 1996). Only the full-length isoform was phosphorylated by PKA because the phosphorylation site believed to be Serine 1928 is cleaved in the shorter isoform (Davare et al., 1999; De Jongh et al., 1996; Hell et al., 1995). Although the prevailing isoform found in the heart is the short form (De Jongh et al., 1996), Gao et al. 1997 and Gerhardstein et al. 2000 indicated the full-length isoform is also present in the heart, but the cleaved C-terminal fragment remains functionally tethered to the short isoform, hence instilling functional PKA regulation in the short isoform. In 1996, Hasse colleagues showed the β subunits of the cardiac Ca^{2+}-channel are also phosphorylated by β-adrenergic agonists. Further evidence was provided by Bünemann et al. (1999), they showed the truncated isoform of the α_{1C} subunit could be stimulated by more than 2-fold by the application of activated PKA when it is co-transfected with the β_{2a} subunit into human embryonic kidney cells. In summary these studies indicate there are PKA phosphorylation sites on both the α_{1C} subunit and the β_2 subunit. Please refer to Walker and De Waard (1998) and Catterell (2000) for a more complete review of the topic.
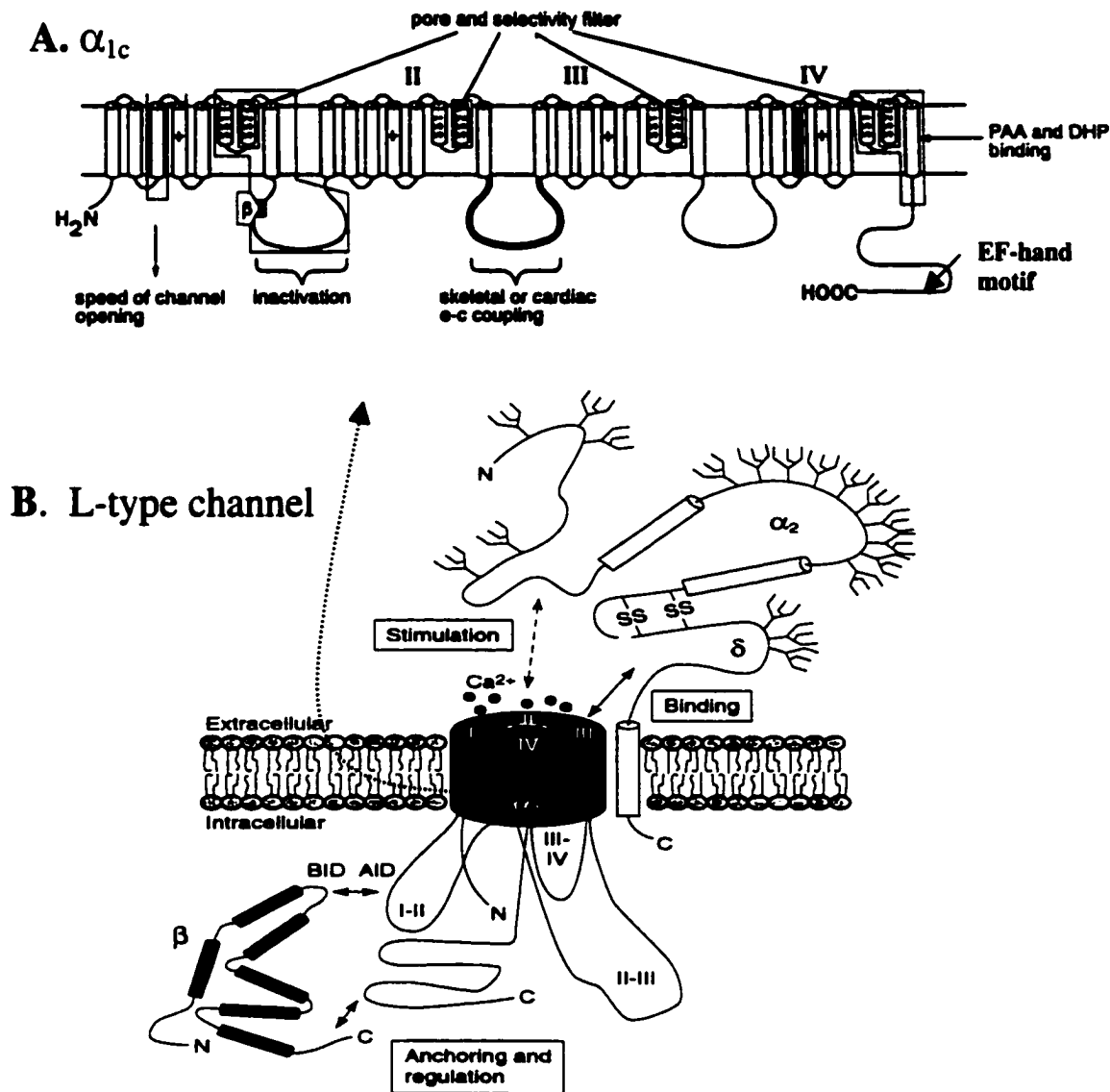
Figure 2: Structural organization of the L-type Ca^{2+}-channel. (A) The α_{1c} subunit for the L-type Ca^{2+}-channel contains four repeats (I-IV), each of which contains six transmembrane spanning α helices (S1-S6). The voltage sensing mechanism lies within the S4 segment of each repeat. The intracellular loop between repeats II and III is involved in E-C coupling, and the EF-hand Ca^{2+}-binding motif is located on the carboxyl tail. (B) The cardiac L-type channel contains at least four subunits: α_{1c}, α_2, δ, and β_2. The shaded region is the channel pore as formed by the α_{1c} subunit. AID (α_{1c} interaction domain) is the cytoplasmic loop between the repeats I and II and is required for interaction with the β_2 subunit. BID (β-interaction domain) is the portion of the $\beta2$ subunit that interacts with the AID. (diagram modified from Walker and DeWaard, 1998).

SECTION D. L-TYPE Ca^{2+}-CHANNEL REGULATION:

(1) Modulation by voltage

This introduction will briefly discuss the voltage regulation by $I_{Ca,L}$ since this route of $I_{Ca,L}$ regulation, except for some surface charge screening effect at high Mg^{2+}_i levels, is for the most part, unaltered by Mg^{2+}_i. Activation refers to the opening of Ca^{2+}-channels in response to a depolarization. The activation of cardiac L-type current is dependent on the membrane potential in a sigmoidal manner (Lee and Tsien 1984; Pelzer et al., 1986; Richard et al., 1993). Generally the threshold potential is approximately -40 mV when the external solution contains 2mM Ca^{2+} or Ba^{2+} (Isenberg and Klockner 1982; Tseng et al., 1987); full activation is obtained at +20 mV, and the potential eliciting half-maximal activation (V_h) is around -15 mV (Richard et al., 1993; McDonald et al., 1994 review). In addition to the increase in the number of opened channels, higher membrane potentials also increase the rate of channel opening (McDonald et al., 1994 review).

The average current in a multi-channel patch can be represented by the equation (McDonald et al., 1994 review):

$$I = N_t \times P_o \times P_f \times i$$

I= whole-cell current

i= single-channel current

N_t= the total number of channels available and unavailable

P_o= is the open-state probability of traces with openings, i.e. the probability that an available channel will be open

13

$P_f=$ the fraction of channels that are available to be opened, it can be calculated by the equation: $P_f = (n_t-n_b)/n_t$ where n_t is the total number of single channel records, and n_b is the number of blank records. P_o and P_f are generally lumped together as P. Generally the modulation of the whole-cell current is made by altering the open channel probability P_o and P_f.

As shown in the above equation, the whole-cell current is simply an aggregation of many single-channel currents within the cell. In practice, the average current flowing through the single channel during a series of identical depolarizations has been shown to reflect the characteristics of a whole-cell channel current (Pelzer et al., 1986). Although the shape of the open probability (P_o) curve is similar to that of whole-cell currents, it is shifted to the right by approximately +20 mV.

Inactivation refers to the decay of the Ca^{2+} current during a maintained depolarization. Inactivation of $I_{Ca,L}$ is governed by both membrane potential and Ca^{2+} entry (Kass and Sanguinetti 1984). Ca^{2+} dependent inactivation will be discussed in more detail in section B2. Evidence from whole-cell and single-channel studies shows voltage dependent inactivation is an intrinsic property of the $I_{Ca,L}$. This is demonstrated in the fact that L-type Ca^{2+}-channel current inactivates even if divalent ions other than Ca^{2+} or monovalent cations carry the current (Hess and Tsien 1984; McDonald et al., 1986; Hadley and Hume 1987; Katzka and Morad 1989). The inactivation of Ca^{2+} current has been shown to display both single and double exponential decay characteristics in multi-cellular preparations, although only double exponential properties are observed for single myocytes (Isenberg and Klockner 1982). Studies into the rate of inactivation for cardiomyocytes show the early phase of $I_{Ca,L}$ inactivation is generally 5 to 20 times faster than the later phase of inactivation (for example Isenberg

and Klockner 1982; Kass and Saguinetti 1984; Carmeliet et al., 1986; You et al 1995).

At the single-channel level, inactivation has also been described with double exponential decay characteristics.

Under physiological conditions, long prepulses at potentials more positive to -50 mV will lead to smaller amplitudes for subsequent activating test potentials. This relationship between the membrane potential and the degree of $I_{Ca,L}$ reduction, termed steady state inactivation, can be best represented by a sigmoidal function (Reuter et al., 1982; Cavalie et al., 1983; McDonald et al., 1986). For $I_{Ca,L}$, channel availability is near 100% at holding potentials negative to -50 mV, and declines at more positive potentials. For the L-type Ca^{2+}-channel the voltage at which steady state half inactivation (V_h) occurs at is around -30 mV and complete steady state inactivation occurs at potentials positive to +10 mV (Isenberg and Klockner 1982; Josephson et al., 1984; Campbell et al., 1988).

Table 2: Summary of the measured values of L-type Ca^{2+}-current voltage dependent steady state activation and inactivation.

Parameters	Whole-cell current	Single-channel current
steady-state activation		
threshold:	-40 mV	-20mV
V_h:	-10 mV	+15 mV
V_{max}:	0 mV	+30 mV
steady-state inactivation		
threshold:	-50 mV	-40 mV
V_h:	-30 mV	-10 mV
V_{max}:	0 mV	+30 mV

(2) Modulation by Ca^{2+}

Negative feedback is a system employed by biological systems to maintain homeostasis. Negative feedback in myocytes is crucial to survival since sustained high levels of free internal Ca^{2+} can lead to cell malfunction at ~ $1\mu M$ and even cell death at 10 μM. The negative feedback action of Ca^{2+} on Ca^{2+}-channel is termed Ca^{2+} dependent inactivation and was first observed by Brehm and Eckert in 1978. They found Ca^{2+} entry into the paramecium inactivates Ca^{2+}-channels. By 1984 a review by Eckert and Chad demonstrated Ca^{2+} dependent inactivation was ubiquitous across all phyla. Ten years later, though a complete mechanistic view of Ca^{2+} dependent inactivation of Ca^{2+}-channels was still not achieved, there was consensus for $I_{Ca,L}$ and many of the related physical aspects: 1) Ca^{2+} dependent inactivation is a distinct and separate process from voltage dependent inactivation; 2) Ca^{2+} dependent inactivation is specific for Ca^{2+} as the charge carrier, while currents carried by others such as Ba^{2+} or Sr^{2+} do not lead to the same kind of inactivation; 3) intracellular chelators slow, but do not abolish the inactivation of the Ca^{2+} current. Apart from these consensuses, there were many divergent opinions concerning the fundamental aspects of mechanisms. The central concern was the location of the calcium "sensor" where the inactivation would initiate. Studies by Sherman and colleagues (1990), and Keizer and Maki (1992), favoured the location of the sensor in the channel pore, whereas Chad and Eckert (1984; 1986), and Imredy and Yue (1992) proposed a Ca^{2+}-sensitive domain around the cytoplasmic entrance of the channel.

In addition to these disagreements, there were also questions about the mechanical factor that induces inactivation. Standen and Stanfield (1982), Sherman et al. (1990) and Keizer and Maki (1992) proposed that direct Ca^{2+} binding onto the channel causes it to inactivate. Using *Helix aspera* neurons Chad and Eckert (1986) proposed the inactivation was mainly caused by Ca^{2+} induced channel dephosphorylation. Another theory involved a known Ca^{2+} sensitive enzyme calmodulin. Armstrong (1989) proposed that Ca^{2+} activation of calmodulin leads to inactivation of the Ca^{2+}-channel, mainly through the stimulation of phosphodiesterases and the inhibition of phosphatase inhibitors. However in 1994, Imredy and Yue dismissed channel dephosphorylation or calmodulin as the key chemical switch by demonstrating that Ca^{2+} dependent inactivation did not diminish with the application of either phosphatase or calmodulin inhibitors. They concluded the direct binding of Ca^{2+} to the channel was the likely cause of channel inactivation. Further support for the direct binding theory was provided by Trautwein and Hescheler (1990) and You et al. (1995). Their work with trypsin showed that Ca^{2+} dependent inactivation could be inhibited by trypsin on the cytoplasmic side. This work led to the idea that Ca^{2+} dependent inactivation requires a regulatory component on the channel that is sensitive to being cleaved by trypsin.

In 1995, Dr. Yue's group transiently expressed the complementary DNA α_{1C} which encodes the L-type Ca^{2+}-channel and a neuronal Ca^{2+}-channel lacking Ca^{2+} dependent inactivation encoded by α_{1E} into HEK293 cells. That study demonstrated a consensus Ca^{2+}-binding motif, and an EF hand located on the carboxyl end of the α_{1C}

subunit were required for Ca^{2+} dependent inactivation, since donation of the α_{1C} EF hand region to the α_{1E} channel conferred the properties of Ca^{2+} dependent inactivation (de Leon et al., 1995). These observations reinforced the notion that Ca^{2+} dependent inhibition occurs as a result of direct calcium binding to the channel.

In 1998, Zuhlke and Reuter identified three amino acid sequences from the carboxyl end of the α_{1C} subunit, the presence of which was required for Ca^{2+} dependent inactivation to occur: 1) a putative Ca^{2+} binding EF-hand motif; 2) two hydrophilic residues (asparagine and glutamic acid) 77-78 amino acids downstream of the EF-hand motif; 3) a putative IQ calmodulin binding motif. Thus four years after Imredy and Yue dismissed calmodulin as a candidate for the chemical "switch", calmodulin returned to become the focal point of Ca^{2+} dependent inactivation (the lack of effect by the calmodulin inhibitors in their previous study could have been caused by the limited diffusion of a large molecule in the restricted space at the channel pore). The importance of calmodulin as the chemical switch was no longer in question, as exemplified by an article titled "Calmodulin is the Ca^{2+} sensor for Ca^{2+} dependent inactivation of L-type channel" (Peterson et al., 1999). A subsequent study (Peterson et al., 2000), revealed that calmodulin is constitutively tethered to the channel α_{1C} complex. Peterson and his group (2000) proposed that inactivation occurs by the interaction of the tethered calmodulin with an IQ like motif on the carboxyl tail of the α_{1C} by the following sequence: 1) Ca^{2+} entering through the channel pore binds onto and activates a calmodulin that is tethered to the α_{1C} subunit, 2) the activation of the tethered calmodulin causes an increase for the affinity of the IQ motif, located down-

stream of the EF hand, and binds to it, and 3) the channel which still conducts Ca^{2+} in this state, undergoes a final conformational change in the EF-hand motif, stabilizing and closing the cytoplasmic gate, thereby shutting the channel pore.

(3) β-adrenergic modulation

The sympathetic branch of the autonomic nervous system is one of the key players in the regulation of heart rate, AV nodal conduction and cardiac contractility. The binding of β-adrenergic agonists to their receptor typically increases $I_{Ca,L}$ amplitude 2 to 4-fold in mammalian ventricular myocytes and up to 10-fold in frog ventricular myocytes (Fischmeister and Shrier 1989; Hartzell and Budnitz 1992; Hartzell and Fischmeister 1987). $I_{Ca,L}$ stimulation is generally ascribed to enhanced cAMP dependent phosphorylation of Ca^{2+}-channels via activated cAMP dependent protein kinase (PKA) after β-adrenergic activation of the guanosine nucleotide-binding (G) protein G_s, and G_s activation of the adenylyl cyclase cascade (Rodbell, 1996 review). In addition to the cytoplasmic PKA phosphorylation pathway, evidence seems to indicate that β-adrenergic regulation of $I_{Ca,L}$ may also occur through the G-protein via a more direct fashion (Hille 1994 review). "Direct" regulation implies a fast membrane-delimited interaction between the G-protein and the L-type Ca^{2+}-channel, although fast processes such as phosphorylation occurring near the membrane cannot be excluded (Pitcher et al., 1992).

Ca^{2+}-channel regulation by cAMP ultimately implies the activation of the PKA system and PKA phosphorylation of the channel. Evidence for support of this pathway

was observed as early as 1973, when Tsien observed $I_{Ca,L}$ stimulation in cardiac Purkinje fibers after cAMP injection; he proposed that cAMP dependent phosphorylation of the Ca^{2+}-channel was the cause (Tsien 1973). Three years later, Sperelakis and Schneider (1976), found that not only was cAMP required for activation but adenosine triphosphate (ATP) was essential to maintain the phosphorylated channels in an available state. Reuter and Scholz in 1977 showed dephosphoryation by phosphatase could shift the channels into an unavailable state.

Elevation of cAMP concentration

The intracellular cAMP level can be modified by a number of methods: either indirectly by increasing its production with an adenylyl cyclase stimulator or by impeding its breakdown with the use of a phosphodiesterase inhibitor; or directly through injections or by photolysis of caged cAMP. The most common indirect method relies on the use of forskolin (FSK), a diterpene which is known to directly activate adenylyl cyclase by bypassing the β-adrenergic receptor and stimulatory G-protein (G_s) (Seamon and Daly 1983; 1986). In guinea pig ventricular myocytes micromolar levels of FSK typically elevated the amplitude of the $I_{Ca,L}$ by 100-400%, without affecting the kinetics of the current (Trautwein et al., 1986; Walsh et at., 1989).

The other indirect method of elevating cAMP is through the use of a phosphodiesterase inhibitor such as caffeine (Butcher and Sutherland 1962). The use of the caffeine analogue 3-isobutyl-1-methylxanthine (IBMX), a non-specific phosphodiesterase inhibitor (Strada et al., 1984), demonstrated that elevating the level

of cAMP by inhibiting its breakdown, can greatly enhance basal $I_{Ca,L}$ amplitude in guinea pig ventricular myocytes (Trautwein et al., 1986; Ono and Trautwein 1991). The results from these experiments also revealed that the $I_{Ca,L}$ amplitude was increased without affecting the current kinetics.

Direct elevation of cAMP has been achieved with dialysis (Irisawa and Kokubun 1983; Kameyama et al., 1985b), or photo-released caged cAMP (Nargeot et al., 1983; Frace et al., 1993), and by extra-cellular application of membrane permeable cAMP analogues (Pelzer et al., 1993; Walsh and Long 1992). In line with studies that utilized indirect elevation of cAMP, these investigations also showed a three to four-fold increase in basal $I_{Ca,L}$ amplitude.

Modification of PKA activity

The most direct and convincing evidence for PKA stimulation of the Ca^{2+}-channel is the application of PKA into the cytoplasm. $I_{Ca,L}$ was stimulated in guinea pig ventricular myocytes following injection (Osterrieder et al., 1982, and Brum et al., 1983) or dialysis (Kameyama et al., 1985, Shuba et al., 1990a) of the catalytic subunit of the PKA enzyme. Finally, additional confirmation that PKA phosphorylation is a necessary process in $I_{Ca,L}$ stimulation was obtained through the use of PKA inhibitors H89 (Yuan and Bers, 1995) and PKI (Kameyama et al., 1986; Pelzer et al., 1990; Hartzell et al., 1991). These studies showed that $I_{Ca,L}$ stimulation via the β-adrenergic pathway could be inhibited by H89 and PKI.

Modification of ATP supply utilization

Implicit in the cAMP dependent phosphorylation pathway is the requirement for ATP. It provides both the substrate and the energy to maintain cAMP levels and channel phosphorylation. Hence, it is not unexpected that investigations that either inhibit ATP production with the use of cyanide (Goldhaber et al., 1991) or use non-hydrolyzable ATP analogues (Shuba et al., 1990b) observed diminished $I_{Ca,L}$ amplitudes. Conversely, Noma and Shibasaki (1985) observed a marked increase in $I_{Ca,L}$ as dialysate ATP was augmented from 0.5 to 10 mM, and Keung and Karliner (1990) showed that the inhibitory effects of pertussis toxin could be reversed with the application of 5 mM ATP.

Channel dephosphorylation

Since cAMP stimulation culminates in the phosphorylation of the Ca^{2+}-channel, it is probable that any interventions that would influence dephosphorylation would likely affect the $I_{Ca,L}$. For example, stimulation of the phosphatase system has been shown to suppress the stimulatory effects of β-adrenergic stimulation (Hescheler et al., 1987) and inhibit basal $I_{Ca,L}$ (Trautwein et al., 1986; Hescheler et al., 1987). In contrast, protecting the phosphorylated channel from being dephosphorylated can greatly enhance the responsiveness to β-adrenergic stimulation and also deter $I_{Ca,L}$ rundown. For instance, the use of ATPγS to promote channel thiophosphorylation resulted in a doubling of $I_{Ca,L}$ and also enhanced responsiveness to isoproterenol (Kameyama et al.,

1986), as well as maintained stimulation after agonist withdrawal (Hescheler et al., 1987; Scamps et al., 1992).

Regulation of L-type Ca^{2+}-channel by β-adrenergic receptor stimulation

Stimulation of the β-adrenergic receptors activates the receptor-coupled Gs-protein resulting in stimulation of the adenylyl cyclase and the cAMP cascade. β-adrenergic stimulation of cardiac myocytes typically produces an increase in the current amplitude, and aside from this macroscopic change, this section will also review the effects of β-adrenergic stimulation on single-channel properties.

Whole-cell current changes

Application of 0.01 to 10 μM of the β-adrenergic agonist isoproterenol typically amplifies whole-cell currents carried by Ca^{2+}, Ba^{2+}, or Na^+ by 1 to 4-fold. This result is observed in a wide variety of systems including: cardiac multicellular preparations (Reuter, 1979; McDonald, 1982; Tsein et al., 1986); sino-atrial nodal cells (Belardinelli et al., 1988: Petit-Jacques et al., 1993); and guinea pig ventricular myocytes (Isenberg and Klockner, 1982; Kameyama et al., 1985; Balke and Wier, 1992; refer to McDonald et al., 1994 review).

Average and unitary current amplitudes

Although the whole-cell current increased several-fold with β-adrenergic stimulation, the single-channel unitary current amplitude is unaltered. Single-channel recording in experiments by Brum and colleagues (1984), Tsein's group (1986), Ochi and Yawashima (1990), and Yue and others (1990) suggest the increase in whole-cell current amplitude is caused by changes to channel gating properties, altering the channel open probabilities.

Fast-gating kinetics

Channel phosphorylation via β-adrenergic stimulation has the effect of enhancing both open state probability (P_o) and the fraction of available channels (P_f). The increase in P_o is caused by the lengthening of millisecond-long openings and the abreviation of millisecond-long closings (Brum et al., 1984; Trautwein and Pelzer 1988). Ono and Fozzard (1992) detected a second class of longer lasting openings ($\tau \sim 1$ ms), in addition to the normal openings ($\tau \sim 0.3$ ms), when high (16 μM) isoproterenol was applied to the cells. These changes to the fast-gating kinetics however can only account for a small portion of the increase in P_o and whole-cell $I_{Ca,L}$ amplitude.

Slow-gating kinetics

The bulk of the β-adrenergic stimulation is caused by changes to the slow-gating kinetics. In most studies, β-adrenergic stimulation caused an increase in the proportion of non-blank sweeps within ensembles of single-channel currents. The increase in the

proportion of non-blank sweeps represents an increase in the number of available channels P_f. For example the application of isoproterenol in guinea pig ventricular myocytes can raise the number of non-blank sweeps by 200% (Yue et al., 1990), 300% (Trautwein et al., 1986) and 400% (Tsien et al., 1986). Non-blank records tend to occur in consecutive sweeps (Tsein et al., 1986), while the number of consecutive non-blank sweeps were increased by several-fold with β-adrenergic stimulation (Ochi and Kawashima 1990).

The higher number of non-blank sweeps can be interpreted as a shift from channel inactivation towards channel activation. This shift has been witnessed as a slowing of the whole-cell current decay when Ba^{2+} is the charge carrier (Brum et al., 1984; Trautwein and Pelzer 1988; Ochi and Kawashima 1990). However, this phenomenon was not observed when Ca^{2+} is the charge carrier because Ca^{2+} dependent inactivation overrides this effect (Pelzer et al., 1990). In addition to the slowing of current inactivation, voltage dependent activation is shifted to the left by 5-10 mV (Shuba et al., 1990a; Ono and Trautwein 1991; Tiaho et al., 1991; Osaka and Joyner 1992).

Shifts in gating modes

In addition to the prolongation in millisecond open times, Yue and colleagues (1990) found a pronounced increase in extra long openings. They interpreted this transformation as a shift towards a different gating mode, that favours long openings (mode-2). Hess et al. (1984) first described mode-2 gating as unitary currents

displaying long-lived open times (~10 ms) and short-lived closed times. A shift

towards mode-2 conductance was shown by Tiaho and coworkers (1991) to slow the

deactivation of whole-cell Ca^{2+} currents.

(4) $I_{Ca,L}$ modulation via direct G_s stimulation

The first evidence supporting the direct stimulation of $I_{Ca,L}$ by G-protein was

provided by Yatani and colleagues between 1987 and 1989 (Yatani et al., 1987; Yatani

et al., 1988; Imoto et al., 1988; Yatani and Brown 1989). They showed that $G\alpha s$-

GTPγs, but not $G\alpha_i$ or $G\beta\gamma$, stimulated $I_{Ca,L}$ activity in inside-out cardiomyocyte patches

and lipid bilayers and was able to resolve the fast and slow receptor dependent

components of the regulation. Further support for this mechanism was provided by

Shuba et al. in 1990b and 1991, Trautwein et al. 1990, Cavalie et al. 1991, and Pelzer et

al. 1991. Collectively, their work showed that stimulation by isoproterenol was

possible in the absence of ATP, cAMP or other supplements which would allow

phosphorylation to occur. In spite these findings, Hartzell and colleagues did not report

any fast membrane delimited pathway in either guinea pig or frog myocytes (Hartzell et

al., 1991).

(5) Ca^{2+} and adenylyl cyclase

There are at least 9 different isoforms of adenylyl cyclases with differing responses to Ca^{2+}. Adenylyl cyclase isoforms AC1, AC3 and AC8 are positively modulated by Ca^{2+}; isoforms AC5 and AC6 are inhibited by Ca^{2+}; and isoforms AC2, AC4, AC7 and AC9 are not influenced by fluctuations in Ca^{2+} level (reviews Cooper et al., 1998; Tang and Hurley 1998) refer to table 3. The brain is one of the few tissues which has stimulatory Ca^{2+}-calmodulin (Ca^{2+}-CaM) adenylyl cyclase effect. In most tissues cyclase activity is inhibited by free Ca^{2+} via Ca^{2+}-CaM. Such inhibition was observed in rat bone and osteosarcoma membranes (Rodan et al., 1980), rat fat cell membranes (Birnbaumer et al., 1969), guinea pig hearts (Drummond and Duncan 1970; Colvin et al., 1991), rat liver membranes (Pohl et al., 1971), and turkey erythrocytes (Steer and Levitski 1975a; Steer and Levitski 1975b). In addition to the inhibition by Ca^{2+}-CaM, Levitski and colleagues proposed the existence of allosteric binding sites for free Ca^{2+} on the turkey erythrocyte adenylyl cyclase complex distinct from free Mg^{2+} binding sites. They argued that Ca^{2+}-binding decreases the V$_{max}$ of the erythrocyte enzyme without affecting the K$_m$ for MgATP^{2-}. Further evidence for the existence of inhibitory Ca^{2+} binding sites on the adenylyl cyclase was reported in 1991. Using cardiac sarcolemmal preparations, Colvin et al., 1991 demonstrated the existence of a high affinity (K$_m$ < 1 µM) and a low affinity (K$_m$ > 100 µM) Ca^{2+} binding site on the adenylyl cyclase. At the low affinity site Ca^{2+} competes with Mg^{2+} for the allosteric Me^{2+} binding site; whereas the high affinity binding site is most likely non-competitive

with Mg^{2+}, and is regulated by G-protein stimulation which decreases the affinity for Ca^{2+}.

Results from recent studies seem to indicate that Ca^{2+} modulation of cardiac adenylyl cyclase is highly dependent on Ca^{2+} entry through the Ca^{2+}-channel and to a lesser extent on bulk cytoplasmic Ca^{2+} (Cooper et al., 1995). You and colleauges (1997) demonstrated that $I_{Ca,L}$ stimulation by 40 mM BAPTA was caused by the hindrance of Ca^{2+} dependent inhibition of the adenylyl cyclase from Ca^{2+}-channel entry.

Table 3: Properties of cloned mammalian adenylyl cyclases grouped by structural relatedness, modified from Cooper et al. (1995 and 1998). The regulatory susceptibilities of the adenylyl cyclase families the Ca^{2+}, G-protein $\beta\gamma$ subunits, $G_{\alpha s}$, and protein kinase C (PKC). Location of cyclase is defined by mRNA expression: DG/HO dentate gyrus/hippocampus, OE olfactory neuroepithelium.

AC family	Ca^{2+} effect	$\beta\gamma$ effect	Gs stimulation	PKC stimulation	mRNA source
AC1	stimulation	inhibition	Mild	No	DG/HO
AC3	stimulation	inhibition	Yes	No	OE
AC8	stimulation	inhibition	Yes	No	hippocampus
AC2	No	stimulation	Yes	Yes	cerebellum
AC4	inhibition	stimulation	Yes	No	heart
AC7	No	stimulation	Yes	Yes	cerebellum
AC5	inhibition	No	Yes	No	caudate nucleus
AC6	inhibition	No	Yes	No	heart
AC9	inhibition	No	Yes	?	widely expressed

(6) L-type Ca^{2+}-channel run-down

During the course of an electrophysiological experiment involving the patch clamp technique, it is common for the amplitude of the Ca^{2+} current to decline. This phenomenon referred to as run-down is most pronounced when the cells are dialyzed during whole-cell recordings or during experiments involving inside-out patches (McDonald et al., 1994). Run-down is believed to be caused by the wash-out of important endogenous cytosolic components (Kameyama et al., 1988) leading to dephosphorylation or proteolysis of constituents involved in Ca^{2+}-channel regulation (Romanin et al., 1991). A number of different mechanisms have been suggested as the cause of run-down. Some of the mechanisms which were initially suggested as the cause of run-down are:

1) Run-down caused by the progressive loss of high energy compounds such as ATP and cAMP. Irisawa and Kokubon (1983) and Belles et al. (1988) showed that the application of ATP into the cytoplasmic side of the membrane could slow down the rate of run-down.

2) Run-down caused by the increase in intracellular Ca^{2+}. Belles et al. (1988b) indicated the addition of Ca^{2+} buffers could dramatically reduce of the rate of channel run-down.

3) Run-down caused by dephosphorylation of the L-type channel. Yatani et al. (1987) showed that run-down could be reduced in cardiac cells by the addition of compounds that stimulate the PKA phosphorylation cascade. Further evidence was supplied by

Ono and Fozzard (1992); these researchers showed the addition of MgATP^{2-} and PKA could temporarily reverse the effects of run-down.

4) Involvement of proteolysis in run-down. Belles et al. (1988a) demonstrated that run-down of the L-type Ca^{2+}-current in guinea pig myocytes was accelerated by the Ca^{2+} dependent proteases calpain I and II, whereas the endogenous protease inhibitor calpastatin impeded the rate of run-down. Romanin et al. (1991) also showed that in addition to calpastatin, the application of ATP and GTP could further enhance the "protective" properties of calpastatin. However, research from Romanin's and Kameyama's labs suggested the mode of action of calpastatin on $I_{Ca,L}$ run-down may not be through the inhibition of calpain but by an undetermined pathway (Seydl et al., 1995; Kameyama et al., 1998). By 2000 Romanin's research determined the mode of action of calpastatin was focused on the portion of the α_{1C} subunit containing the C-terminal sequence 1572-1651 (Kepplinger et al., 2000).

SECTION E. Mg^{2+}_i HOMEOSTASIS:

The concentration of cytoplasmic magnesium is generally kept to within narrow limits in spite of wide changes in magnesium levels in the external medium under experimental conditions. This implies the existence of specialized magnesium transport systems, because magnesium can pass across the cellular membrane, and because the internal level is kept well below the electrochemical gradient. Alterations of free intracellular magnesium can be accomplished by a number of processes, some of which are direct, and others indirect.

Investigations into the amount of magnesium in rat hepatocytes indicate that only 5-10% of the total intracellular magnesium is in the free ionized form (Corkey et al., 1986). The large pool of bound-intracellular Mg^{2+} has the potential to elevate the free-intracellular Mg^{2+} level significantly, especially as an indirect effect to changes in the level of H^+, ATP and to a lesser extent intracellular calcium. Indirect elevation of Mg^{2+}_i is most significant under situations of metabolic compromise; for example in simulated ischemic conditions on cardiac cells, the Mg^{2+}_i level could rise greatly due to the fall in cellular ATP, and rise in H^+ ions. Silverman et al., (1994), showed that the Mg^{2+}_i could increase by more than 200% in single adult rat ventricular myocytes subjected to hypoxic conditions. ATP is normally a major cytoplasmic magnesium buffer because of its high concentration and high magnesium affinity. As ATP breaks down, it forms products with much lower magnesium affinities, causing the Mg^{2+}_i level to be elevated. In addition, the ATP may fall to levels at which Mg^{2+} transport is

31

compromised, such that the elevated Mg^{2+}_i could not be transported to the extracellular medium (McDonald et al.,1994 review). The example described above exemplifies an indirect response of intracellular magnesium to a stimulus, but does not necessarily represent a regulatory mechanism.

Although the influx of Mg^{2+} into the cardiac myocyte remains unclear, the efflux is handled by an active sodium-dependent and imipramine-sensitive mechanism, which is most likely a Na-Mg exchanger (Handy et al., 1996). Even though the regulation of intracellular magnesium is still not well understood, there seems to be agreement that the intracellular level is regulated by hormones. β-adrenergic stimulation leads to a reduction in Mg^{2+}_i, whereas muscarinic receptor stimulation leads to an increase in Mg^{2+}_i (Romani et al., 1992; Watanabe et al., 1998). The muscarinic stimulation acts via (protein kinase C) PKC activation and can antagonize the effects of β-adrenergic stimulation (Amano 2000). More work has to be completed in this area before Mg^{2+}_i homeostasis can be completely understood. Given the current information, it is proposed that regulation of Mg^{2+}_i occurs via the Na-Mg exchanger; β-adrenergic stimulation increases the rate of Mg^{2+}_i efflux via the Na-Mg exchanger leading to a reduction in Mg^{2+}_i, whereas muscarinic stimulation slows down the rate of Mg^{2+}_i efflux by the same exchanger thus resulting in a build-up of Mg^{2+}_i.

The measured cytoplasmic free-Mg^{2+} levels in heart cells range between 0.4 mM and 1.2 mM, for basal conditions. In rat myocytes β-adrenergic stimulation results in a ~25% decline in free Mg^{2+} levels (Watanabe et al., 1998), and a ~15% reduction in total Mg^{2+} level (Romani et al., 1993). Watanabe et al. (1998) showed that although PKC

antagonized the effects of β-adrenergic stimulation it did not raise the Mg^{2+}_i level; in contrast, Romani et al. (1993) found that PKC stimulation by carbachol elevated the Mg^{2+}_i level by ~20%.

Table 4. Summary of the measured values of internal magnesium levels in heart cells in the last ten years.

Cell type	$[Mg^{2+}]_i$ (mM)	Conditions	Year	Authors
rat myocytes	0.40 0.30 0.40	basal ISO PKC	1998	Watanabe et al.
rat myocytes	0.60 0.73 0.46	basal electrical stim. caffeine	1997	Hong-ying and Quame
rat myocytes	0.80-0.90 0.90 1.40 0.90	basal Ca-free ext. Ca-Na-Free ext. Ca-Na-Free and Impramine	1996	Handy et al.
sheep myocytes	0.60 ± 0.19	basal	1995	Gow et al.,
rat myocytes	1.02 ± 0.03 1.3-2.8 10-17	basal hypoxia extended hypoxia	1994	Silverman et al.
guinea pig myocytes	0.42-1.23 mean 0.72	basal	1993	Buri et al.
chicken myocytes	0.48 ± 0.03 1.50	basal Na-Free ext.	1989	Murphy et al.
ferret myocytes	0.40 0.90	basal K-Na-Free ext.	1988	Balatter and McGuigan
	Total Magnesium			
perfused rat heart	10.5 8.76 12.35 10.5-11.5	Basal Nor-epinephrine PKC stimulation basal	1993 1990	Romani et al. Romani and Scarpa

SECTION F. Mg^{2+}_i AND THE β-ADRENERGIC SYSTEM:

The final product of β-adrenergic stimulation is an increase in the level of cAMP. Conversion of ATP to cAMP is catalyzed by adenylyl cyclase, which is regulated by a system comprised of a G-protein coupled receptor, and a heterotrimeric G-protein. Conversely the metabolism of cAMP into 5'-AMP is catalyzed by phosphodiesterases (PDEs). This simple outline indicates at least four different junctions where β-adrenergic stimulation could be regulated: the receptor, G-protein, adenylyl cyclase and phosphodiesterase. In varying degrees each of these regulatory steps requires Mg^{2+}_i.

This part of the introduction will be divided into two sections, the first elaborates on the involvement of magnesium in the synthesis of cAMP, and the second focuses on the degradation of cAMP. Since the influence of magnesium on the synthesis of cAMP was the focus of much attention during the 1970's, this research dominates the first section. Most of the information about the influence of magnesium in the metabolism of cAMP was acquired later, and thus, the majority of the works cited in the second section is from the 1990's.

(1) Mg^{2+}_i influence on ligand binding

In 1977 Ross and his colleagues were one of the first groups to investigate the regulatory role of divalent cations on β-adrenergic receptor affinity. Using S49 murine lymphoma cells, they discovered that raising the level of free Mg^{2+} from nominal amounts to 40 mM increases the receptor's affinity for their agonist isoproterenol by as much as 30-fold, without increasing the affinity for their antagonist propanolol. The half maximal effect was observed at 2 mM free Mg^{2+}. An intriguing aspect of the ability of Mg^{2+} to alter agonist affinity is its effect on the apparent Hill coefficient of the agonist for β-adrenergic receptors. While antagonists bind with a Hill coefficient close to 1.0, agonists in the absence of guanosine triphosphate (GTP) or Mg^{2+} have a coefficient of about 0.8. The addition of Mg^{2+} progressively lowers the Hill coefficient to 0.4 - 0.5, while the addition of GTP increases the Hill coefficient back to the same level observed for antagonists. This led Ross and his group to study the interaction of GTP and Mg^{2+} with regard to modulation of agonist affinity for β-receptors. In the absence of Mg^{2+}, GTP has little if any ability to decrease agonist affinity. However, after addition of Mg^{2+}, when agonist affinity has been increased to 20-fold or more, addition of GTP in the micromolar range progressively decreased agonist affinity. A curious fact about Mg^{2+}/GTP interaction is that it is non-competitive. Raising the Mg^{2+} level as high as 100 mM does not reverse the loss of agonist affinity. The decrease in agonist affinity is concentration dependent when GTP is added to membranes in the presence of Mg^{2+} and occurs over a range of GTP concentrations similar to those

required for agonist/GTP-stimulation of adenylyl cyclase. These findings led Ross and colleagues to postulate the existence of four β-adrenergic receptor conformational states: 1) a low affinity receptor state in the absence of agonist, GTP and free Mg^{2+}; 2) a low affinity state when agonist alone is bound; 3) a high affinity agonist-bound state induced by Mg^{2+}; 4) a low affinity agonist-bound state induced by GTP and Mg^{2+} (Ross et al., 1977).

(2) Mg^{2+}_i dependence of G-protein dissociation

In addition to Mg^{2+}'s direct influence on the adenylyl cyclase, it plays a major role in the dissociation of the G-protein:

$$GDP\text{-}G\alpha\beta\gamma + GTP \rightleftharpoons GTP\text{-}G\alpha + G\beta\gamma + GDP.$$

Mg^{2+} shifts the equilibrium for this reaction strongly to the right. The concentration of Mg^{2+} required to shift the equilibrium in favour of G-protein dissociation varies for different types of G-proteins: 1-10 mM for the "olfactory" G-proteins $G\alpha_{olf}$ (Katada and Oinuma 1986), 5-50 mM for the inhibitory G-proteins $G\alpha_i$ (Higashijima et al., 1987) and greater than 10 mM for the stimulatory G-proteins $G\alpha_s$ (Brandt and Ross 1985). As demonstrated in those reports, Mg^{2+} can either be stimulatory or inhibitory to the production of cAMP depending on the type of G-proteins expressed.

(3) Mg^{2+}_i dependence of adenylyl cyclase

Using cardiac and skeletal sarcolemma preparations, Narayanan and Sulakhe researched the effects of Mg^{2+} on unstimulated and β-adrenergic receptor-stimulated cyclases (Narayanan and Sulakhe 1977; Narayanan et al., 1979). Both cardiac and skeletal preparations appeared to have stimulatory free Mg^{2+} binding sites associated with the cyclase. Mg^{2+} binding to these sites tended to increase the rate of reaction (V_{max}) without affecting the substrate binding affinity (K_m) for $MgATP^{2-}$. This result was observed in both basal and stimulated conditions. For example, as the Mg^{2+} was raised from 50 μM to 1.2 mM, both basal adenylyl cyclase activity and that stimulated via the receptor by epinephrine or the G-protein by GTP or Gpp(NH)p (a non-hydrolyzable GTP analog) V_{max} was increased with no alteration in the apparent K_m for the substrate $MgATP^{2-}$.

In studies on rat liver adenylyl cyclase, Londos and Preston (1977) revealed that increasing concentrations of Mg^{2+} can increase the catalytic activity. The K_m value for Mg^{2+} under basal conditions was between 5 and 10 mM. However when the adenylyl cyclase was activated by either glucagon or GTP, the K_m for Mg^{2+} was lowered to physiological concentrations. This was one of the first pieces of evidence to link adenylyl cyclase regulation to the combination of hormones and Mg^{2+}. A possible interpretation of this result is that adenylyl cyclase activity is kept at a minimum by the lack of bound Mg^{2+} under basal conditions due to the relatively high K_m value. However under hormonally stimulated conditions, when the K_m is within the

physiological range, adenylyl cyclase activity is stimulated by the increased number of activated Mg^{2+}-bound catalysts.

Published data about the influence of free Mg^{2+} on adenylyl cyclase activity was, for the most part, consistent with other experiments indicating that free Mg^{2+} was required for optimal adenylyl cyclase activity. However it was not until Rodan's report in 1980 that a mechanistic view of Mg^{2+} regulation emerged. Rodan et al. (1980), investigated the effects of Mg^{2+} and Ca^{2+} on basal activity of adenylyl cyclase in plasma membrane from bone and osteosarcoma cells. As seen by other researchers, they observed that the primary effect of Mg^{2+} was that of an activator, increasing V_{max} without significant impact on the K_m for the substrate $MgATP^{2-}$. However, the most interesting aspect of their report was the discovery of two distinct allosteric Mg^{2+} regulatory binding sites. As revealed by double reciprocal plots, two different K_ms were evident, giving indication of two possible binding sites (the K_m values were 1 and 8 mM). But it was not until 1998, 18 years later, that the role of Mg^{2+} was understood. Using X-ray crystallography and mutated adenylyl cyclases, Zimmerman et al. (1998) proposed that the mechanism of the adenylyl cyclase was very similar to that of DNA polymerase, in which two Mg^{2+} ions facilitate the nucleophilic attack of the 3'-hydroxyl group of the ATP and the subsequent elimination of pyrophosphate.

39

(4) Mg^{2+}_i dependence of phosphodiesterase

Cyclic nucleotide phosphodiesterase plays an equal but opposite role to adenylyl cyclase in the regulation of cAMP. Phosphodiesterase was first described by Rall and Sutherland in 1958 shortly after the discovery of cAMP; but it was the subsequent identification of PDE as a catalyst for the hydrolysis of cAMP which led to the determination of cAMP as a physiologically relevant molecule. Similarly, the revelation that most preparations of PDE also hydrolyze cGMP was used as a basis for proving the physiological relevance of cGMP as a second messenger molecule.

The initial purification and characterization of phosphodiesterase activity was reported by Butcher and Sutherland in 1962. This and subsequent early studies documented the inhibitory effect of methylxanthine, caffeine, and theophylline on PDE activity and also demonstrated the specificity of the reaction for the hydrolysis of the 3'-phosphoester bond of the 3',5'-purine ribose cyclic monophosphates cAMP and cGMP. Much of the difficulty and confusion in the early interpretation of PDE regulation was due to the fact that PDE is a major mediator of cross talk between different second messenger signaling pathways. However, there seems to be a consensus that Mg^{2+} is required for catalytic activity, and Ca^{2+}, depending on its concentration, can be either a stimulator or inhibitor (Yamamoto et al., 1983).

At present, there are eight different families of phosphodiesterases with many unique isozymes within each family; in total 15 different phosphodiesterase genes generate over 21 different isozymes (Antoni 2000). The families are categorized based on their substrate affinity for either cGMP or cAMP, dependence on regulatory

compounds such as Ca^{2+}/CaM or cGMP, primary amino acid sequence, and inhibitors. All phosphodiesterase families except for PDE5 are able to hydrolyze both cAMP and cGMP with varying K_m and V_{max}. The PDE5 family is cGMP specific, while PDE1, PDE2, and PDE6 are more selective for cGMP than cAMP. A recombinant expressed PDE7 exhibited a high affinity for cAMP ~0.1 μM (Han et al., 1997), however this enzyme has not been detected in heart cells (Bloom and Beavo 1996). The physiological properties of the PDEs that tend to have higher affinities for cAMP than cGMP and their presence in cardiomyocytes are shown in table 3. These PDEs include those from the PDE3, PDE4, and PDE8 families.

Table 5: Summary of the cAMP selective phosphodiesterases that are expressed in mammalian heart cells. cGMP inhibits PDE3 because it has the same affinity as cAMP but is very poorly hydrolyzed.

Family	Gene Products	Stimulators	Inhibitors	EC_{50} for Mg^{2+}	Affinity	Reference:
PDE3	PDE3A PDE3B	PKA	cGMP	200 μM	cAMP = cGMP	Meacci et al., 1992; MacPhee et al., 1988; Omburo et al., 1995

Importance: attenuate amplitude of cAMP signal due to its high V_{max} but lower affinity for cAMP (compared to PDE8). cGMP acts as a competitive inhibitor of cAMP.

PDE4	PDE4A, PDE4B, PDE4C, PDE4D	PKA	?	3 mM basal 50 μM PKA	cAMP >> cGMP	Rahn et al., 1994; Sette et al., 1994; Sette and Conti 1996; Percival et al., 1997

Importance: attenuate amplitude of cAMP signal; PKA phosphorylation stimulates enzyme by lowering requirements for Mg^{2+}.

PDE8	PDE8A	?	?	400 μM	cAMP >> cGMP	Fisher et al., 1998;

Importance: maintaining low basal level of cAMP due to its low V_{max} but high affinity for cAMP.

SECTION G. Mg^{2+}_i REGULATION OF $I_{Ca,L}$:

Only a few of groups have studied the effects of cytoplasmic Mg^{2+} on $I_{Ca,L}$ in the past 13 years. Of the four groups, two researched the effects of Mg^{2+} on $I_{Ca,L}$ in the frog myocyte while the others studied the guinea pig myocyte. The outcome from these investigations revealed little consensus aside from the observation that milli-molar levels of free Mg^{2+} tend to inhibit $I_{Ca,L}$.

(1) Mg^{2+}_i effects on frog $I_{Ca,L}$ myocytes

White and Hartzell (1988) were the first to look at the effects of Mg^{2+}_i on $I_{Ca,L}$ in frog ventricular myocytes. Their study found inhibition of $I_{Ca,L}$ by Mg^{2+}_i was greater under β-adrenergic stimulation than basal conditions. When they increased the Mg^{2+}_i level from 0.3 mM to 3 mM they observed a 20% inhibition under basal conditions, as opposed to 50% inhibition under β-adrenergic stimulation. Although they did not rule out possible effects from Mg^{2+}-activated phosphatases, they postulated that the inhibition by Mg^{2+} was most likely caused by direct Mg^{2+}-binding at the calcium channel, which is exacerbated by phosphorylation.

In contrast to White's and Hartzell's study, Yamaoka and Seyama (1996a), observed a 700% increase in $I_{Ca,L}$ when Mg^{2+}_i was reduced from 1mM to 1 μM under basal conditions. Single channel studies under this condition revealed that the augmentation was caused by an increase in the number of available channels and not by channel open probability (P_o). Although the characteristics of the stimulation were very

similar to that observed for phosphorylated channels, they showed that the stimulation was independent of phosphorylation, because application of the non-hydrolysable AMP-PCP could not suppress the potentiation by 1 μM Mg^{2+}. Later that same year Yamaoka and Seyama (1996b) showed that the potentiation by 1 μM Mg^{2+} could be inhibited by GTP. From these results, they concluded that both GTP and Mg^{2+} act directly but independently to inhibit $I_{Ca,L}$. By 1998, again contrasting White's and Hartzell's study, Yamaoka and Seyama showed that Ca^{2+}-channels phosphorylated by PKA were insensitive to blockage by Mg^{2+} and GTP. They were able to propose a model of the interactions between Mg^{2+}, GTP and the Ca^{2+}-channel. According to Figure 7 from Yamaoka and Seyama (1998), the model is comprised of one inhibitory binding site for Mg^{2+}, one inhibitory binding site for GTP, and one stimulatory phosphorylation site on the Ca^{2+}-channel. They argued that both GTP and Mg^{2+} can bind onto and inhibit the Ca^{2+}-channel independently, whereas phosphorylation of the channel blocks the binding of Mg^{2+} and GTP, and allows the channel to be available for activation.

(2) Mg^{2+}_i effects on guinea pig $I_{Ca,L}$ myocytes

The effects of Mg^{2+} on mammalian cardiomyocytes $I_{Ca,L}$ were first studied by Agus and colleagues (1989). Their results showed a 140% stimulation when Mg^{2+}_i was reduced from 1.3 mM to 0 mM, whereas inhibition was observed when Mg^{2+}_i was elevated to 9.4 mM. The inhibition observed by dialysis of 9.4 mM Mg^{2+}_i was powerful, and regardless of the state of channel phosphorylation the peak currents at 9.4

mM Mg^{2+}_i were less than 3% of that observed at 0 mM Mg^{2+}_i. Based on their findings, they proposed that Mg^{2+}_i enhanced the steady state inactivation of the channel, thus making it unavailable for activation.

While Agus's experiment focused on very low and very high levels of Mg^{2+}_i. Backx et al. (1991), and O'Rourke et al. (1992) chose to study the effects of altering Mg^{2+}_i in the micro-molar range. Their experiments showed that rapid elevation of Mg^{2+}_i in the low micro-molar range (0.06 to 58 μM, and 25 to ≤ 200 μM), stimulated $I_{Ca,L}$ but only in the presence of ATP or non-hydrolyzable ATP analogues. They were able to prove that the stimulation was independent of PKA phosphorylation, and hypothesized the presence of a Mg-ATP stimulatory binding site on the L-type Ca^{2+}-channel.

As shown by this brief summary, the effects of Mg^{2+}_i on L-type Ca^{2+}-channel, especially in mammalian cardiomyocytes are not well understood. To gain a better comprehension of the effects of Mg^{2+} on $I_{Ca,L}$ in mammalian cardiomyocytes, the present study will assess whether effects of Mg^{2+}_i on phosphorylation/dephosphorylation processes contribute to the Mg^{2+}_i dependence of $I_{Ca,L}$ in guinea pig cardiomyocytes.

II. METHODS

The methods section is divided into four parts: (A) myocyte preparation, (B) electrophysiology recording and analysis (C) experimental solutions and drugs, (D) statistics.

SECTION A. MYOCYTE PREPARATION, CELL DIMENSIONS, AND COMPOSITION OF SOLUTIONS FOR MYOCYTE ISOLATION:

(1) Myocyte preparation

In accordance with local regulations on animal experimentation, guinea pigs (300-600g) of either sex were killed by cervical dislocation. The heart was quickly excised, the ascending aorta cannulated, and attached to the base of a Langendorff column for retrograde perfusion through the aorta. The perfusion consisted of 1-2 minutes with physiological salt (PS) solution, 4-8 minutes with Ca^{2+}-free solution, 8-12 minutes with Ca^{2+}-free solution containing collagenase (0.1 mg/ml: Yakult Pharmaceutical Co., Tokyo Japan), and 4-5 minutes with a high-K^+, low-Na^+ "KB" storage solution. All perfusates were oxygenated with 100% O_2 and maintained at 37° C. The ventricles were cut into small pieces and agitated to disperse the cells. The cell-dispersed solution was filtered through a 200 μm polyethylene mesh. The isolated myocytes were stored in "KB medium" at room temperature before experiments, and used within 12 hours.

(2) Cell dimensions

Observation of a typical sample of the KB medium containing the isolated cells reveals a mixture of cell debris, rounded cells, and rod-shaped cells. The cells that were selected for experimentation were rod shaped. These cells were deemed appropriate because they would have had low and uniformly distributed resting levels of Ca^{2+}_i (Wier et al., 1987), whereas the other two types of cells, spontaneously contracting, and rounded cells would have had much higher levels of Ca^{2+}_i (Wier et al., 1987). The size of the rod-shaped cells were in the range of ~20 μm by 130 μm. Although the thickness of the cells is hard to determine, occasionally the cells get turned over on their sides (from turbulence created by superfusion) and the thickness can be ascertained. The measurements from these cells indicate the thickness is in the 10-15 μm range.

(3) Composition of solutions for myocyte isolation

Physiological salt (PS) solution (in mM): 140 NaCl, 5.4 KCl, 1.8 $CaCl_2$, 1.0 $MgCl_2$, 10 N-2-hydroxyethylpiperazine-N'-2-ethanesulfonic acid (HEPES), 10 glucose (pH 7.4 with NaOH).

Ca^{2+}-free solution (in mM): 125 NaCl, 4.6 KCl, 1.15 $MgCl_2$, 20 taurine, 20 glucose, and 5 HEPES (pH 7.4 with NaOH).

KB solution (in mM): 30 KCl, 80 KOH, 30 KH_2PO_4, 50 glutamic acid, 3 $MgSO_4$, 20 taurine, 10 glucose, 0.5 ethylene glycol-bis(b-aminoethyl ether)-N,N,N',N'-tetraacetic acid (EGTA), and 10 HEPES (pH 7.4 with KOH).

SECTION B. ELECTROPHYSIOLOGICAL RECORDING, AND
ANALYSIS:

(1) Electrophysiological recording

Experiments were performed using the whole-cell configuration of the patch clamp technique (Hamill et al., 1981) to record L-type Ca^{2+} currents in single ventricular myocytes. Pipettes were pulled from thick-walled borosilicate glass capillaries. The outer diameter of the glass capillaries was ~2.0 mm and the inner diameter ~1.25 mm (H15/10/137, Jencon's Scientific, Bedfordshire, UK). The pipettes were made daily using a 2-stage pulling technique (Corey and Stevens 1983), and were neither heat polished nor treated with surface coating agents. The quality of the pipettes was checked by using a Carl Zeiss microscope at 100X magnification. Only unbroken tips with inner diameters between 1.5-2.5 μm were selected. The pipette resistance was typically between 1.5 - 3 MΩ when immersed in PS solution.

For experimental recordings, isolated cells were transferred into a superfusion chamber positioned on top of an inverted microscope stage (Olympus IMT-2). Once the myocytes had adhered to the glass bottom of the chamber, they were superfused with PS solution; after 5 minutes, the superfusate was changed to K^+-free PS solution (KCl replaced by CsCl). The cells selected for electrical recordings were quiescent, rod-shaped, and appeared relaxed with well-defined striations. These cells were deemed appropriate because they would have had low and uniformly distributed resting levels of Ca^{2+}_i (Wier et al. 1987).

To patch clamp a cell, the first step was to apply a light positive pressure (applied orally via a plastic tube) to the pipette tip (this was done to prevent external debris from attaching to and clogging the tip). Next, using the micro-manipulators, the top surface of the cell was lightly touched with the pipette tip. The positive pressure was released causing a seal to form. Slight negative pressure was sometimes provided at this point if the seal was slow to develop. The holding potential was changed to -80 mV. After a giga-ohm seal had been formed, a quick but strong suction was applied to rupture the patch to provide access to the cell's interior. After giga-seal formation and patch breakthrough, cells were dialyzed via the patch pipette with a K^+-free solution. Continuous voltage clamp was applied with a single electrode with an EPC9 amplifier (Heka, Lambrecht/Pfalz, Germany) using the whole-cell configuration of the patch clamp technique. $I_{Ca,L}$ was elicited by step depolarizations from -80 to $+10$ mV applied at 0.03 Hz. Na^+ current was minimized by 50-ms prepulses to -40 mV and the presence of 100 μM Tetrodotoxin or 0.2 mM 4,4'-diisothiocyanatostilbene-2,2'-disulfonic acid (Liu et al., 1998) in the superfusate. Cell capacitance was monitored and updated with each depolarizing pulse. Current was recorded at 2-10 kHz bandwidth using Pulse (version 8.21, Instrutech Corp., Elmont, NY) and analyzed using PulseFit (version 8.21, Instrutech Corp., Elmont, NY), on an IBM PC. All experiments were performed at 22 $\pm$ 1 C°.

(2) Series resistance and capacitance

In the whole-cell voltage clamp recording, the series resistance (R_s) is a measure of the resistance of the pipette itself and the access resistance between the pipette and the cell interior. The magnitude of the resistance can limit the quality of the voltage control of the patch. A large R_s can slow the charging of the cell membrane capacitance because it impedes the flow of the capacitative charging currents when a voltage step is applied to the pipette electrode. The time constant of charging is represented by the equation: $\tau = R_s \times C_m$, where C_m is the membrane capacitance. A long time constant may limit the quality of current recordings of fast voltage-activated currents. Another hindrance of a large R_s is the loss of voltage control when a large current flows. The major determinant of the magnitude of the R_s is the size of the pipette tip and the quality of the patch break. In these experiments the R_s was typically 2 times that of the resistance of the pipette alone. Although it is more desirable to use a larger pipette to achieve a smaller resistance, the trade-off is that it becomes increasingly more difficult to seal and patch with larger pipette tips. The majority of the R_s's were between 4-6 $M\Omega$ in these experiments, and sometimes the R_s increased during the experiments; in these circumstances the experiment was aborted if the R_s reached 8 $M\Omega$ or higher.

The cell membrane capacitance (C_m) is a good indicator of cell size, the measured C_m in my experiments were generally between 90 to 150 pF. The value of C_m is derived from the change in total charge (ΔQ) that is displaced during a step voltage potential (ΔV), according the following equation $C_m = \Delta Q/\Delta V$. The cell capacitance is

50

used to standardize the current amplitudes, making it possible to compare the magnitude of the current from cells of different sizes. The units of these measurements are pA/pF.

(3) $I_{Ca,L}$ Measurement

$I_{Ca,L}$ was recorded from guinea pig ventricular myocytes superfused with K^+-free Tyrode's solution and dialyzed with K^+-free internal solution. The holding potential was -80 mV and 50 ms prepulses to -40 mV were applied prior to all test pulses. This combination of solution and pulse protocol were used to minimize cation movements through ion channels, pumps, and exchangers: (i) Cs^+ was substituted for K^+ in both external and internal solutions to eliminate the effects of K^+ as a charge carrier through K^+ channels; (ii) Na^+ current and T-type Ca^{2+} currents were minimized by the prepulse to -40 mV; (iii) Na^+-K+ pump current was abolished by the K^+-free solutions; and (iv) Na^+-Ca^{2+} exchange current was minimized by a low free-Ca^{2+} dialysate adjusted with Ca^{2+} buffers. The same external solution was used for all experiments. $I_{Ca,L}$ amplitude was measured as the peak inward current with reference to zero current; it was readily blocked by the L-type Ca^{2+}-channel blocker Cd^{2+}. Over 95% of $I_{Ca,L}$ was blocked by the addition of 0.2 mM Cd^{2+} (e.g. You et al., 1997), suggesting that most of the currents I measured went through L-type Ca^{2+}-channels.

The current voltage relations were measured after 30 minutes of dialysis. The $I_{Ca,L}$ was elicited every 10 seconds by step depolarizations from -80 mV to -40 mV for 50 ms then to test potentials for 1500 ms. The initial test potential was -40 mV and increased by 10 mV increments to +80 mV. The V_{max} of each current voltage relation

was determined by B-spline approximation (Microcal origin 6.0, Originlab Corporation, Northampton, MA). The V_{max} values shown on Figures 4,7 and 10 represent the average values of the B-spline approximations.

(4) Effects of run-down

As described in the introduction, run-down refers to the reduction in I_{CaL} during the course of an experiment. The complexity of this phenomenon is further complicated by the effect of cell dialysis in the early stages of the experiments. Research by Pusch and Neher (1988) indicate that the rate of dialysis of a certain molecule is dependent on its molecular mass (m), the access resistance of the pipette (R_A), and the volume of the cell (Vol). They incorporated these factors into an empirical equation to estimate the time constant (τ) for the dialysis of constituents from the pipette into the cell cytoplasm:

$$\tau = 0.6 \times R_A \times m^{1/3} \times Vol \times 1897^{-1},$$

the unit of τ is in seconds when R_A is in MΩ and Vol is in μm^3. Pusch and Neher (1988) indicated that the R_A is generally higher than the pipette tip resistance, and the factor 0.6 has a standard deviation of 0.17; in addition, deviations are likely in unusually shaped non-spherical cells. In consideration of these factors, I calculated the τ for the dialysis of Ca^{2+}, Mg^{2+}, ATP, BAPTA, and EGTA into an average cell with dimensions 20μm × 10μm × 130μm and an access resistance of 5 MΩ. The calculated τ values are Mg^{2+} ~119s, Ca^{2+} ~141s, BAPTA ~320s, EGTA ~298s, and ATP ~327s. The calculated results indicate that it takes at least 5 minutes for sufficient dialysis of large molecules such as BAPTA and ATP to occur, and for these reasons it is difficult

to interpret results before the first 10 minutes of cell dialysis. However, by 10 minutes the dialysis of most of the compounds should be complete, therefore the currents recorded after this time should reflect both the regulatory effects of Mg^{2+}_i and run-down. After, 15 to 20 minutes of cell dialysis, the $I_{Ca,L}$ currents were by and large stable and declined only minimally for the remainder of the experiments. Because of these factors, the comparison of effects is usually made from currents that are recorded after 30 minutes of cell dialysis, which I postulate at this point to be steady state condition (because the current amplitudes are generally very stable at this point). Although Mg^{2+}_i could affect run-down, these experiments are not however designed to study it. As such I hypothesize that the density of the currents recorded after 20 minutes is the final outcome of Mg^{2+}'s regulatory effect, therefore I do not try to discriminate between Mg^{2+}'s effect on run-down and that of phosphorylation.

SECTION C. COMPOSITION OF EXPERIMENTAL SOLUTIONS:

(1) Extra-cellular solutions

K^+-free PS solution (in mM) 140 NaCl, 5.4 CsCl 1.8 $CaCl_2$, 1.0 $MgCl_2$, 10 N-2-hydroxyethylpiperazine-N'-2-ethanesulfonic acid (HEPES), 10 glucose (pH 7.4 with NaOH). This solution was used for all experiments.

Attributes of the drugs used:

(i)   Forskolin (FSK) (Calbiochem) is a compound extracted from the roots of the *Coleus forskohlii*, and is a direct activator of adenylyl cyclase (Seamon and Daly 1986). FSK was added to K^+-free PS solution from 10 mM stock solution in dimethyl sulfoxide (DMSO), (Sigma). The final working concentration of FSK was 10 μM, and the final DMSO concentration was ~0.1% (v/v) in the experimental solutions.

(ii)   Isoproterenol (ISO) (a.k.a. isoprenaline; Calbiochem) is a synthetic non-specific β-receptor agonist, and was added to K^+-free PS solution from 1 mM stock solution. The final working concentration was 3 μM ISO.

(iii)   3-isobutyl-1-methylxanthine (IBMX) (Sigma) is a broad spectrum phosphodiesterase inhibitor (Beavo and Reifsnyder 1990). The IBMX was dissolved in DMSO to yield a stock concentration of 20 mM. The stock solution was added to K^+-free PS solution, to produce a final working concentration of 50 μM IBMX, and ~0.25% (v/v) DMSO.

(iv)   K252a (Calbiochem) is a non-hydrolyzable ATP analogue, and is used as a broad spectrum protein kinase inhibitor in this study. Its effectiveness as a cAMP

53

dependent kinase (PKA) inhibitor was ascertained by performing a positive control test with FSK and IBMX. These tests indicated that 10 μM of K252a was sufficient to block $I_{Ca,L}$ stimulation by FSK (3 μM) and IBMX (50 μM). The experiments involving K252a are shown in Figures 6-8, the cells in these experiments were preincubated for 10 minutes prior to patching and had continuous superfusion for the duration of the experiment with 10 μM K252a.

To enhance dissolution, most of the solutions were sonicated (Elma Transonic sonicator, Mandel Scientific). For all external solutions the final DMSO concentration was less than 0.25%. Experiments previously performed in the Pelzer lab showed that DMSO at this level and as high as 1.2% vol/vol would have no noticeable side effects on the $I_{Ca,L}$ (Kaspar and Pelzer 1995).

(2) Internal solutions

Dialysates (pipette solutions): after giga-seal formation and patch breakthrough, cells were dialyzed via the patch pipette with a K^+-free solution containing (in mM) 50 CsCl, 110 Cs-aspartate, 10 HEPES, 10 BAPTA, 4 NaATP, (pH 7.2 with CsOH). Free Ca^{2+} (180 nM) and free Mg^{2+} were adjusted to the desired concentrations by adding appropriate amounts of $MgCl_2$ and $CaCl_2$ (free Ca^{2+} and free Mg^{2+} calculated after Schoenmakers and colleagues, 1992). To obtain 1 μM free Mg^{2+} a total of > 30 μM Mg^{2+} was required, most of which is bound to ATP. All experiments used the dialysate solution described above except for the experiments shown on Figures 9-11. These

experiments used a similar dialysate solution but with 20 BAPTA, 20 EGTA, and with either 90nM or 180 nM free Ca^{2+}.

Reports by Backx et al., 1991 and O'Rourke et al., 1992, indicated that magnesium-adenosine triphosphate complexes ($MgATP^{2-}$) may stimulate the L-type Ca^{2+}-channel independent of PKA phosphorylation. According to their 1992 paper, O'Rourke and colleagues indicated that elevating the Mg^{2+} level to ~58 μM in the presence of ATP can stimulate $I_{Ca,L}$. Therefore it was important for me to know the level of $MgATP^{2-}$ in the dialysate solutions. Except for 1 μM Mg^{2+}_i, I feel that the level of $MgATP^{2-}$ in the pipettes does not play a major factor in the interpretation of my results; the reason being that the level of $MgATP^{2-}$ in my internal solutions, even at 10 and 17μM free Mg^{2+}, is 5 and 9 times of the amount required for stimulation via direct $MgATP^{2-}$ interaction with the L-type Ca^{2+}-channel respectively. As shown in Table 6-8, even at 1 μM free Mg^{2+}, the level of $MgATP^{2-}$ is ~31 μM. Although I am unsure if this is enough for direct $MgATP^{2-}$ stimulation, this level was sufficient to fulfill the requirements for phosphorylation in my experiments (see Figure 15).

Table 6: Amount of MgATP^{2-} corresponding to the free Mg^{2+} levels in the dialysate solutions. The ATP concentration is 4 mM, BAPTA is 10 mM, free Ca^{2+} is 180 nM, pH 7.2, temperature 22° C, and ionic strength is 0.160 mM.

Free Mg^{2+}	MgATP^{2-}	Total MgCl
1 μM	30.9 μM	31.1 μM
10 μM	288 μM	300 μM
17 μM	468 μM	488 μM
30 μM	758 μM	793 μM
80 μM	1.54 mM	1.63 mM
100 μM	1.75 mM	1.87 mM
300 μM	2.80 mM	3.15 mM
500 μM	3.18 mM	3.76 mM
1 mM	3.54 mM	4.70 mM
3 mM	3.84 mM	7.29 mM
5 mM	3.90 mM	9.64 mM
10 mM	3.95 mM	15.3 mM

Table 7: Amount of MgATP^{2-} corresponding to the free Mg^{2+} levels in the dialysate solutions. The ATP concentration is 4 mM, BAPTA is 10 mM, free Ca^{2+} is 180 nM, pH 7.2, temperature 22° C, and ionic strength is 0.160 mM.

Free Mg^{2+}	MgATP^{2-}	Total MgCl
1 μM	31.0 μM	32.7 μM
17 μM	467 μM	497 μM
30 μM	758 μM	810 μM
100 μM	1.75 mM	1.92 mM
1 mM	3.54 mM	5.25 mM
5mM	3.89 mM	12.2 mM

Table 8: Amount of MgATP^{2-} corresponding to the free Mg^{2+} levels in the dialysate solutions. The ATP concentration is 4 mM, BAPTA is 10 mM, free Ca^{2+} is 90 nM, pH 7.2, temperature 22° C, and ionic strength is 0.160 mM.

Free Mg^{2+}	MgATP^{2-}	Total MgCl
1 μM	30.9 μM	32.8 μM
17 μM	468 μM	501 μM
30 μM	758 μM	812 μM
100 μM	1.75 mM	1.94 mM
1 mM	3.54 mM	5.43 mM
5mM	3.90 mM	12.9 mM

All biochemicals were reagent to analytical grade from Calbiochem (San Diego, CA), Research Biochemicals International (Natick, MA), and Sigma (St. Louis, MO).

(3) Switching of solutions during experiments

Solution exchange in the experimental chamber was regulated by a 5-way valve connected to 5 tubes. The tubes were connected to beakers of solutions situated 55 cm above the experimental chamber. To minimize the lag time between solution switches, the tubes were thoroughly siphoned and filled with the experiment solutions prior to the experiments. The delay time between switches was generally in the 20-40 second range, and this is reflected by the time it takes to observe a stimulatory response by switching to an isoproterenol PS solution from a PS solution alone.

SECTION D. STATISTICS:

Statistical analysis was carried out using the Microcal origin version 6.0 software package. Except for the time courses, which show the current amplitude recorded during the dialysis of one cell, all other data points represent the average values for all cells recorded under that condition. The error bars represent the standard error of the mean (SEM). In the results section, data values will be expressed as mean ± SEM.

For most of the experimental conditions the sample size has an n-value of ~5, a small number which makes it hard to determine whether or not the sample comes from a population that follows a Gaussian distribution. The determination of the distribution is important because it would dictate whether a parametric or non-parametric test should be used. Although it is impossible to determine if the samples come from a population that follows a Gaussian distribution with such low n-values, I chose the parametric mainly because there are no better alternatives. The assumptions and limitations of the tests used in this study are discussed below. The statistical significance criterion was set at $p<0.05$. In the results section, the actual p value is expressed to three decimal places, if the value is smaller it will be expressed as < 0.001. In the discussion section, the actual p values any references to significant differences are assumed to meet the criterion $p<0.05$ and will already be shown in the results section.

(1) One-way analysis of variance (ANOVA) for two independent groups

Used in Figure 4B and Figure 7B: to compare the difference in V_{max} values between basal condition and K252a treated cells at 17 μM Mg^{2+}_i.

Used in Figure 5: to determine if the values recorded from cells under basal condition differed statistically from those dialyzed with 0.2 mM GTP.

Used in Figure 11: to determine if the values recorded from cells with 90 nM Ca^{2+}_i differed statistically from those dialyzed with 180 nM Ca^{2+}_i.

Used in Figure 17: to determine if there was a statistical difference between $I_{Ca,L}$ amplitudes recorded from cells treated with FSK alone and cells treated with FSK and IBMX, at 5 mM Mg^{2+}_i.

The assumptions of these tests were:

1. The samples selected are a good representation of the larger populations.

2. The samples were obtained independently. In the case where the two samples represent before and after measurements, then the paired t-test was used.

3. The standard deviation of the two populations is similar.

4. The data are obtained from larger populations that approximate a Gaussian distribution. This assumption is important especially since I am dealing with small samples (small n values). Generally, this test is robust to deviations from the Gaussian distribution if large samples are being compared, however for small samples the tests are not robust. Nevertheless, I did not chose the alternative to this test, which would be a nonparametric test, such as a Mann-Whitney test (which assumes the population does

not follow a Gaussian distribution), because it lacks statistical power with small samples and the P values tend to be too high.

(2) One-way ANOVA for more than two groups

Used in Figure 16C: to determine if there was a significant difference in the degree of stimulation by ISO by the varying levels of Mg^{2+}_i .

Used in Figure 18 and 19: to compare the inactivation constants under the various conditions at each Mg^{2+}_i concentration. The null hypothesis for these tests is the inactivation constants are the same for cells dialyzed with the same Mg^{2+}_i concentration regardless of the drug treatment, and the alternative hypothesis is that one or more of the populations differ from the rest. The tests were performed by comparing the different conditions in both figures in one test for each Mg^{2+}_i concentration. In the instance where the null hypothesis is true, this test attributes the differences among the sample values to random scatter around the same population mean. Multiple t-tests were not chosen because of limitations inherent in interpreting the P values. As more groups are added to the study the chance of observing a significant P value by chance would also increase. For example even if I were to perform 21 different t-tests to compare all seven different conditions at 1 μM Mg^{2+}, the chance of randomly observing a P value less than 0.05 would increase significantly. In fact the probability of obtaining one or more P values less than 0.05 by chance would increase to ~64%.

The assumptions of these tests were:

1. The samples selected are a good representation of the larger populations.

2. The samples were obtained independently.

3. The standard deviation of the two populations is similar.

4. The data are obtained from larger populations that approximate a Gaussian distribution.

In these tests the P value was set at 0.05. Since all the results from these tests revealed P values that were much higher than 0.05, no other tests were performed to determine which group was significantly different than the others.

(3) Paired t-tests

Used in Figure 15: to determine if the addition of the drugs, ISO, IBMX, and FSK significantly altered the $I_{Ca,L}$ amplitude from basal condition.

In this case, where the two samples being compared represent before and after measurements, the paired t-test was used.

The assumptions of the paired t-tests were:

1. The pairs must be randomly selected and are representative of a larger population.

2. The samples are matched from measurements of basal and drug applications from the same cell.

3. The pairs are selected independently of the others.

4. The distribution of the differences approximates a Gaussian distribution.

In these tests the P value was set at 0.05.

III. RESULTS

The results of this study are organized into three main sections. The first section (A) deals with the experiments designed to assess whether effects of Mg^{2+}_i on phosphorylation and dephosphorylation processes contribute to the Mg^{2+}_i dependence of $I_{Ca,L}$. These experimental results are presented under three subheadings according to the three different experimental conditions used here: (1) Mg^{2+}_i dependence of $I_{Ca,L}$ under basal conditions; (2) Mg^{2+}_i dependence of $I_{Ca,L}$ under general protein phosphorylation inhibition conditions; and (3) Mg^{2+}_i dependence of $I_{Ca,L}$ under cAMP-stimulated conditions. The second section (B) is concerned with the requirements of Mg^{2+}_i for $I_{Ca,L}$ stimulation via: β-adrenergic receptor stimulation with ISO; direct adenylyl cyclase stimulation with FSK; and inhibition of PDE with IBMX. The third section (C) will consider the effects of Mg^{2+}_i on Ca^{2+}-channel inactivation.

SECTION A. EFFECTS OF PHOSPHORYLATION/DEPHOSPHORYLATION ON Mg^{2+}_i REGULATION OF $I_{Ca,L}$:

(1) Mg^{2+}_i dependence of basal $I_{Ca,L}$ (Figures 3-5)

Figure 3 shows recordings of $I_{Ca,L}$ (left panel) and time courses of $I_{Ca,L}$ density (right panel) during cell dialysis with solution containing five different concentrations of free Mg^{2+} ranging from 1 μM to 10 mM. $I_{Ca,L}$ density shortly after patch breakthrough was usually between -5 and -6 pA/pF. With dialysate concentrations of

free Mg^{2+} close to the cytoplasmic Mg^{2+}_i in isolated guinea pig ventricular myocytes

($\sim$1 mM, Buri et al.,1993), $I_{Ca,L}$ declined over time. This phenomenon, known as run-down, is commonly observed during whole cell recordings of $I_{Ca,L}$ using the patch clamp technique and is likely caused by a combination of factors resulting from the change in the intracellular environment during cell dialysis (McDonald et al., 1994). Typically $I_{Ca,L}$ run-down was most noticeable early in dialysis. In myocytes dialyzed with 1 mM Mg^{2+} solution (O), $I_{Ca,L}$ declined by $\sim$25% within 10 minutes, which accounted for 95% of the run-down. When higher concentrations of Mg^{2+}_i were used, $I_{Ca,L}$ declined faster and to a larger extent. For example, the $I_{Ca,L}$ decreased by almost 40% within the first 5 minutes of cell dialysis with 10 mM Mg^{2+}_i solution ($\triangle$).

$I_{Ca,L}$ time courses were however quite different when the cells were dialyzed with low Mg^{2+}_i concentrations ($\leq$100 μM). Typically, an increase in $I_{Ca,L}$ density was observed for the first 5 - 8 minutes after patch breakthrough, which was followed by a long period of run-down before the current finally stabilized at $\geq$20 minutes. The increase in $I_{Ca,L}$ was most pronounced with solution containing $\sim$20 μM Mg^{2+}_i. In the myocytes shown (Figure 3), $I_{Ca,L}$ density recorded after 5 minutes of dialysis with 1 μM (∇), 17 μM ($\Diamond$), and 100 μM ($\square$) Mg^{2+} solution exceeded that in 1 mM-Mg^{2+} dialysate (O) by 2.7, 3.2, and 1.6 times, respectively (compare sample currents 2). With 1 μM (∇) and 100 μM ($\square$) Mg^{2+}_i solution the initial increase in $I_{Ca,L}$ was completely occluded by the following run-down. In contrast, $I_{Ca,L}$ with 17 μM dialysate Mg^{2+} ($\Diamond$) stabilized after >20 minutes at a significantly elevated level (compare sample currents 4 and 5 on Figure 3, for a summary see Figure 5).

These time courses show that $Mg^{2+}{}_i$ significantly affects $I_{Ca,L}$ density in guinea

pig ventricular myocytes. Furthermore, $Mg^{2+}{}_i$ alters the extent and duration of $I_{Ca,L}$ run-

down that occurs during dialysis.

I next examined possible effects of $Mg^{2+}{}_i$ on the voltage dependence of $I_{Ca,L}$.

Mg^{2+} is a weak blocker of the Ca^{2+} channel (Kuo and Hess, 1993) and, being the major

divalent cation present in the cytoplasm, might also affect the potential drop across the

membrane by shielding negative charges fixed at the cytoplasmic side of the membrane.

Figure 4 shows example currents recorded at -10 mV, +10 mV and +30 mV (left panel)

and corresponding $I_{Ca,L}$-voltage relations (right panel) at five different $Mg^{2+}{}_i$

concentrations ranging from 1 µM (Figure 4A) to 10 mM (Figure 4E). The data were

collected after extensive cell dialysis (≥ 28 minutes), when $I_{Ca,L}$ had reached a steady

state (see Figure 3). Typical bell-shaped $I_{Ca,L}$-voltage relations were observed at all

$Mg^{2+}{}_i$. However at concentrations > 100 µM increasing $Mg^{2+}{}_i$ caused a negative shift of

the potential eliciting maximal inward current (V_{max}, indicated by arrows) from V_{max} =

13 ± 1 mV with 100 µM $Mg^{2+}{}_i$ (n = 5, Figure 4C) to $V_{max} = 1 \pm 1$ mV with 10 mM

$Mg^{2+}{}_i$ (n=4, Figure 4E). $I_{Ca,L}$ density at V_{max} was similar with 1 µM, 100 µM and 1 mM

$Mg^{2+}{}_i$ (compare Figures 4A, C, D) and somewhat (~25%) smaller with 10 mM $Mg^{2+}{}_i$

(Figure 4E). With 17 µM $Mg^{2+}{}_i$ (Figure 4B), $I_{Ca,L}$ was considerably larger in size and

the $I_{Ca,L}$-voltage relation peaked at a less positive potential than with 1 µM $Mg^{2+}{}_i$

(Figure 4A) or 100 µM $Mg^{2+}{}_i$ (Figure 4C). This negative shift appears to be unrelated

to the leftward shift of V_{max} at higher $Mg^{2+}{}_i$ and seems to be associated with the

mechanism causing the elevation of $I_{Ca,L}$ (see below).

The information summarized in Figure 5 illustrates the Mg^{2+}_i dependence of

basal $I_{Ca,L}$. All $I_{Ca,L}$ densities shown are average values measured from 5 to 13

myocytes. Figure 5A depicts changes in the relation between $I_{Ca,L}$ at +10 mV and Mg^{2+}_i

during cell dialysis. Shown are $I_{Ca,L}$ densities measured after 10 minutes of cell dialysis

(●) (a time when dialysis with the low molecular weight compounds contained in my

pipette solution can be expected to be complete), and $I_{Ca,L}$ densities measured after ≥ 28

minutes (■) (when $I_{Ca,L}$ had reached a steady state at all Mg^{2+}_i) (see Figure 3). While at

millimolar Mg^{2+}_i levels, $I_{Ca,L}$ densities were similar at both times and decreased with

increasing Mg^{2+}_i; at sub-millimolar concentrations cell dialysis altered the Mg^{2+}_i

dependence of $I_{Ca,L}$ significantly. Ten minutes after patch breakthrough (●) $I_{Ca,L}$

density with 1 μM Mg^{2+}_i was elevated (1.8 times larger than with 1 mM Mg^{2+}_i),

increased to a maximum at 17 μM Mg^{2+}_i and decreased steeply at higher Mg^{2+}_i

suggesting that Mg^{2+}_i exerts both stimulatory and inhibitory actions on $I_{Ca,L}$. After ≥ 28

minutes of dialysis (■) $I_{Ca,L}$ densities in 1 μM Mg^{2+}_i and 1 mM Mg^{2+}_i were similar, and

bimodal changes of $I_{Ca,L}$ density occurred only in a small concentration range around 20

μM Mg^{2+}_i. Apparently, much of the inhibitory action of Mg^{2+}_i had been masked by the

decline of $I_{Ca,L}$ at low Mg^{2+}_i with progressing cell dialysis (see Figure 3). The

stimulatory effect of Mg^{2+}_i appeared to be little altered by cell dialysis. After 10

minutes of dialysis, $I_{Ca,L}$ density at 17 μM Mg^{2+}_i exceeded that at 1 μM Mg^{2+}_i by 3.0 ±

1.0 pA/pF (n = 13 for $I_{Ca,L}$ at 17 μM Mg^{2+}_i, and n = 7 for $I_{Ca,L}$ at 1 μM Mg^{2+}_i); after ≥ 28

minutes of dialysis the elevation in $I_{Ca,L}$ density was of similar size (3.8 ± 0.7 pA/pF (n

= 6 for $I_{Ca,L}$ in 17 μM Mg^{2+}_i, and n = 3 for $I_{Ca,L}$ in 1 μM Mg^{2+}_i)).

Both stimulatory and inhibitory effects of Mg^{2+}_i were also apparent at other test

potentials (see Figure 5B, filled symbols). The stimulatory action of Mg^{2+}_i appeared to

be reduced with increasing test potential. A comparison of the $I_{Ca,L}$ densities measured

in 1μM and 17μM Mg^{2+}_i shows that $I_{Ca,L}$ density at -10 mV increased by 3.7-fold

compared to 2.3-fold, 1.6-fold, 1.5-fold and 1.4-fold at 0, +10, +30 and +50 mV

(compare Figures 4A and 4B), respectively. Also noticeable, particularly at millimolar

Mg^{2+}_i, was the tendency of $I_{Ca,L}$ to decrease with increasing Mg^{2+}_i at positive potentials

and increase at -10 mV, which is in keeping with the Mg^{2+}_i-induced leftward shift of

$I_{Ca,L}$-voltage relations (see Figure 4).

It is worth noting that $I_{Ca,L}$ densities in GTP-containing dialysates were similar

to those which were dialyzed with my standard GTP-free pipette solution at 1mM Mg^{2+}_i

after 10 minutes (p=0.221) and after 30 minutes (p=0.763) of dialysis, but were

significantly lower at 17 μM Mg^{2+}_i for both 10 and 30 minutes (p<0.001) after dialysis

(open symbols in Figure 5A and 5B).

These data indicate that Mg^{2+}_i affects basal $I_{Ca,L}$ in a complex manner, which

comprises both stimulatory and inhibitory mechanisms. Stimulatory effects of Mg^{2+}_i

prevail at low (< 20 μM) Mg^{2+}_i levels. They appear to be enhanced at negative

potentials and are altered only slightly by cell dialysis. Inhibitory effects of Mg^{2+}_i

become predominant at Mg^{2+}_i levels > 20 μM. However, they are masked by the run-

down of $I_{Ca,L}$ as cell dialysis progresses. Furthermore, the regulatory effects of Mg^{2+}_i appear to depend on the cellular concentration of GTP.
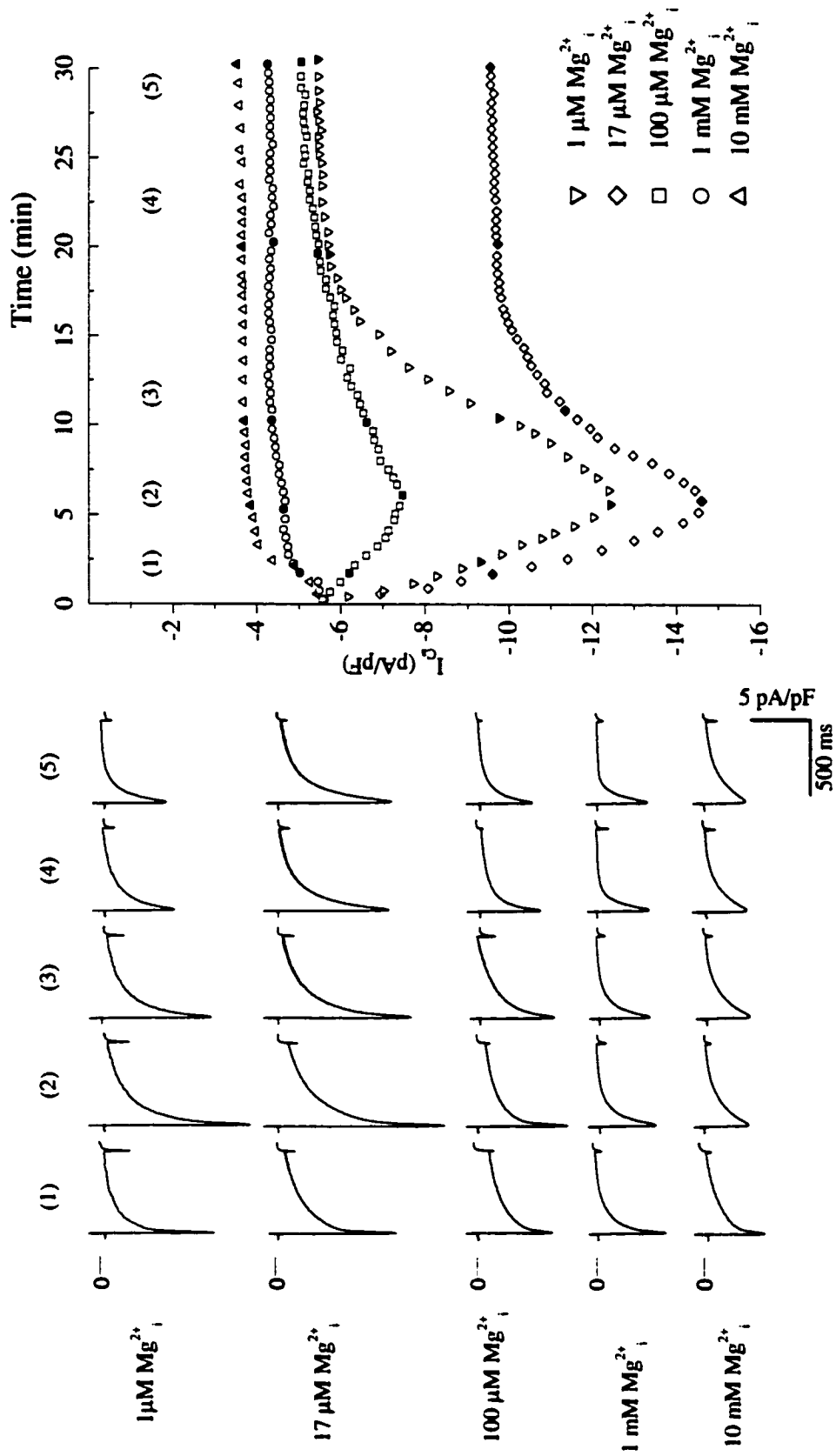
Figure 3: $I_{Ca,L}$ in guinea pig ventricular cardiomyocytes during dialysis with solution containing different concentrations of free Mg^{2+} ranging from 1 μM to 10 mM. $I_{Ca,L}$ was elicited every 30 seconds by step depolarizations from -80 to -40 mV for 50 ms then to test potential +10 mV for 500 ms. The right panel shows time diaries of $I_{Ca,L}$ density at a test potential of +10 mV. "0" time represents the moment of patch breakthrough. Filled symbols (1-5) in each time course correspond to sample currents shown on the left.
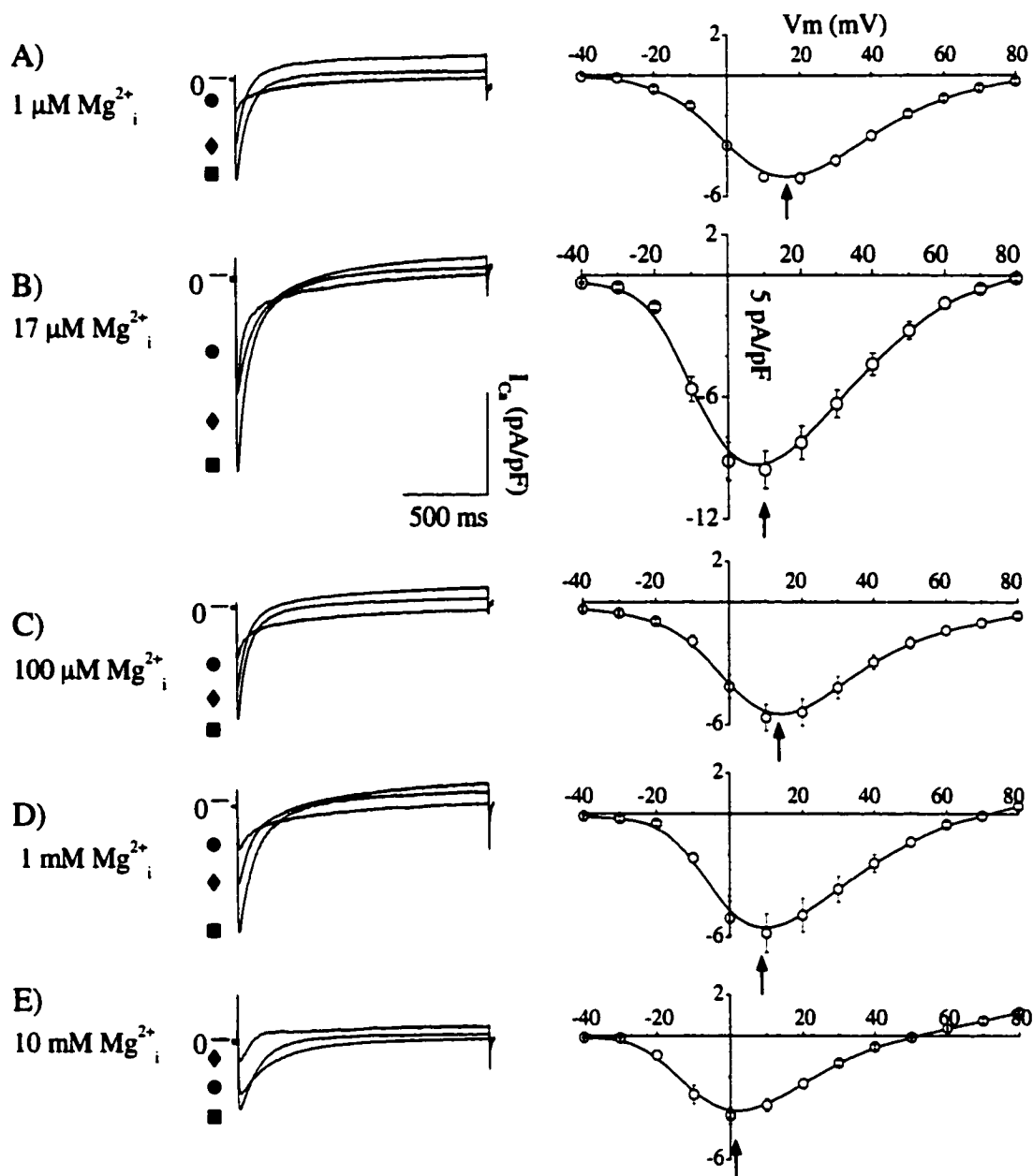
Figure 4: Voltage dependence of $I_{Ca,L}$ with different $[Mg^{2+}]_i$ ranging from 1 µM to 10 mM (1 µM (A),17 µM (B), 100 µM (C), 1 mM (D) and 10 mM (E)). The $I_{Ca,L}$ was elicited every 10 seconds by step depolarizations from -80 to -40 mV for 50 ms then to test potentials ranging from -40 mV to +80 mV for 1500 ms. The right panel shows time courses of $I_{Ca,L}$ density at a test potential of +10 mV. The left panel shows original currents recorded at test potentials of -10 mV (●), +10 mV (■) and +30 mV (◆) after > 28 minutes of cell dialysis. Corresponding complete I_{Ca}-voltage relations are shown in the right panel. Each point represents the average $I_{Ca,L}$ density measured in 3-6 cells. Where error bars are absent, they are smaller than the symbol size. Arrows indicate the average potential eliciting maximal inward current (V_{max}) obtained from Spline approximations of the $I_{Ca,L}$-voltage relations. V_{max} was 16 ± 1 mV (A), 6 ± 1 mV (B), 13 ± 1 mV (C), 8 ± 1 mV (D),and 1 ± 1 mV (E).

A)

B)
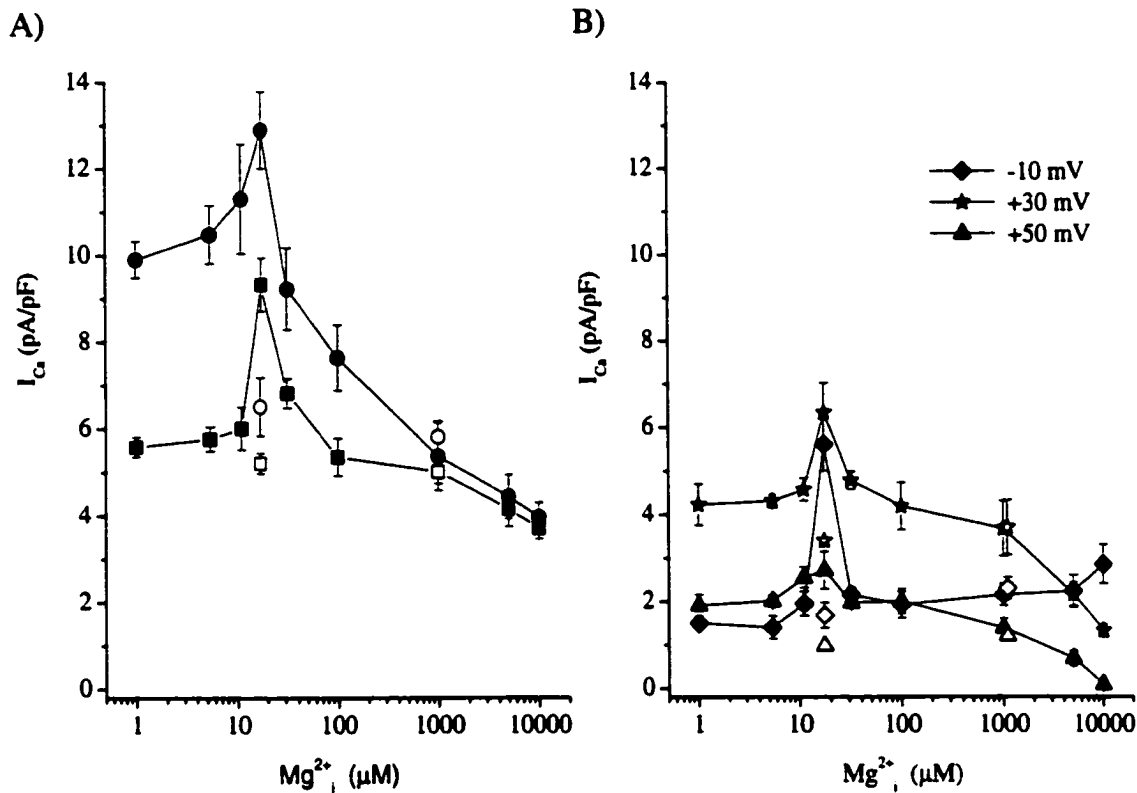
Figure 5: Concentration dependence of $I_{Ca,L}$ on free $[Mg^{2+}]_i$ after different times of cell dialysis (A),and at different test potentials (B). (A) $I_{Ca,L}$ density at a test potential of +10 mV measured after 10 minutes (●) and 30 minutes of cell dialysis (■). Points represent the mean of 4 - 13 cells.(B) $I_{Ca,L}$ density after 30 minutes of cell dialysis at test potentials of -10 mV ─◆─, +30 mV ─★─, and +50 mV ─▲─. Each point represents the mean of 3-6 cells. The open symbols represent cells that have the addition of 0.2 mM GTP in the dialysate. Where error bars are absent, they are smaller than the symbol size.

(2) Mg^{2+}_i dependence of $I_{Ca,L}$ after protein kinase inhibition (Figures 6-8)

Possible targets for interactions with Mg^{2+} are the Ca^{2+}-channel itself as well as several systems involved in the regulation of protein phosphorylation. To separate phosphorylation-related from direct effects of Mg^{2+}_i on $I_{Ca,L}$, I used the non-hydrolyzable ATP analogue K252a. This compound abolishes the enzymatic activity of a wide array of kinases including PKA, calmodulin dependent kinase II, and protein kinase C, all of which contribute to the regulation of cardiac $I_{Ca,L}$ (McDonald et al., 1994 review). Figure 6 illustrates sample $I_{Ca,L}$ records (left panel) and time courses of $I_{Ca,L}$ density (right panel) recorded from K252a-treated myocytes. Regardless of the concentration of free Mg^{2+} in the dialysate, which ranged from 1 μM (Figure 6A) to 5 mM (Figure 6D), $I_{Ca,L}$ density at a test potential of +10 mV immediately after patch breakthrough was considerably lower than under basal conditions (around -3 pA/pF) and changed little during cell dialysis.

The voltage dependence of $I_{Ca,L}$ in K252a-treated cells (Figure 7) was determined under steady state conditions after $\geq$ 28 minutes of cell dialysis. Again, all $I_{Ca,L}$-voltage relations had the typical bell shape and increasing Mg^{2+}_i from 1 μM (Figure 7A) to 5 mM (Figure 7D) caused a progressive negative shift of V_{max} (indicated by arrows in the right panel). With 17 μM Mg^{2+}_i, the V_{max} was similar to that observed with 1 μM Mg^{2+}_i (compare Figures 7A and 7B) but significantly more positive (p < 0.001) than under basal conditions (compare Figures 4B and 7B). K252a seemingly abolished the leftward shift in the voltage dependence of basal $I_{Ca,L}$ at 17 μM Mg^{2+}_i suggesting that this leftward shift requires protein kinase activity.

The information in Figure 8 summarizes the Mg^{2+}_i-dependence of $I_{Ca,L}$ in K252a-treated myocytes. $I_{Ca,L}$ densities at +10 mV were similar after 10 minutes (Figure 8A, ○) and after ≥ 28 minutes (●) of cell dialysis and were unaffected by changes in Mg^{2+}_i between 1 μM and 5 mM. $I_{Ca,L}$ at +30 mV and +50 mV (Figure 8B) declined with increasing Mg^{2+}_i; at -10 mV $I_{Ca,L}$ rose at higher Mg^{2+}_i. These changes are interpreted as the Mg^{2+}-induced negative shift of the voltage dependence of $I_{Ca,L}$ (see Figure 7).

These data show that the inhibition of protein phosphorylation with K252a reduced $I_{Ca,L}$ density and rendered the remaining current unresponsive to modulatory effects of Mg^{2+}_i. The only noticeable effect of Mg^{2+}_i on the permeation of Ca^{2+} through unphosphorylated Ca^{2+} channels is a negative shift of $I_{Ca,L}$-voltage relations at Mg^{2+}_i > 100 μM, which was most likely caused by the screening of intracellular negative surface charges by Mg^{2+}_i.

It is also worth noting that there was no detectable $I_{Ca,L}$ run-down in K252a treated cells (see Figure 6). Hence one has to assume that the run-down of $I_{Ca,L}$ under basal conditions (see Figure 3) either results from a decline in the activity of phosphorylated Ca^{2+}-channels or that the processes causing run-down involve protein kinase activity.
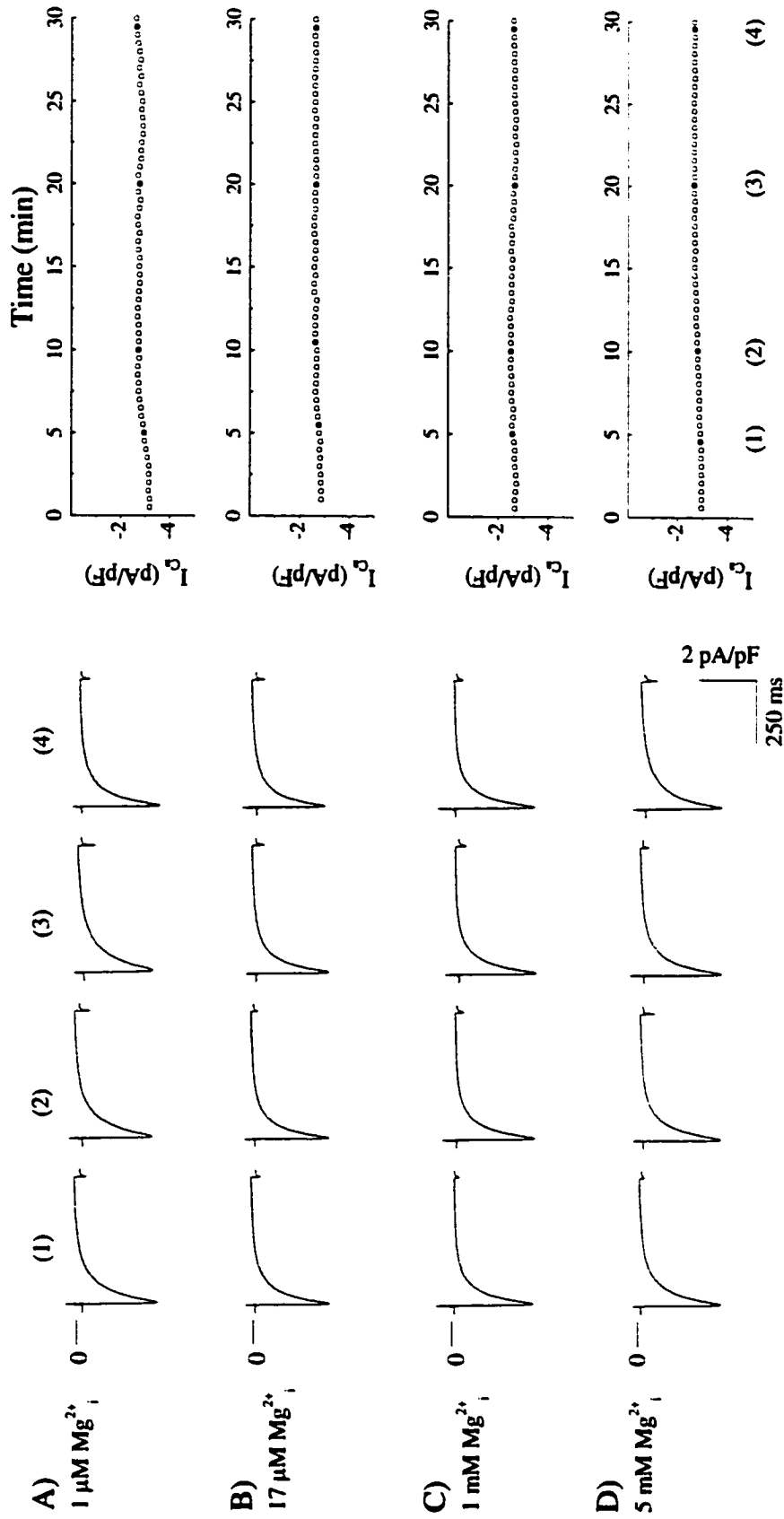
Figure 6: $I_{Ca,L}$ in K252a-treated myocytes during dialysis with solution containing 1 μM (A), 17 μM (B), 1 mM (C), and 5 mM (D) free Mg^{2+}. $I_{Ca,L}$ was elicited every 30 seconds by step depolarizations from -80 to -40 mV for 50 ms then to test potential +10 mV for 500 ms. The right panel shows time courses of $I_{Ca,L}$ density at a test potential of +10 mV. Illustrated are sample currents (left panel) and time courses of $I_{Ca,L}$ density (right panel) recorded from myocytes which were preincubated for 10-20 minutes in and subsequently superfused with 10 mM K252a solution. "0" time represents the moment of patch breakthrough and the start of cell dialysis. The filled symbols (1-4) in each time course correspond to the sample currents shown.
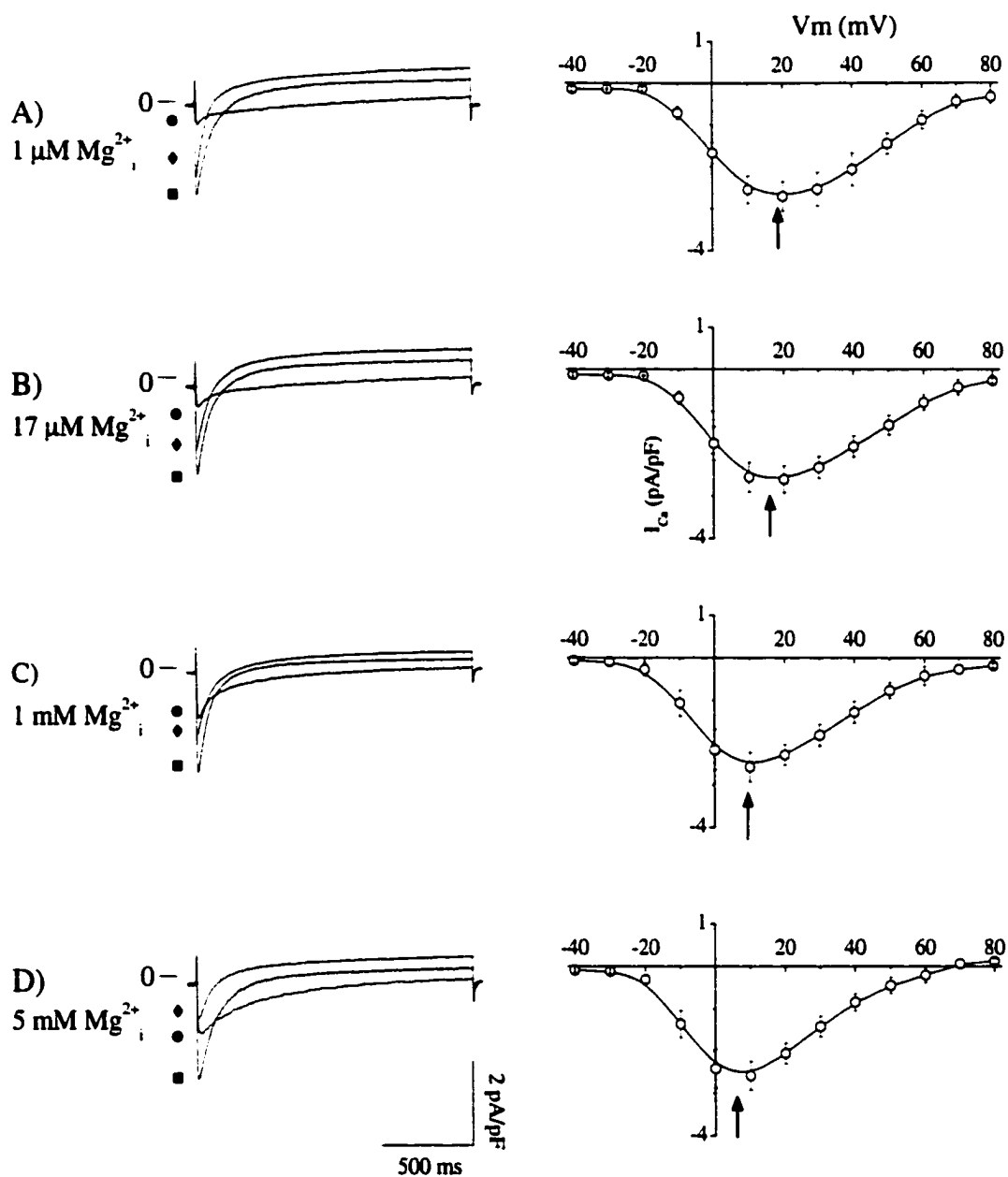
Figure 7: Voltage dependence of I_{CaL} in K252a-treated myocytes with different $[Mg^{2+}]_i$ ranging from 1 μM to 5 mM (1 μM (A), 17 μM (B), 1 mM (C), and 5 mM (D)). The I_{CaL} was elicited every 10 seconds by step depolarizations from -80 to -40 mV for 50 ms then to test potentials ranging from -40 mV to +80 mV for 1500 ms. The left panel shows original currents recorded at test potentials of -10 mV ($\bullet$), +10 mV ($\blacksquare$) and +30 mV ($\blacklozenge$) after 30 minutes of cell dialysis. Corresponding complete I_{CaL}-voltage relations are shown in the right panel. Each point represents the average I_{CaL} density measured in 3-6 cells. Where error bars are absent, they are smaller than the symbol size. Arrows indicate V_{max} which was 18 ± 2 mV (A), 17 ± 1 mV (B), 11 ± 1 mV (C), and 6 ± 1 mV (D).
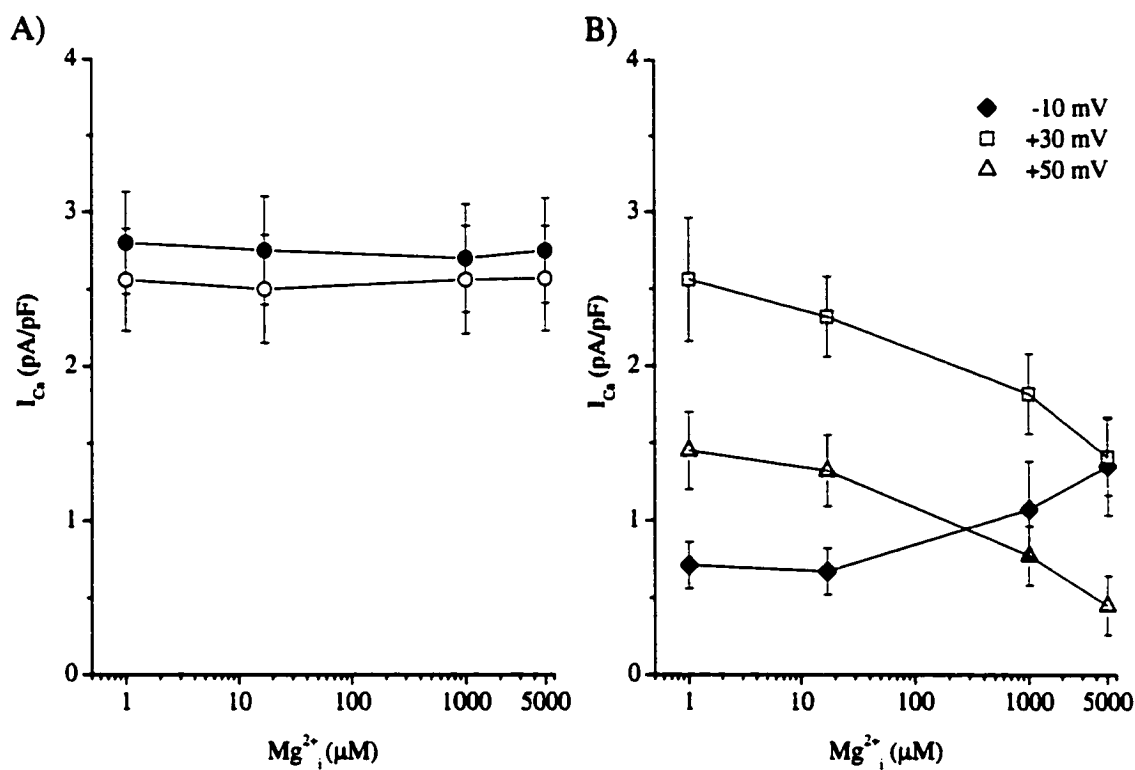
Figure 8: Concentration dependence of $I_{Ca,L}$ on $[Mg^{2+}]_i$ in K252a-treated myocytes measured after different times of cell dialysis (A) and at different test potentials (B). (A) $I_{Ca,L}$ density measured at a test potential of +10 mV after 10 minutes (●) and 30 minutes of cell dialysis (○). (B) $I_{Ca,L}$ density after 30 minutes of cell dialysis at test potentials of -10 mV (◆),+30 mV (□), and +50 mV (△). Each point represents the mean of 3-6 cells. Where error bars are absent, they are smaller than the symbol size.

(3) Effects of Mg^{2+}_i on $I_{Ca,L}$ in cAMP-loaded myocytes (Figures 9-11)

Previous experiments performed in the Pelzer lab have shown that bath application of the adenylyl cyclase activator FSK together with the PDE inhibitor IBMX elevates cAMP sufficiently to maximally stimulate the cAMP-mediated phosphorylation of Ca^{2+}-channels (You et al., 1997). Figure 9 shows typical $I_{Ca,L}$ records (left panel) and time courses of $I_{Ca,L}$ density (right panel) recorded with different concentrations of dialysate Mg^{2+}. Shortly after patch breakthrough $I_{Ca,L}$ density at +10 mV was usually in the range of -25 to -35 pA/pF. With 1 mM Mg^{2+} dialysate (see Figure 9D), typically an increase in $I_{Ca,L}$ during the first 5-7 minutes of dialysis was observed and followed by rundown that lasted for the entire 30-minute observation period. Considering that the pre-dialysis Mg^{2+}_i in guinea pig ventricular myocytes is ~1 mM, cell dialysis is unlikely to cause a significant change in Mg^{2+}_i. Hence, the assumption must be made that the initial increase in $I_{Ca,L}$ is not related to a change in Mg^{2+}_i concentration. It is more likely the initial increase in $I_{Ca,L}$ represents relief from Ca^{2+}-induced inhibition of $I_{Ca,L}$ caused by the reduction of cytoplasmic Ca^{2+} to the dialysate concentration of 90 nM, from a possibly higher pre-dialysis Ca^{2+} level. Similar $I_{Ca,L}$ time courses were seen when sub-millimolar concentrations of free Mg^{2+} were used to decrease Mg^{2+}_i (Figures 9A – 9C). However, when Mg^{2+}_i was increased to 10 mM, $I_{Ca,L}$ declined throughout the entire observation period but most noticeably during early dialysis (Figure 9E).

The voltage dependence of $I_{Ca,L}$ in cAMP-loaded myocytes is illustrated in Figure 10. Sample records of $I_{Ca,L}$ at different membrane potentials (left panel) and

$I_{Ca,L}$-voltage relations (right panel) were measured after 30 minutes of dialysis with Mg^{2+}_i levels ranging from 1 μM (Figure 10A) to 10 mM (Figure 10E). All $I_{Ca,L}$-voltage relations were bell shaped with V_{max} (indicated by arrows) clustering between -4 and +1 mV. At all Mg^{2+}_i concentrations, V_{max} was noticeably less positive than under basal conditions (see Figure 4) or in K252a-treated cells (see Figure 7). This confirms observations by others (McDonald et al., 1994 review) that cAMP-mediated phosphorylation shifts the voltage dependence of the Ca^{2+}-channel to more negative potentials.

Figure 11 summarizes the dependence of $I_{Ca,L}$ on Mg^{2+}_i in cAMP-loaded cells for two different internal Ca^{2+} concentrations. The filled symbols represent current densities recorded from cells that are dialyzed with 90 nM free Ca^{2+}, and the open symbols represent current densities recorded from cells that are dialyzed with 180 nM free Ca^{2+}. The $I_{Ca,L}$-Mg^{2+}_i relations shown in Figure 11A were determined at +10 mV after 10 minutes (circles) and 30 minutes (squares) of cell dialysis. As seen in Figure 11A, the current densities recorded with the different Ca^{2+} concentrations were very similar. At both times cAMP-upregulated $I_{Ca,L}$ was unresponsive to variations of Mg^{2+}_i between 1 μM and 1 mM; increasing Mg^{2+}_i in the millimolar range caused a noticeable reduction in $I_{Ca,L}$ density.

$I_{Ca,L}$ at -10 mV displayed a very similar dependence on Mg^{2+}_i (see Figure 11B) as currents recorded at +10 mV. At more positive test potentials a decline of $I_{Ca,L}$ density at sub-millimolar Mg^{2+}_i was noticeable, and the stimulation of cAMP-mediated

phosphorylation appears to confer considerable protection against the inhibitory effects of Mg^{2+}_i on I_{CaL} seen under basal conditions (see Figure 5).

These data demonstrate the Mg^{2+}_i dependence of I_{CaL} under basal conditions and in cAMP-loaded cells differs considerably in several respects. In cAMP-loaded cells stimulatory effects of Mg^{2+}_i were occluded, while inhibitory effects of Mg^{2+}_i occurred only at millimolar concentrations of the ion (compare Figures 5 and 11). In contrast to both basal conditions and K252a-treated cells, there was no clear effect of Mg^{2+}_i on the voltage dependence of I_{CaL} in cAMP-loaded cells.
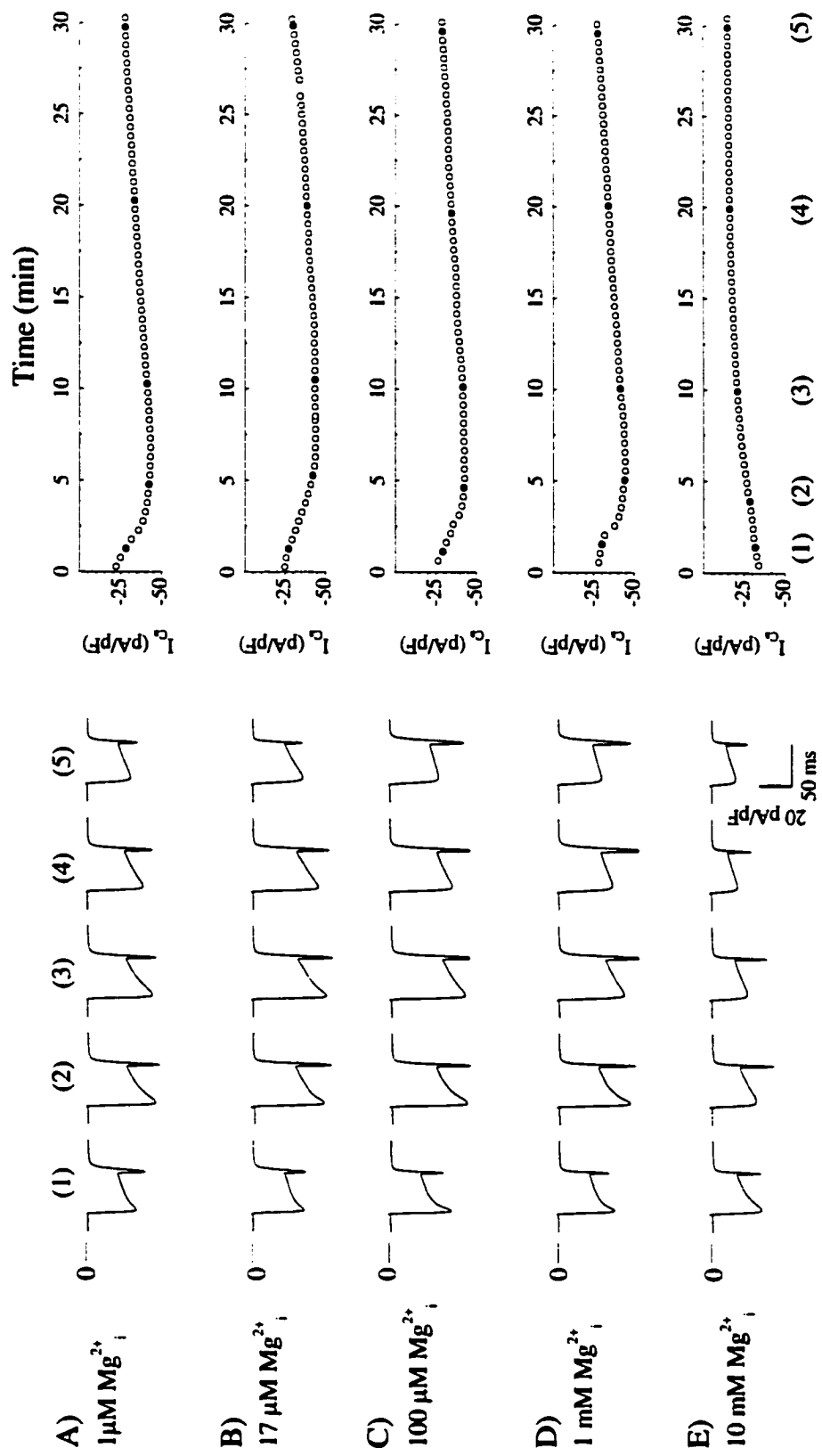
Figure 9: $I_{Ca,L}$ in cAMP-loaded myocytes during dialysis with 1 µM (A),17 µM (B), 100 µM (C), 1 mM (D) and 10 mM (E) Mg^{2+} solution. $I_{Ca,L}$ was elicited every 30 seconds by step depolarizations from -80 to -40 mV for 50 ms then to test potential +10 mV for 50 ms. The right panel shows time diaries of $I_{Ca,L}$, and the left panel shows sample currents from myocytes preincubated for 10-20 minutes in and superfused with solution containing 10 mM forskolin and 50 mM IBMX. "0" time represents the moment of patch breakthrough and the start of cell dialysis. Filled symbols (1-5) in each time course correspond to the sample currents shown on the left.
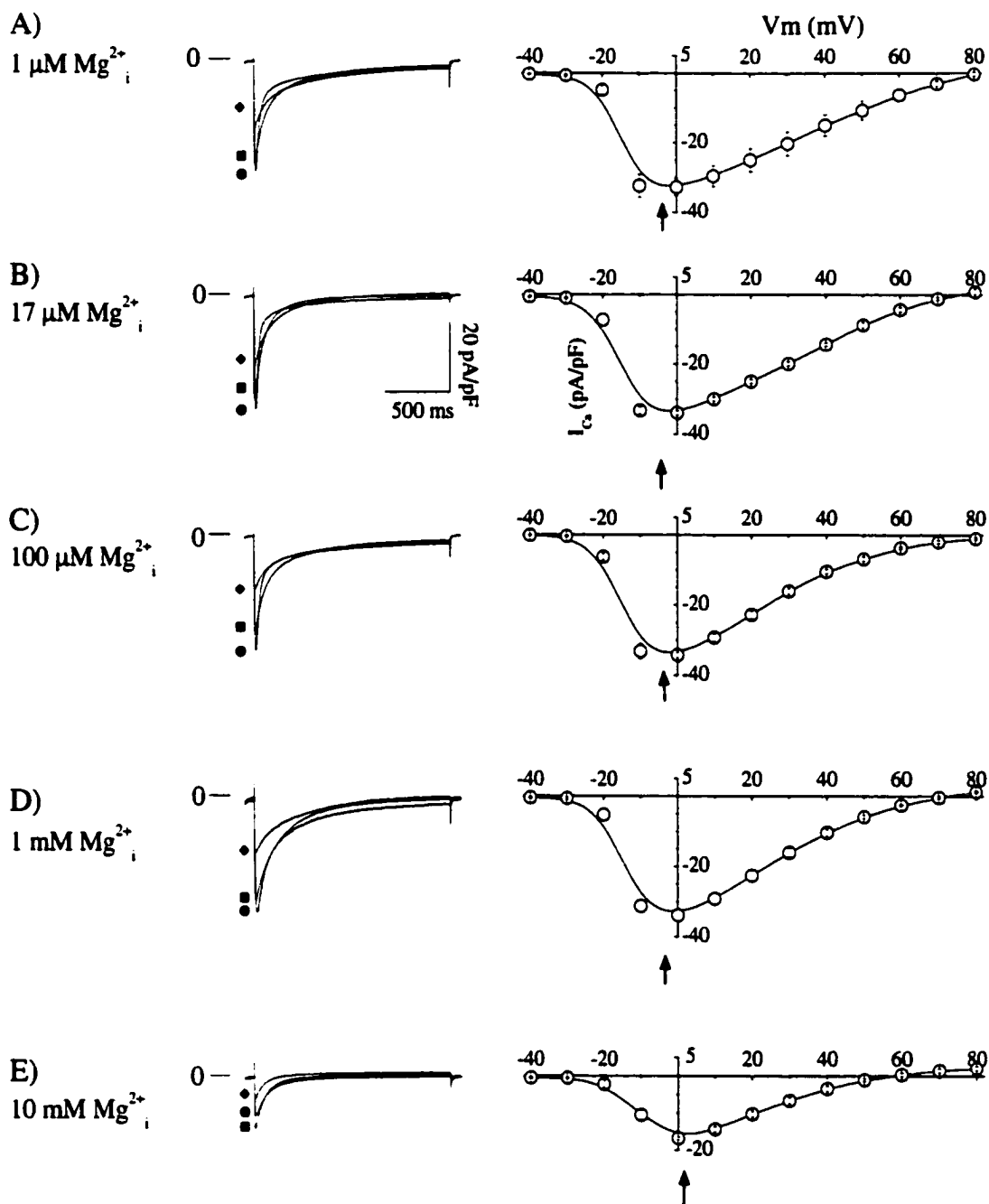
Figure 10: Voltage dependence of cAMP-upregulated $I_{Ca,L}$ at different $[Mg^{2+}]_i$ ranging from 1 μM to 10 mM (1 μM (A), 17 μM (B), 100 μM (C), 1 mM (D) and 10 mM (E)). The $I_{Ca,L}$ was elicited every 10 seconds by step depolarizations from -80 to -40 mV for 50 ms then to test potentials ranging from -40 mV to +80 mV for 1500 ms. The left panel shows original currents recorded at test potentials of -10 mV (●), +10 mV (■) and +30 mV (◆) after 30 minutes of cell dialysis. Corresponding complete $I_{Ca,L}$-voltage relations are shown in the right panel. Each point represents the average $I_{Ca,L}$ density measured in 2-5 cells. Where error bars are absent, they are smaller than the symbol size. The arrows indicate V_{max} which was -3 ± 1 mV (A), -3 ± 1 mV (B), -4 ± 1 mV (C), -2 ± 2 mV (D) and 1 ± 1 mV (E).
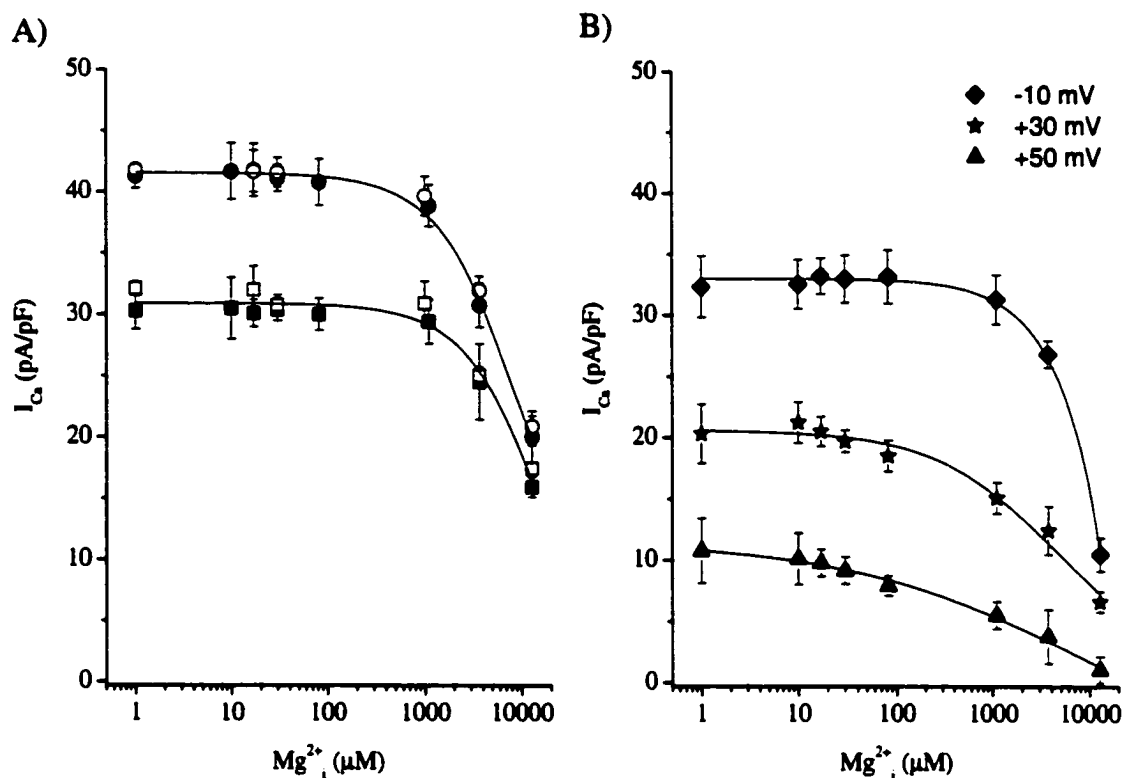
Figure 11: $[Mg^{2+}]_i$-dependence of cAMP-upregulated $I_{Ca,L}$ measured after different times of cell dialysis (A) and at different test potentials (B). (A) $I_{Ca,L}$ density measured at a test potential of +10 mV after 10 minutes (circles) and 30 minutes of cell dialysis (squares). The filled symbols represent cells that are dialyzed with solutions containing 90 nM Ca^{2+}, and the open symbols represent cells that are dialyzed with solutions containing 180 nM free Ca^{2+}. (B) $I_{Ca,L}$ density after 30 minutes of cell dialysis with solutions containing 90 nM Ca^{2+} at test potentials of -10 mV (—◆—), +30 mV (—★—), and +50 mV (—▲—). Each point represents the mean of 4-6 cells. Where error bars are absent, they are smaller than the symbol size.

SECTION B. EFFECTS OF $Mg^{2+}{}_i$ AND cAMP-STIMULATION ON $I_{Ca,L}$:

Several proteins involved in the regulation of cAMP-mediated phosphorylation are Mg^{2+} dependent. To assess how this manifests in intact cells, the effects of $Mg^{2+}{}_i$ on the stimulation of $I_{Ca,L}$ by elevations of cAMP induced by β-adrenoceptor stimulation, direct stimulation of AC, and inhibition of PDE activity were studied. The first section will show typical examples of cAMP-induced changes in $I_{Ca,L}$ (Figures 12-14), and the latter part will present summaries of the $Mg^{2+}{}_i$ dependence of pertinent parameters, (Figure 15 - 19).

(1) $Mg^{2+}{}_i$ effects on the stimulation of $I_{Ca,L}$ by β-adrenergic receptor stimulation

Figure 12 shows sample records (left panel) and typical time courses of $I_{Ca,L}$ density (right panel) seen in response to β-adrenergic stimulation with ISO (3 μM) after dialysis with solutions containing different concentrations of $Mg^{2+}{}_i$ ranging from 1 μM (Figure 12A) to 5 mM (Figure 12D). ISO was applied only after 20 minutes of dialysis in order to minimize interferences with the transient $I_{Ca,L}$ changes during dialysis with low $Mg^{2+}{}_i$ solutions (compare Figure 3). In cells dialyzed with solution containing 1 mM Mg^{2+}, ISO typically induced a ~3-fold increase in $I_{Ca,L}$ density within ~3 minutes, which faded somewhat during a 10 minute observation period (see Figure 12C). Similar responses to the β-agonist were seen with 5 mM Mg^{2+} dialysates (see Figure 12 D), but not with dialysates containing sub-millimolar concentrations (>100 μM) of Mg^{2+}. In these cells, ISO-induced increases in $I_{Ca,L}$ were significantly slower, weaker

and faded more noticeably. A typical example is the cell dialysed with 30 μM Mg^{2+} solution

(Figure 12B) where β-adrenergic stimulation caused an increase of $I_{Ca,L}$ by 91 % within ~6 minutes which faded by 36 % during a 10 minute observation period (for a summary see Figures 16 and 18). In 1 μM Mg^{2+} dialysates, ISO failed to induce any significant changes in $I_{Ca,L}$ density.

(2) Mg^{2+}_i effects on the stimulation of $I_{Ca,L}$ by the phosphodiesterase inhibitor IBMX

Figure 13 shows sample records (left panel) and typical time courses of $I_{Ca,L}$ density (right panel) seen in response to PDE inhibition with IBMX, after dialysis with solutions containing different concentrations of free Mg^{2+}_i ranging from 1 μM (Figure 12A) to 5 mM (Figure 12D). As above, IBMX was applied only after 20 minutes of dialysis. In cells dialyzed with solution containing 1 mM Mg^{2+}_i, IBMX typically induced a ~3-fold increase in $I_{Ca,L}$ density within ~4 minutes, which faded slightly during a 10 minute observation period (see Figure 13C). Similar stimulatory responses to the PDE inhibitor were seen with 5 mM Mg^{2+}_i dialysates (see Figure 13D). In 30 μM Mg^{2+}_i dialysates, IBMX produced elevations in $I_{Ca,L}$ which were notably smaller, and slower than the millimolar Mg^{2+}_i levels. A typical example of a cell dialyzed with 30 μM Mg^{2+} is shown (Figure 13B), the IBMX in this case caused an increase in the density by ~67 % in ~6 minutes. At 1 μM Mg^{2+}_i (Figure 13A), the currents were unaffected by the addition of IBMX.

(3) Mg^{2+}_i effects on the stimulation of $I_{Ca,L}$ by FSK

Figure 14 shows sample records (left panel) and typical time courses of $I_{Ca,L}$ density (right panel) seen in response to direct adenylyl cyclase stimulation with FSK, and after dialysis with solutions containing different concentrations of free Mg^{2+} ranging from 1 μM (Figure 14A) to 5 mM (Figure 14D). In all dialysates, the addition of FSK after 20 minutes of dialysis produced a 3-fold increase in density. Although the increase in density caused by FSK application was not appreciably different for the varying levels of Mg^{2+}_i, higher levels of Mg^{2+}_i seemed to produce more stable responses. For example, the $I_{Ca,L}$ density from the cell dialyzed with 1 μM Mg^{2+}_i shown on Figure 14A declined by ~40% ten minutes after the peak of stimulation, whereas the cell dialyzed with 1 mM Mg^{2+}_i shown on Figure 14C showed run-down less than 10% after the same period.
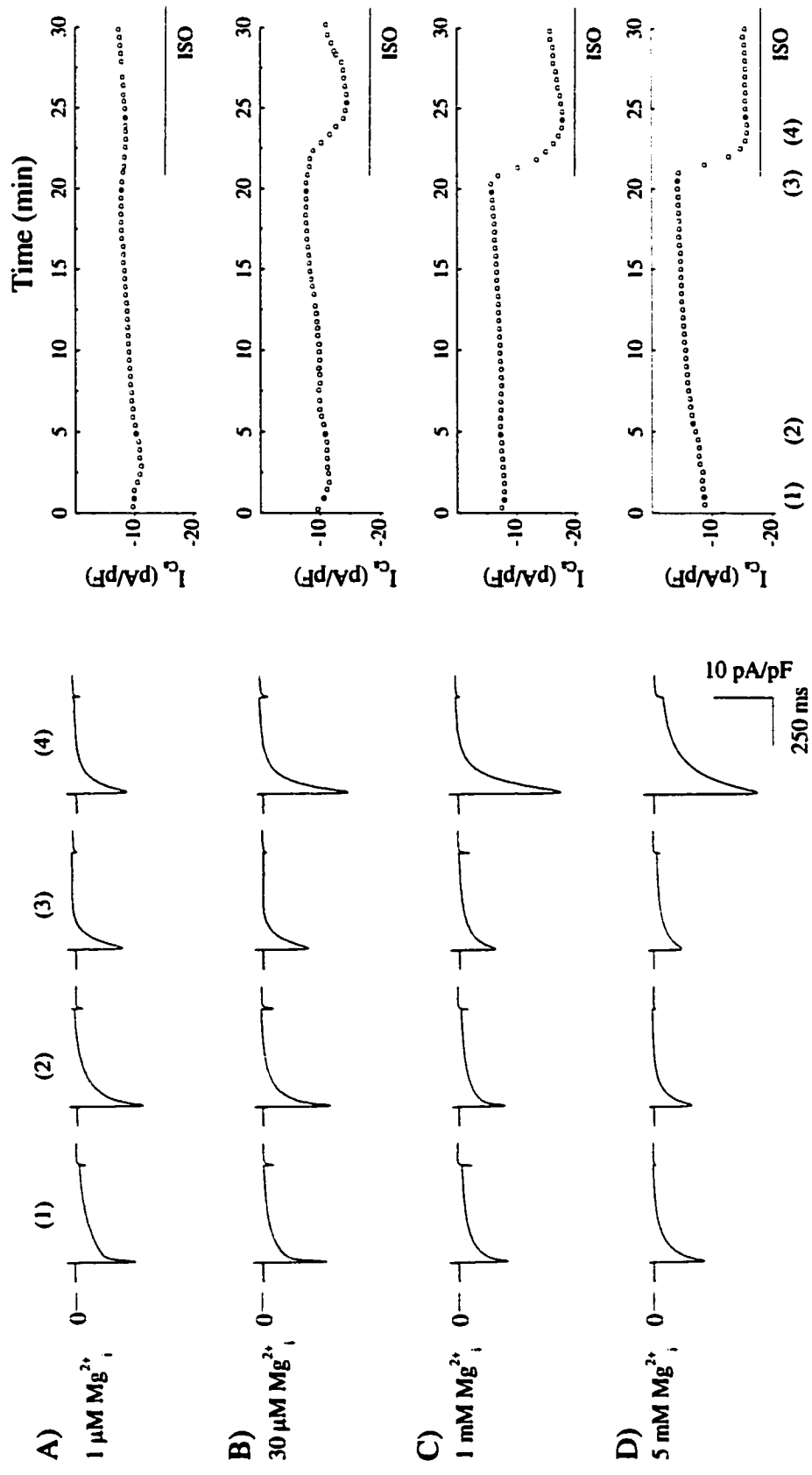
Figure 12: ISO stimulation of $I_{Ca,L}$ following dialysis with (a) 1μM, (b) 30 μM, (c) 1 mM, and (d) 5 mM Mg^{2+}_i solution. $I_{Ca,L}$ was elicited every 30 seconds by step depolarizations from -80 to -40 mV for 50 ms then to test potential +10 mV for 500 ms. ISO (3 μM) was applied after 20 minutes of dialysis. Time diaries of $I_{Ca,L}$ current density recorded at +10 mV are shown on the right panel, example currents corresponding to the filled symbols are shown on the left panel. Time zero represents patch break-through and the start of cell dialysis.
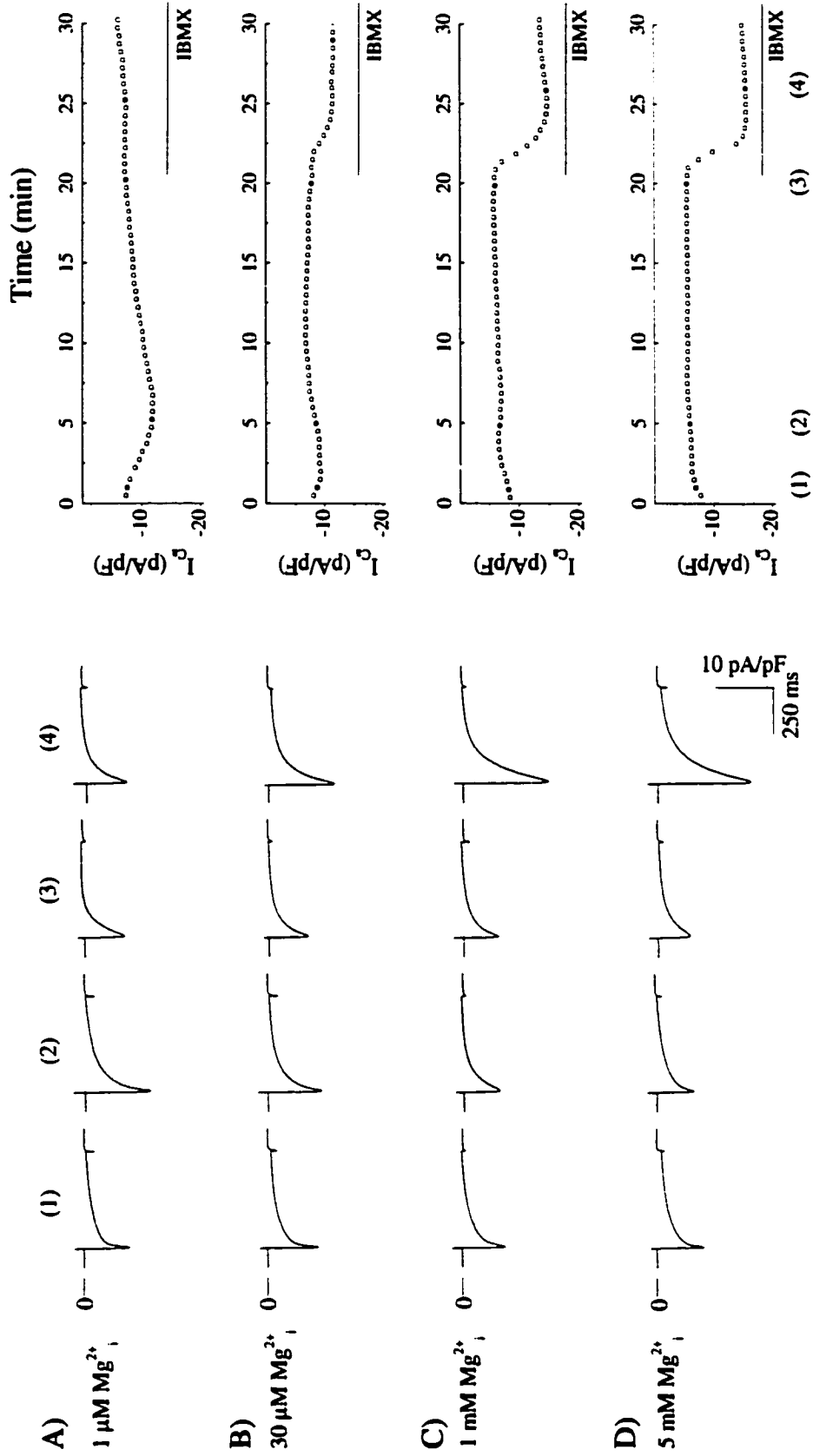
Figure 13: IBMX stimulation of $I_{Ca,L}$ following dialysis with (a) 1 μM, (b) 30 μM, (c) 1 mM, and (d) 5 mM Mg^{2+}_i solution. $I_{Ca,L}$ was elicited every 30 seconds by step depolarizations from -80 to -40 mV for 50 ms then to test potential +10 mV for 500 ms. IBMX (50 μM) was applied after 20 minutes of dialysis. Time diaries of $I_{Ca,L}$ current denisty recorded at +10 mV are shown on the right panel, example currents corresponding to the filled symbols are shown on the left panel. Time zero represents patch break-through and the start of cell dialysis.
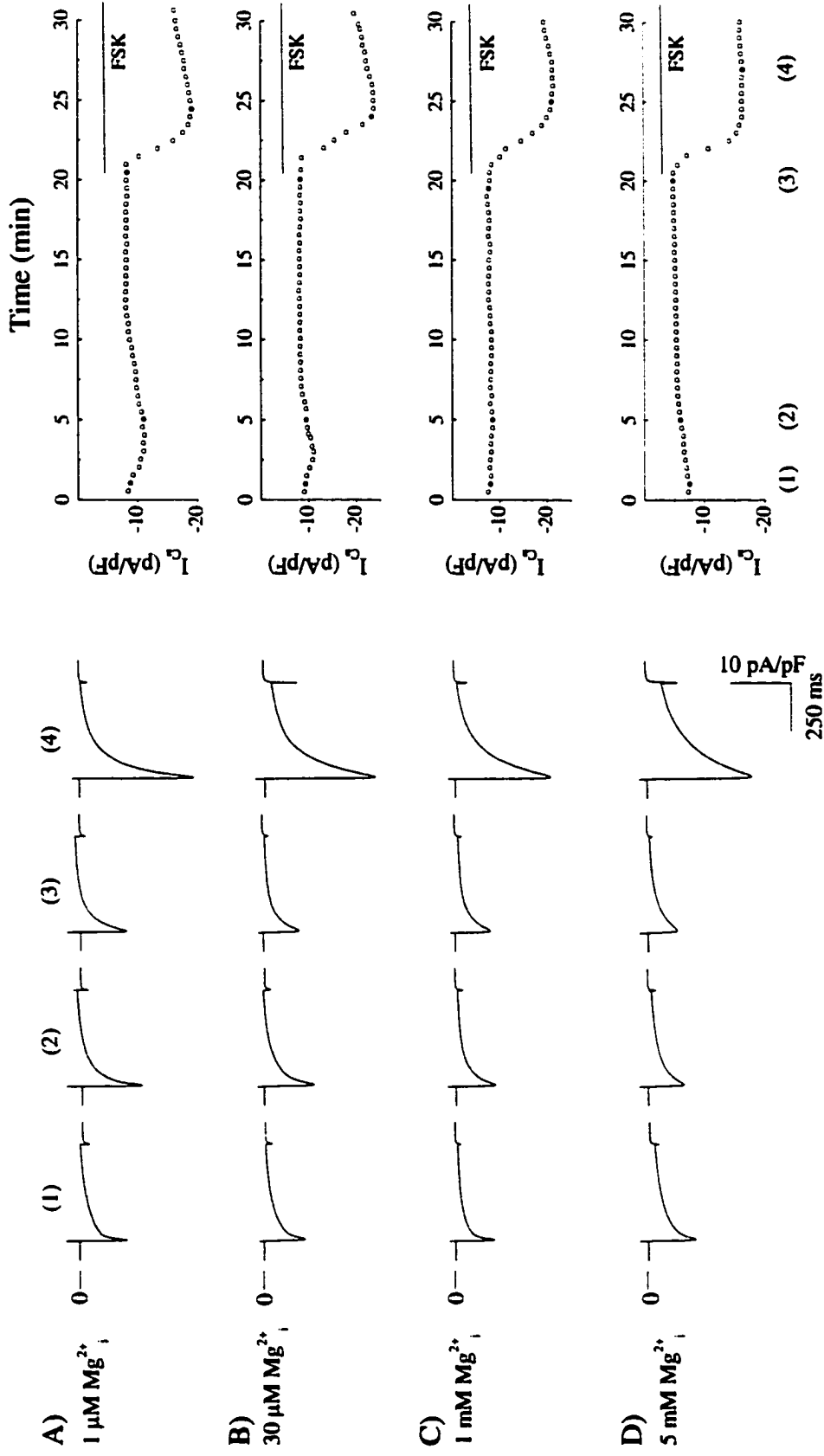
Figure 14: FSK stimulation of $I_{Ca,L}$ following dialysis with (a) 1μM, (b) 30 μM, (c) 1 mM, and (d) 5 mM Mg^{2+}_i solution. $I_{Ca,L}$ was elicited every 30 seconds by step depolarizations from -80 to -40 mV for 50 ms then to test potential +10 mV for 500 ms. FSK (10 μM) was applied after 20 minutes of dialysis. Time diaries of $I_{Ca,L}$ current density recorded at +10 mV are shown on the right panel, example currents corresponding to the filled symbols are shown on the left panel. Time zero represents patch break-through and the start of cell dialysis.

(4) Mg^{2+}_i dependence of $I_{Ca,L}$ by cAMP stimulators

The information summarized in Figure 15 illustrates the relationship between Mg^{2+}_i concentration and $I_{Ca,L}$ density before (O) and after (●) the stimulation of cAMP-mediated phosphorylation by ISO (Figure 15A), IBMX (Figure 15B) and FSK (Figure 15C). Basal $I_{Ca,L}$ density, which was recorded 20 minutes after patch breakthrough, showed the same typical bimodal dependence on Mg^{2+}_i which was observed after 30 minutes (compare Figure 5).

$I_{Ca,L}$ density after β-adrenergic stimulation (Figure 15A) also displayed a bimodal Mg^{2+}_i dependence. At 1 μM Mg^{2+}_i, the $I_{Ca,L}$ density was similar to those observed with basal conditions (P=0.115), the density increased with rising Mg^{2+}_i to a maximum at 100 μM Mg^{2+}_i (P<0.001) and declined at higher Mg^{2+}_i concentrations. Note that while basal $I_{Ca,L}$ was maximal at 17 μM Mg^{2+}_i, the largest current after ISO stimulation occurred at 100 μM Mg^{2+}_i.

The response of the IBMX-stimulated $I_{Ca,L}$ (●, Figure 15B) did not follow the same bimodal pattern of the basal or ISO stimulated conditions. The IBMX application had no significant effect at 1 μM Mg^{2+}_i (p=0.453) and 17 μM Mg^{2+}_i (p=0.076). However at higher Mg^{2+}_i levels, the $I_{Ca,L}$ density increased dramatically and significantly (p<0.001 for all concentration above 17 μM) from the basal condition. The peak $I_{Ca,L}$ was recorded at 100 μM (18.6 ± 1.2 pA/pF), and declined only slightly at greater levels of Mg^{2+}_i dialysate (15.9 ± 1.1 pA/pF at 5 M Mg^{2+}_i).

When FSK was used to stimulate $I_{Ca,L}$ the relationship between cAMP-upregulated $I_{Ca,L}$ density and Mg^{2+}_i followed a bimodal pattern similar to that seen under basal conditions. At 1 μM Mg^{2+}_i, $I_{Ca,L}$ density was considerably higher than under basal conditions ($p<0.001$), the $I_{Ca,L}$ density increased to a maximum at 17 μM, and declined considerably at higher Mg^{2+}_i concentrations. To determine if the activation of PDE at millimolar Mg^{2+}_i was limiting the stimulation by FSK, IBMX was applied along with FSK to four cells at 5 mM Mg^{2+}_i (filled square in Figure 15C). The results showed a further increase of 2 pA/pF, and the test of significance revealed a $p=0.01$.
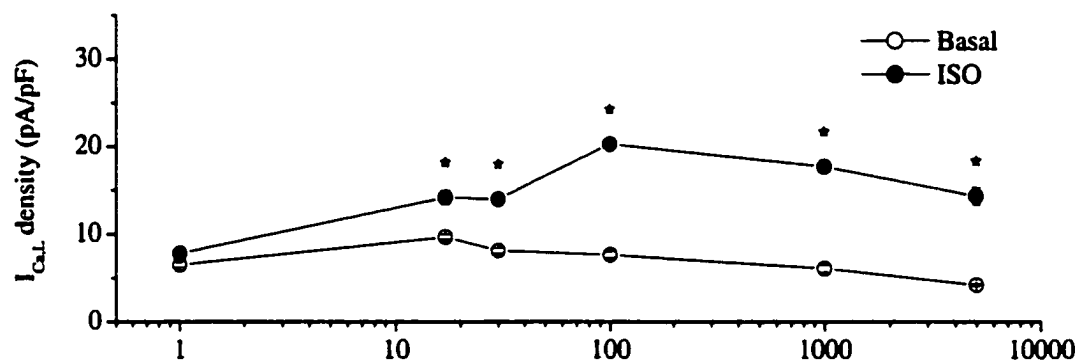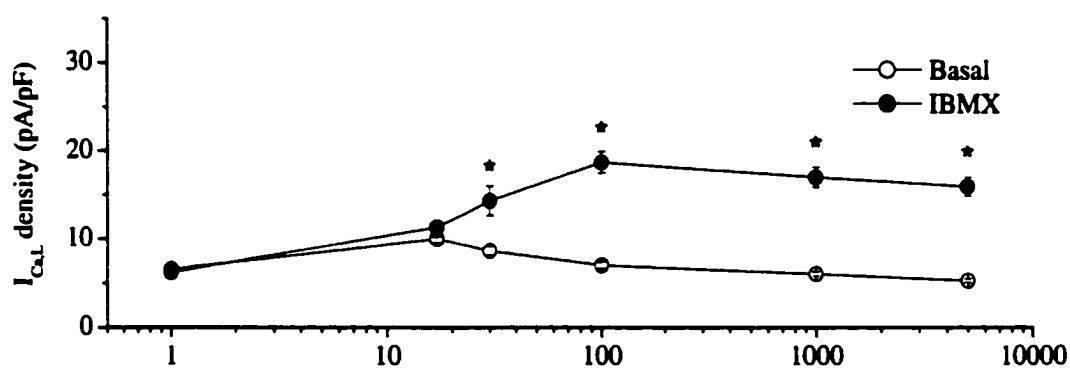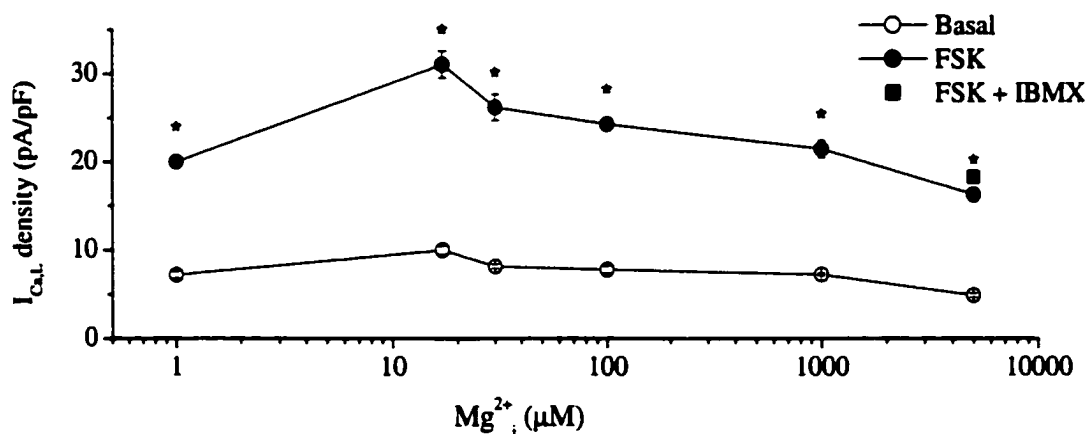
Figure 15: Mg^{2+}_i dependence of basal and cAMP stimulated $I_{Ca,L}$. Basal $I_{Ca,L}$ density (◯) was measured at +10 mV after 20 minutes of cell dialysis. The cAMP stimulated $I_{Ca,L}$ (●) shown are the largest measured currents at +10 mV after drug stimulation by:
(A) ISO (3 μM); (B) IBMX (50 μM); and (C) FSK (10 μM), and FSK 10 (μM) + IBMX (50 μM) (■). Each point represents the average of 4-6 cells. Where error bars are absent, they are smaller than the symbol size. The stars indicate a signifcant change (p<0.05) after the addition of drug.

(5) Mg^{2+}_i dependence of cAMP-induced elevations of $I_{Ca,L}$

Figure 16 compares the responses of $I_{Ca,L}$ at different Mg^{2+}_i concentrations to stimulation with ISO (Figure 16A), IBMX (Figure 16B), and FSK (Figure 16C). The level of stimulation is expressed as the maximum increase in the $I_{Ca,L}$ after the addition of the cAMP stimulators. Figure 16A shows that the response of $I_{Ca,L}$ to stimulation by ISO rose noticeably with increasing Mg^{2+}_i. The amount of increase ranged from 20 ± 6.4% at 1 µM Mg^{2+}_i to 194 ± 18% at 1 mM and 239 ± 22% at 5mM. Application of IBMX (Figure 16B) failed to stimulate $I_{Ca,L}$ when the cells were dialyzed with 1µM Mg^{2+}_i (-5.6 ± 3.7%). At higher levels of Mg^{2+}_i the response to IBMX increased from 13.5 ± 14% at 17 µM, to 203 ± 20% at 5 mM. Unlike ISO and IBMX, the response of the $I_{Ca,L}$ stimulated by FSK (Figure 16C) was insensitive to changes (p=0.617) to Mg^{2+}_i, and the amount of stimulation ranged from 178 ± 23% at 1µM, to 224 ± 24% at 5 mM. At 5 mM Mg^{2+}_i the stimulation with FSK and IBMX produced an even stronger increase than with FSK alone (287 ± 24%, p=0.04), suggesting that activation of PDE at higher Mg^{2+}_i may be a limiting factor in the stimulation by FSK.
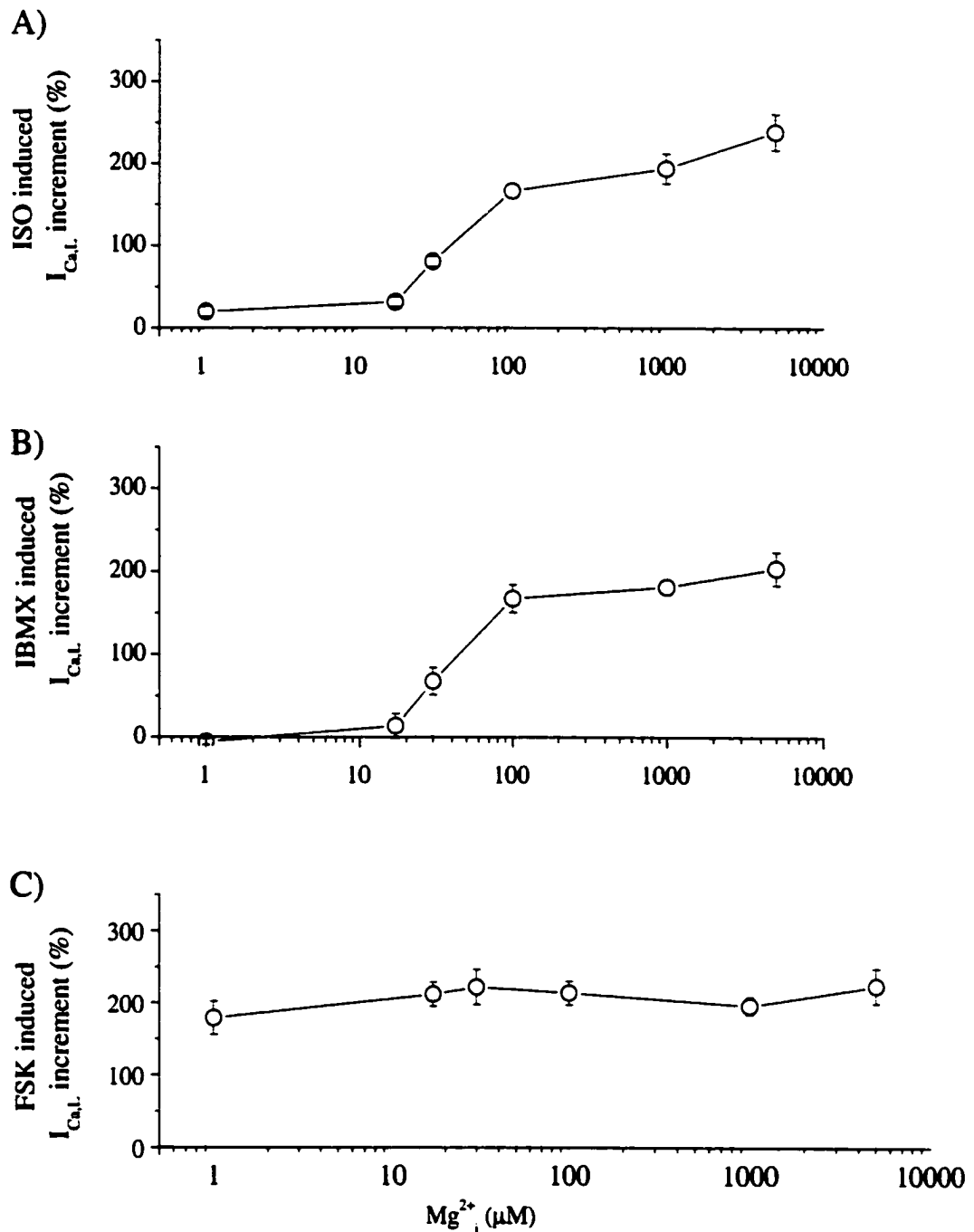
Figure 16: Mg^{2+}_i dependence of (A) ISO (3 μM), (B) IBMX (50 μM) and (C) FSK (10 μM) induced $I_{Ca,L}$ increments at +10 mV. The stimulation, measured as the peak current after drug application, is expressed as a percentage of the basal current after 20 minutes of cell dialysis. Each column represents the average of 3-6 cells.

(6) Mg^{2+}_i dependence of Ca^{2+} influx through the L-type Ca^{2+}-channel

Figure 17 illustrates how Mg^{2+}_i affects the amount of Ca^{2+} that enters the cell during a 500 ms depolarization period via the L-type Ca^{2+}-channel under basal conditions, and in K252a treated cells (Figure 17a), as well as after stimulation with ISO (Figure 17B), IBMX (Figure 17B) and FSK (Figure 17D). For basal conditions (Figure 17A,□), the Ca^{2+} influx increased significantly from 0.60 ± 0.052 pC/pF to 0.91 ± 0.078 pC/pF ($p<0.001$) when the Mg^{2+}_i was elevated from 1 to 17 µM. Further elevations of Mg^{2+}_i did not cause any significant changes in the amount of Ca^{2+} entering the cell. Unlike the basal condition, Ca^{2+} influx after inhibition of protein phosphorylation with K252a (□) was similar at 1 and 17 µM Mg^{2+}_i, but increased at higher Mg^{2+}_i levels, from

0.54 ± 0.04 pC/pF at 100 µM Mg^{2+}_i to 0.75 ± 0.05 pC/pF at 5 mM Mg^{2+}_i. It is also worth noting that when the Mg^{2+}_i levels were ≤ 1 mM, the Ca^{2+} influx was significantly higher under basal conditions than in K252a treated cells ($p<0.001$). However, at 5 mM Mg^{2+}_i the inhibition of protein phosphorylation caused no significant reduction in Ca^{2+} influx ($p=0.083$).

Ca^{2+} influx in response to stimulation with ISO (Figure 17B) increased steadily with increasing levels of Mg^{2+}_i; from 0.75 ± 0.10 pC/pF at 1 µM to 3.08 ± 0.59 pC/pF at 5 mM. A similar increase in Ca^{2+} influx was observed when $I_{Ca,L}$ was stimulated with IBMX (Figure 17C), the amount of influx increased from 0.61 ± 0.04 to 3.38 ± 0.13 pC/pF. After the stimulation of $I_{Ca,L}$ with FSK (Figure 17D) the Ca^{2+} influx at 1 µM Mg^{2+}_i (1.61 ± 0.29 pC/pF) was considerably higher than basal conditions ($p<0.001$), and

increased by over 3-fold to a maximum at 17 μM Mg^{2+}_i. Higher levels of Mg^{2+}_i led to a

slight decreases in the amount of Ca^{2+} influx. $I_{Ca,L}$ stimulation by the combination of

FSK and IBMX did not significantly raise the amount of Ca^{2+} influx above the level

observed with FSK stimulation alone (p=0.342).
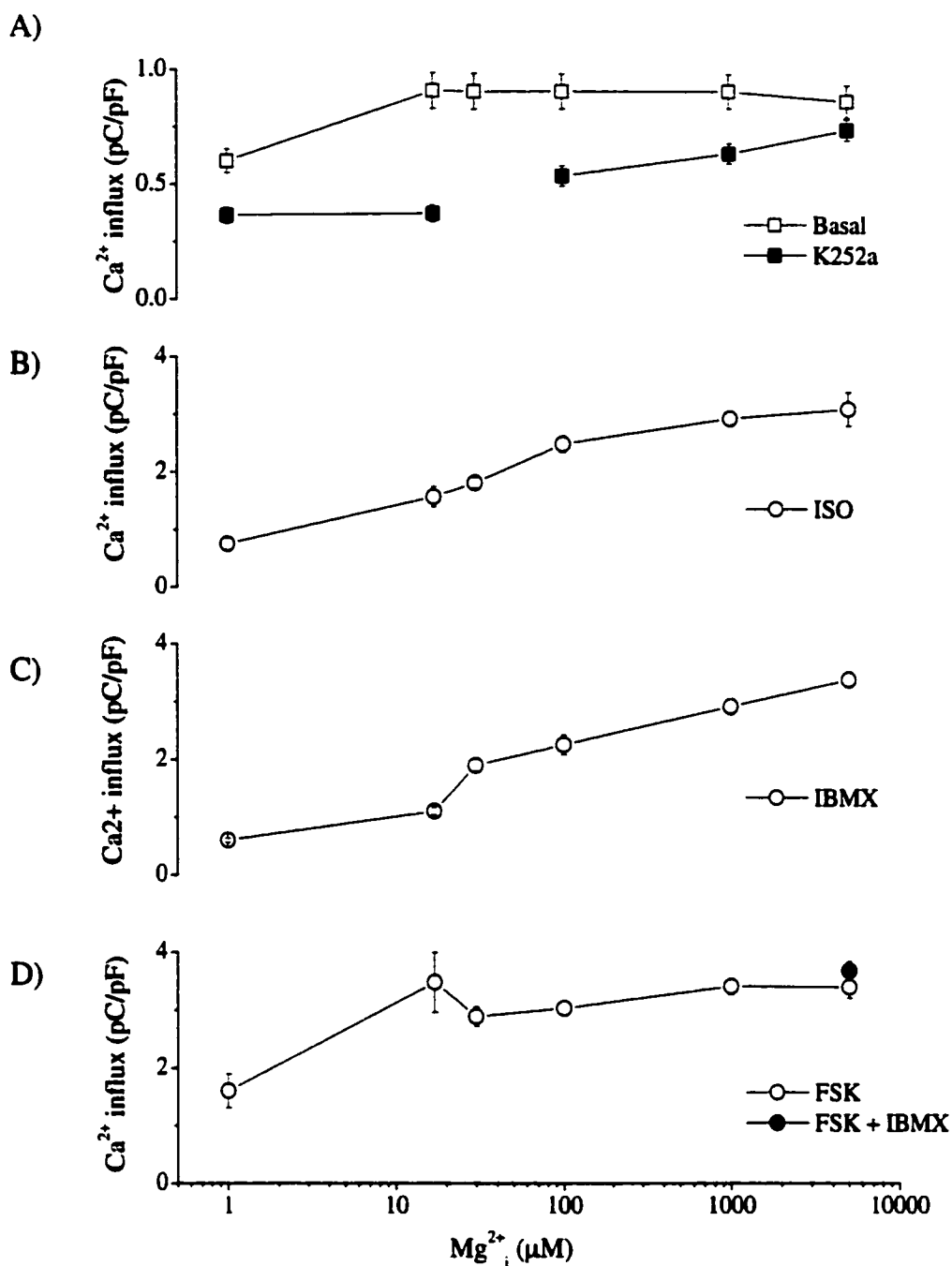
Figure 17: Mg^{2+}_i dependence of Ca^{2+} influx through L-type Ca^{2+}-channels under basal conditions, and in K252a treated cells after 30 minutes of dialysis (A), as well as at the maximum I_{CaL} response to stimulation with (B) ISO, IBMX (C), and FSK (D) after 20 minutes of dialysis. The I_{CaL} was elicited depolarizations from -80 to -40 mV for 50 ms then to test potential +10 mV for 500 ms. The Ca^{2+} influx was calculated by integrating the area outlined by the I_{CaL} current and zero current for the 500 ms test potential. Each point represents the average of 3-6 cells. Where error bars are absent, they are smaller than the symbol size.

SECTION C. EFFECTS OF Mg^{2+}_i AND $I_{Ca,L}$ INACTIVATION:

(1) Mg^{2+}_i dependence of $I_{Ca,L}$ inactivation in varying phosphorylation conditions

The sample records shown in Figures 3,6, and 9 indicate that Mg^{2+}_i does not only affect peak current amplitude but also the inactivation of $I_{Ca,L}$. To quantify effects of Mg^{2+}_i on $I_{Ca,L}$ inactivation, the decay of $I_{Ca,L}$ during test pulses was fitted with 2 exponentials. Figure 18 shows the time constants of inactivation for the fast component (τ_f) and the slow component (τ_s) in $I_{Ca,L}$ decay at different Mg^{2+}_i concentrations under basal conditions (A), and in cells treated with K252a (B), and in cAMP pre-loaded cells dialyzed with 180 nM free dialysate Ca^{2+} (C), and 90 nM free dialysate Ca^{2+} (D). The most noticeable trend among all these conditions was a steady increase in both the τ_f and τ_s with increasing Mg^{2+}_i concentration.

Figure 19 illustrates the influence of Mg^{2+}_i on $I_{Ca,L}$ stimulated after 20 minutes of dialysis with ISO (A), IBMX (B), and FSK (C). Again, regardless of the agonist, the most noticeable trend is a steady increase in the τ_f and τ_s with increasing Mg^{2+}_i concentration.

One-way ANOVA tests were performed by comparing all the different conditions in both figures into one test for each Mg^{2+}_i concentration. The null hypothesis for these tests is the inactivation constants are the same for cells dialyzed with the same Mg^{2+}_i concentration regardless of the drug treatment. The results from these tests (summarized in Table 9) indicate that the null hypothesis could not be rejected (at the $p<0.05$) level. This is quite remarkable considering that the $I_{Ca,L}$

densities were significantly different. For example, the current densities exhibited by the cAMP-loaded cells is generally 10-fold larger than the K252a-treated current density (compare Figures 8A and 11A), but there is no significant difference in the inactivation times between these conditions.

Table 9: P values from one-way ANOVA tests comparing the time constants for basal, K252a, FSK+IBMX (180 nM Ca^{2+}), and FSK+IBMX (90 nM Ca^{2+}) from Figure 18, and ISO , IBMX and FSK from Figure 19.

Mg^{2+}_i	1 μM	17 μM	30 μM	100 μM	1 mM	5 mM
τ_f	p = 0.971	p = 0.718	p = 0.140	p = 0.461	p = 0.189	p = 0.621
τ_s	p = 0.953	p = 0.995	p = 0.811	p = 0.991	p = 0.997	p = 0.991
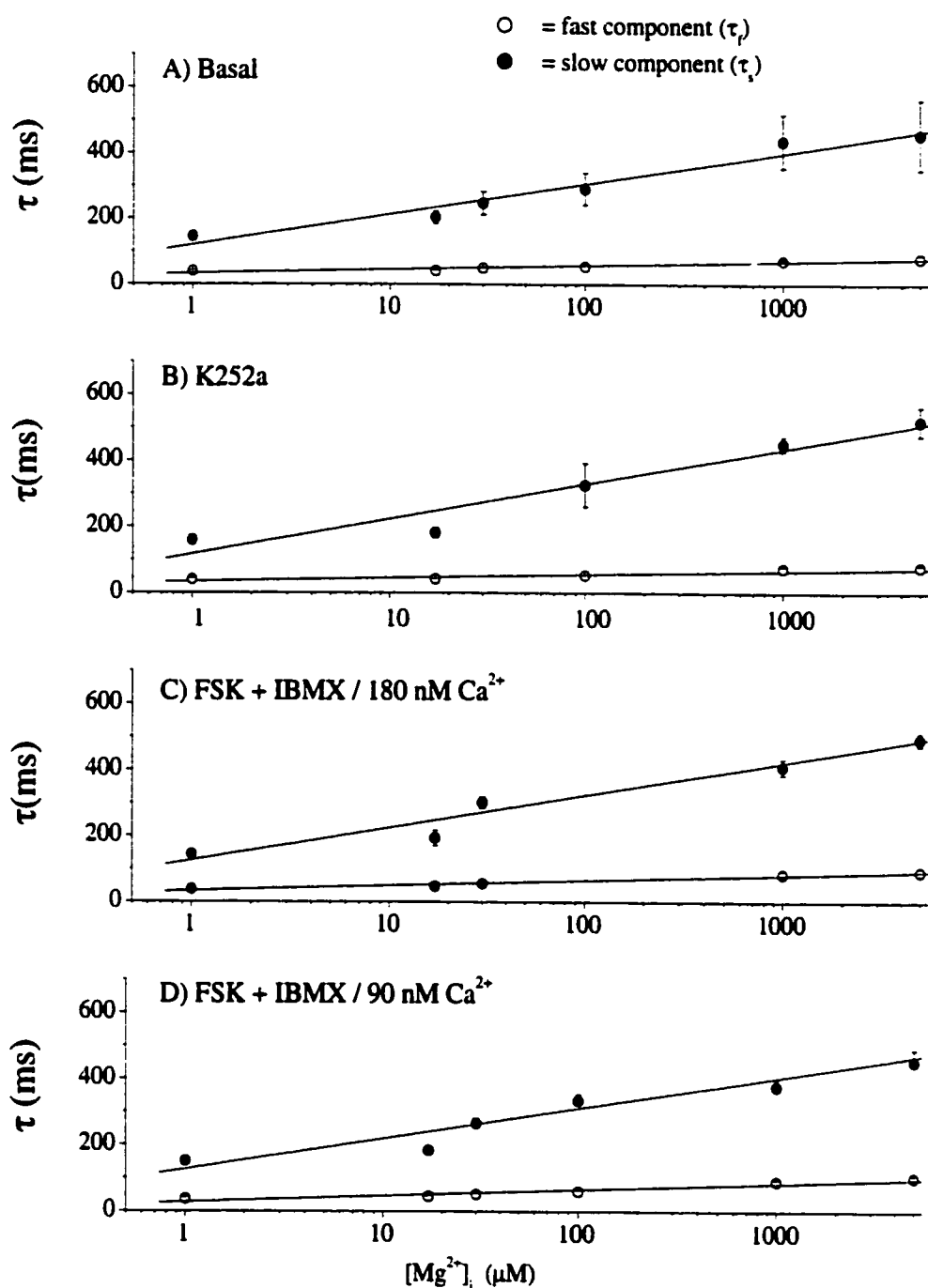
Figure 18: Dependence of $I_{Ca,L}$ inactivation on $[Mg^{2+}]_i$, under basal conditions (A), in K252a-treated cells (B), and in cells pre-stimulated with FKS and IBMX and dialyzed with solutions containing 180 nM free Ca^{2+}_i (C) or 90 nM free Ca^{2+}_i (D). The $I_{Ca,L}$ was elicited by step depolarizations from -80 to -40 mV for 50 ms then to + 10 mV for 500 ms. The time constants of inactivation were calculated by using double exponential decay curve-fitting (Origin 6.0, Microcal Software Inc., Northampton). The fast inactivation component (τ_f) is represented by the open symbol, and the slow inactivation component is represented by the darkened symbol (τ_s).
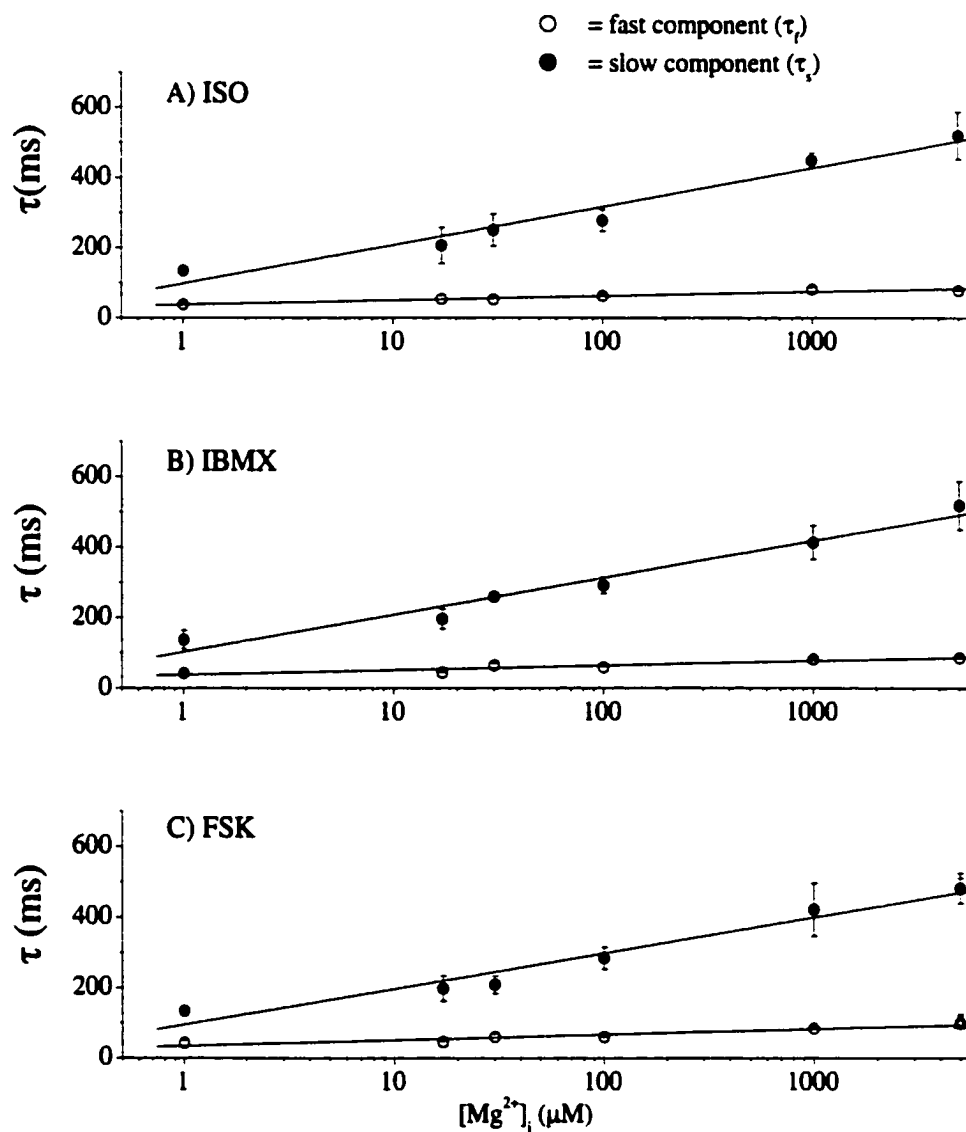
Figure 19: Dependence of $I_{Ca,L}$ inactivation on $[Mg^{2+}]_i$ after stimulation with ISO (A), IBMX (B), or FSK (C). The $I_{Ca,L}$ was elicited by step depolarizations from -80 to -40 mV for 50 ms then to + 10 mV for 500 ms. The time constants of inactivation were calculated by using double exponential decay curve-fitting (Origin 6.0,Microcal Software Inc., Northampton). The fast inactivation component (τ_f) isrepresented by the open symbol, and the slow inactivation component is represented by the filled symbol (τ_s).

IV. DISCUSSION

SECTION A. REVIEW OF RESULTS:

Under basal conditions I observed a bimodal inhibition of the $I_{Ca,L}$. Basal $I_{Ca,L}$ density increased with rising Mg^{2+}_i from 1 μM to 17 μM, while higher Mg^{2+}_i concentrations led to an inhibition of the $I_{Ca,L}$. This bimodal effect was occluded when phosphorylation was eliminated by the use of K252a. The stimulation appeared to be caused by an increase cAMP level and hence PKA mediated phosphorylation, whereas inhibition appears to be the reverse, a reduction in cAMP. The use of K252a greatly reduced the amplitude of the $I_{Ca,L}$ and all modulating effects from Mg^{2+}_i were absent. The use of K252a inhibited the phosphorylation of Ca^{2+}-channels, regardless of the Mg^{2+}_i concentration, thereby eliminating the regulation by Mg^{2+}_i. On the other hand, stimulation by preincubation with FSK and IBMX raised the level of cAMP, which was not subsequently altered by high or low levels of Mg^{2+}_i. The effect was a large stimulation of the $I_{Ca,L}$ that was not influenced by Mg^{2+}_i. From these experiments, I postulated that Mg^{2+}_i controls the balance of phosphorylated Ca^{2+}-channels. But how does that occur? There are four possible sites that Mg^{2+}_i can influence the net production of cAMP: at the receptor site, at the G-protein, at the adenylyl cyclase and at the phosphodiesterase. The results from the second set of experiments designed to determine the Mg^{2+}_i requirements at each site indicate that Mg^{2+}_i acts at all four levels but with different concentration requirements.

100

The discussion of the present study is divided into four sections. The first will analyze the set of experiments performed to assess whether the effects of Mg^{2+}_i on the phosphorylation/dephosphorylation processes contribute to the Mg^{2+}_i dependence of $I_{Ca,L}$. These experiments included cells in basal conditions, phosphorylation compromised, and cAMP-loaded cells. The second section will assess the experiments designed to determine the requirements of Mg^{2+}_i for $I_{Ca,L}$ control when different stages in the regulation of the cellular level of cAMP are altered. I tested its effect at the receptor level, at the level of the adenylyl cyclase and on the phosphodiesterase by using ISO, FSK and IBMX respectively. The third section will discuss the results relating to the effects of Mg^{2+}_i on Ca^{2+}-channel inactivation. Finally, the fourth section will discuss and correlate the findings to the physiological relevance of the study.

SECTION B. Is Mg^{2+}_i regulation of $I_{Ca,L}$ phosphorylation dependent?

(1) Inhibitory effects of Mg^{2+}_i

The inhibitory influence of Mg^{2+}_i on the L-type Ca^{2+}-channel can be explained by two different mechanisms; one is through direct Mg^{2+} binding to the Ca^{2+}-channel and the other is regulation of the basal activity of proteins which curtail or reverse the cAMP-mediated phosphorylation of the Ca^{2+}-channel. The first possibility has been embraced in several studies of the Mg^{2+}_i dependence of $I_{Ca,L}$ in frog (Yamaoka and Seyama, 1996a, 1996b, 1998) and mammalian (Agus et al. 1989) cardiomyocytes. Support for the second theory comes from in vitro studies showing that Mg^{2+} activates

phosphodiesterases (Jost and Rickenberg, 1971), PDE3 (McLaughlin et al. 1993; Torphy et al. 1992), PDE4 (Sette and Conti, 1996, Percival et al. 1997), PDE8 (Fisher et al. 1998), and protein phosphatases (McGowan and Cohen, 1988). The latter would imply that Mg^{2+}_i possibly plays a much broader role in the regulation of cardiac performance than presently anticipated.

In intact frog cardiomyocytes, micromolar Mg^{2+}_i levels increased the open probability but did not alter the conductance of the Ca^{2+}-channel (Yamaoka and Seyama, 1996a, 1998). Channel gating in Mg^{2+}-depleted cardiomyocytes resembled the characteristics of phosphorylated Ca^{2+}-channels in the "willing" mode and shifted at higher levels of Mg^{2+}_i into a "reluctant" mode. Mechanisms that have been associated with such a mode shift are the Ca^{2+}-induced inhibition and the dephosphorylation of the Ca^{2+}-channel (McDonald et al. 1994). One of the key differences between Yamaoka's and Seyama's frog cardiomyocyte experiments and my guinea pig cardiomyocyte tests is the effect of phosphorylation inhibition on Mg^{2+}_i regulation of $I_{Ca,L}$. Yamaoka's and Seyama's use of the "death brew", which inhibits phosphorylation by depleting the cell of ATP, did not affect the Mg^{2+}_i regulation of $I_{Ca,L}$ in frog cardiomyocytes. In fact $I_{Ca,L}$ recorded from cells subjected to the "death brew" were stimulated by as much as 10-fold when the internal Mg^{2+}_i level was lowered to 1 µM (Yamaoka and Seyama 1996b). Conversely in the guinea pig myocytes, phosphorylation inhibition by K252a abolished the Mg^{2+}_i regulation of $I_{Ca,L}$ (Figure 8). Since the Mg^{2+}_i regulation of $I_{Ca,L}$ seemed to be independent of phosphorylation in the frog myocytes, the researchers postulated that the stimulatory effect observed at very low Mg^{2+}_i was caused by the

relief of a direct inhibitory effect at the Ca^{2+}-channel (Yamaoka and Seyama 1996b). In other words, the inhibitory effect of Mg^{2+}_i was attributed to Mg^{2+} acting as an agonist at the regulatory Ca^{2+} binding site responsible for the Ca^{2+}-induced inhibition of $I_{Ca,L}$ (Yamaoka and Seyama, 1998). I found no occurrence of this phenomenon in my results; in fact Mg^{2+}_i seemed to act as an antagonist for Ca^{2+} dependent inactivation (see below). An alternative explanation for the inhibitory effects of Mg^{2+}_i could be suggested by my finding that the inhibition of protein phosphorylation by K252a inhibited $I_{Ca,L}$ for all the Mg^{2+}_i concentrations and rendered the remaining current insensitive to changes in Mg^{2+}_i (see Figures 6). Judging from the effect of K252a after 10 minutes of dialysis, phosphorylated channels appear to carry ~75% of basal $I_{Ca,L}$ in Mg^{2+} depleted cells but only 40% or less at the millimolar level (compare Figures 5A and 8A). This implies that in Mg^{2+}-depleted cells a considerable portion of Ca^{2+}-channels is phosphorylated and that Mg^{2+}_i reduces the contribution of currents through phosphorylated Ca^{2+}-channels to whole-cell $I_{Ca,L}$; this occurs either by the selective inhibition of the current flow through phosphorylated Ca^{2+}-channels or by the reduction of the number of phosphorylated channels. My results argue against an inhibitory action of Mg^{2+}_i on phosphorylated Ca^{2+}-channels, because if this was the case, the inhibitory effect of Mg^{2+} would increase when Ca^{2+}-channel phosphorylation is stimulated. On the contrary, the stimulation of cAMP-mediated phosphorylation decreased the sensitivity of $I_{Ca,L}$ to inhibition by Mg^{2+}_i (compare Figures 3A and 11A). This suggests that Mg^{2+}_i inhibition occurs by activating proteins which curtail and reverse the phosphate transfer by cAMP-dependent protein kinase. Although the nature

of these proteins remains to be determined, likely candidates are Mg^{2+}-dependent phosphodiesterases (Jost and Rickenberg, 1971; Meacci et al., 1992; Percival et al., 1997; Fisher et al., 1998) and/or the Mg^{2+}-dependent protein phosphatase PP2C (McGowan and Cohen, 1988).

(2) Stimulatory effects of Mg^{2+}_i

At very low Mg^{2+}_i levels (<17 µM) the predominant regulatory influence of Mg^{2+}_i on $I_{Ca,L}$ was stimulatory (see Figure 3), whereas the regulatory influence was inhibitory at Mg^{2+}_i levels > 17 µM. This result indicates that the underlying stimulatory mechanism(s) has a higher affinity for Mg^{2+}_i than the Mg^{2+}_i-dependent inhibitory mechanism(s), which overwhelms the ion's stimulatory effect at higher concentrations. Considering that the increase in Mg^{2+}_i levels from 1 µM to 17 µM was accompanied by a similar (~ 3.5 pA/pF) increase in $I_{Ca,L}$ density after 10 and 30 minutes of cell dialysis (see Figure 3A), it appears that the sensitivity of Ca^{2+}-channels to stimulation by Mg^{2+}_i is preserved during cell dialysis and unrelated to the overall density of $I_{Ca,L}$ which declined considerably.

The stimulatory action of low Mg^{2+}_i was suppressed by K252a (see Figure 6). This shows that modulation of $I_{Ca,L}$ by Mg^{2+}_i requires protein kinase activity and points to effects of Mg^{2+}_i on proteins promoting channel phosphorylation. One might hypothesize that Mg^{2+}-induced stimulation results from the phosphorylation of the Ca^{2+}-channel by cAMP dependent protein kinase. In accord with this hypothesis, basal stimulation by Mg^{2+}_i was associated with a leftward shift in the voltage-dependence of

$I_{Ca,L}$ at 17 µM (see Figure 4), which suggests that stimulatory action of Mg^{2+}_i was potential dependent, and most pronounced at negative membrane potentials (see Figure 5B); this is in line with the effects observed during cAMP-mediated phosphorylation of the Ca^{2+}-channel (McDonald et al., 1994). One possible target for Mg^{2+}_i stimulation is the adenylyl cyclase. Mg^{2+}_i is required for the synthesis of cAMP at the catalytic site of the enzyme and stimulates the basal enzymatic activity of cardiac adenylyl cyclase in cell-free preparations (Pignatti et al. 1993; Steinberg et al. 1986). However, the Mg^{2+}_i requirements for these in vitro conditions are much higher than 17 µM; for example Steinberg's group in 1986 reported an apparent activation constant for Mg^{2+}_i of 1.5 mM. Hence one has to assume that either the adenylyl cyclase affinity for Mg^{2+}_i is considerably reduced in cell-free preparations or that another Mg^{2+}_i dependent process is involved. One such possibility could come from Mg^{2+}_i-induced activation of G_s protein, however this is unlikely because (under basal conditions) the activation of G-proteins by GTP-containing dialysates decreased $I_{Ca,L}$ density at 17 µM Mg^{2+}_i (see Figure 5).

(3) Effects of Mg^{2+}_i on unphosphorylated Ca^{2+}-channels

Several actions of Mg^{2+} are expected to affect the current through unphosphorylated Ca^{2+}-channels. Through single channel studies Kuo and Hess (1993) showed that Mg^{2+} binds to sites in the conducting path of the Ca^{2+}-channel exhibiting characteristics of both a weak blocker and a weak permeator. Inhibitory effects of Mg^{2+}_i in intact mammalian cardiomyocytes were attributed not to direct channel block

but another inhibitory interaction of Mg^{2+} with the Ca^{2+}-channel (Agus et al. 1989). I

found the current through unphosphorylated Ca^{2+}-channels to be remarkably insensitive

to the regulatory effects of Mg^{2+}_i. When the phosphorylation-related effects of Mg^{2+}_i

were suppressed by K252a (see Figure 5), the most significant influence of Mg^{2+}_i was a

progressive leftward shift of the $I_{Ca,L}$-voltage relations with increasing Mg^{2+}_i, however

the shape of the $I_{Ca,L}$-voltage relations was unaltered. This argues against significant

direct channel block by Mg^{2+}_i because it would reduce $I_{Ca,L}$ in a potential-dependent

manner, and under the experimental conditions here, impact most prominently at

positive membrane potentials (see Figure 5). The best plausible explanation for the

effects of Mg^{2+}_i on unphosphorylated Ca^{2+}-channels is that Mg^{2+}_i can effectively screen

intracellular negative membrane charges and significantly reduce the voltage drop

across the membrane that is experienced by the Ca^{2+}-channel.

SECTION C. Mg^{2+}_i REQUIREMENTS FOR $I_{Ca,L}$ STIMULATION
BY cAMP REGULATORS:

The results from the experiments outlined in section A indicated that Mg^{2+}_i has

both stimulatory and inhibitory effects on the $I_{Ca,L}$. The stimulatory effects appear to

have a higher affinity for Mg^{2+}_i and dominate at the low micromolar level, whereas the

inhibitory effects have a lower affinity and dominate at the higher Mg^{2+}_i level. These

regulatory impacts require phosphorylation and seem to implicate cAMP-dependent

phosphorylation. Subsequently I investigated the influence of Mg^{2+}_i at the regulation

106

sites involved in modulating the cAMP level. This section will discuss the experiments designed to study the Mg^{2+}_i requirements at the β-adrenergic receptor, G-protein, adenylyl cyclase and the phosphodiesterase.

(1) Mg^{2+}_i requirements for β-adrenergic receptor stimulation of $I_{Ca,L}$

Isoproterenol was used to study the influence of Mg^{2+}_i on β-adrenergic stimulation of the $I_{Ca,L}$. The outcomes from these experiments shown on Figures 15A and 16A had the following features: (i) at least 17 μM Mg^{2+}_i was required for isoproterenol to significantly stimulate $I_{Ca,L}$ beyond the basal level (p<0.001); (ii) between 30-100 μM of Mg^{2+}_i was required to produce 50% of the maximal stimulation; (iii) greater amounts of Mg^{2+}_i yielded increasingly higher levels of $I_{Ca,L}$ stimulation; however, (iv) the overall current density actually declined when the Mg^{2+}_i was elevated from 100 μM to 1 mM (-12%, p=0.006) and 5 mM (-30% p=0.002)(see Figure 15A). These results indicate that a base amount of ~17 μM Mg^{2+}_i is required for β-receptor stimulation to occur, and a higher amount is required for optimal activation (see Figure 16A). Since the pathway from the addition of isoproterenol to $I_{Ca,L}$ stimulation involves dissociation of the G-protein, activation of adenylyl cyclase, and PKA phosphorylation of the L-type Ca^{2+}-channel, this experiment does not allow me to discern the individual Mg^{2+}_i requirements for each of these steps. However, the results do indicate that 17 μM is sufficient to fulfill the minimum requirements for all the steps involved, and that millimolar Mg^{2+}_i is necessary for optimal operation for at least one of the steps. These requirements for Mg^{2+}_i seem to correspond with many of the earlier investigations

involving Mg^{2+}_i and the second messenger system (Rodbell 1992; 1996 reviews). At

the receptor level, Ross et al., (1977) showed that not only was Mg^{2+}_i required but

higher levels of Mg^{2+}_i could increase the agonist binding affinity of β-adrenergic

receptors. At the G-protein level, several researchers demonstrated that a minimum

amount of Mg^{2+}_i is required for G-protein function and millimolar levels are required

for optimal dissociation, (Brandt and Ross 1985; Higashijima et al., 1987; Katada and

Oinuma 1986). At the adenylyl cyclase, Somkuti et al. (1982); and Pieroni (1995)

provided evidence that Mg^{2+}_i was essential for efficient adenylyl cyclase operation.

Their work showed that Mg^{2+}_i could increase the rate (V_{max}) of cAMP production

without altering the affinity (K_m) for the substrate. Finally, I assume that PKA

phosphorylation also requires Mg^{2+}_i, since most kinase activity requires both the Mg^{2+}-

ATP complex and free Mg^{2+}_i to function effectively (Sun and Budde 1997). All of

these studies demonstrated that Mg^{2+}_i is an essential factor for activation, and most

importantly not one of them revealed any inhibitory influence from Mg^{2+}_i, even at the

millimolar level.

As mentioned above, the amount of stimulation increased greatly when the

Mg^{2+}_i level was elevated from 100 μM to 5 mM (see Figure 16A), even though the

overall current density declined by 30 % (p=0.002) (see Figure 15A). I believe this

reduction in current density is similar to the inhibitory process observed under basal

conditions, as it shows the underlying inhibitory process activated by Mg^{2+}_i under basal

conditions is still present with ISO stimulation. Based on the fact that all the research

showed no hindrance by Mg^{2+}_i even in the millimolar range for all the steps involved in

β-adrenergic stimulation, I hypothesize that the smaller ISO stimulated density recorded at 1 and 5 mM Mg^{2+}_i is caused by the activation of an inhibitory process rather than an inhibition of one of the steps involved in the production of cAMP. Although the identity of these proteins remains undetermined, likely candidates include Mg^{2+}-dependent phosphodiesterases (Jost and Rickenberg 1971; Meacci et al., 1992; Percival et al., 1997; Fisher et al., 1998) and/or the Mg^{2+}-dependent protein phosphatase PP2C (McGowan and Cohen 1988).

(2) Mg^{2+}_i requirements for FSK stimulation of $I_{Ca,L}$

In order to distinguish the Mg^{2+}_i requirements for the individual steps involved in $I_{Ca,L}$ stimulation by the β-adrenergic system, FSK was used to bypass the G-protein and directly stimulate the adenylyl cyclase. The findings from these tests shown on Figures 15C and 16C demonstrated the following features: (i) Mg^{2+}_i had a bimodal effect on the $I_{Ca,L}$ density similar to that observed under basal condition; (ii) the amount of $I_{Ca,L}$ stimulation by FSK was significant at all levels of Mg^{2+}_i, even at 1 μM, the amount of stimulation was almost 3-fold ($p<0.001$); (iii) the degree of stimulation did not change significantly above 17 μM Mg^{2+}_i ($p=0.617$) (see Figure 16C) ; although, (iv) the current density decreased when the Mg^{2+}_i was elevated above 17 μM Mg^{2+}_i (see Figure 15C). Since FSK stimulation involves only the adenylyl cyclase and the PKA enzyme, it allows me to discriminate the Mg^{2+}_i requirements at these sites from the rest of the β-adrenergic system. From these results I theorize that the Mg^{2+}_i requirements at the adenylyl cyclase and the PKA are relatively low. The large stimulation observed at

1 μM suggests that the free Mg^{2+} requirements by these enzymes could be less than 1

μM in the guinea pig cardiomyocyte. Although 1 μM Mg^{2+}_i may be enough for

adenylyl cyclase and PKA activity, at least 17 μM is necessary for maximal activation,

and this is reflected by the observation that the maximum density occurred at 17 μM

(see Figure 15C). Although this result complies with prior adenylyl cyclase research to

the extent that a minimum level of Mg^{2+}_i is essential for activation, the concentration

required for maximal stimulation seems relatively low. As explained above, prior

research has shown that Mg^{2+}_i is a vital part of the adenylyl cyclase process, and that

millimolar concentrations of Mg^{2+}_i are necessary for optimum function i.e. EC_{50} ~1.5

mM (Steinberg et al., 1986) to EC_{50} ~ 3.5 mM Mg^{2+}_i (Narayanan and Sulakhe, 1977;

Narayanan et al., 1979). These differences in the apparent Mg^{2+}_i requirements in my

experiments and the in vitro experiments could be explained by the use of different

experimental conditions. The seemingly higher Mg^{2+}_i affinity derived from my results

could be partially explained by the fact that an intact cell as opposed to a membrane

extract is being used. The higher apparent affinity recorded in the intact cell could be

attributed to a less disrupted cytoplasmic environment and membrane-bound adenylyl

cyclase. Although this may account for some of the discrepancies, another possibility

could be the presence of an inhibitory enzyme in the intact cell which is absent in the

membrane extract. As observed on Figure 15C, elevating the Mg^{2+}_i concentrations

beyond the 17 μM level led to increasingly smaller $I_{Ca,L}$ density, even though the

percentage of stimulation was not significantly smaller at the higher concentrations (see

Figure 16C). These results reveal that an inhibitory process similar to the one under

basal conditions is activated when Mg^{2+}_i level exceeds 17 μM. The consequence of this phenomenon is an underestimation of the Mg^{2+}_i requirement, which would account for a portion of the higher apparent affinity for Mg^{2+}_i.

Since the inhibition caused by high Mg^{2+}_i is not likely caused by adenylyl cyclase suppression, or PKA inhibition, other candidates include the Mg^{2+}_i stimulated protein phosphatase PP2C (McGowan and Cohen 1988) or phosphodiesterase stimulation. I did not study the inhibitory influence from PP2C because of the lack of an appropriate inhibitor. This is unfortunate since PP2C is found in the heart and is stimulated by Mg^{2+}. However, the other inhibitory candidate, phosphodiesterase, was studied. To determine if the activation of phosphodiesterase was limiting the stimulation by FSK, IBMX was applied together with FSK at 5 mM Mg^{2+}_i. The results from these experiments showed that there was a further increase in the current amplitude by 2 pA/pF, and the test of significance revealed a p=0.01. This result shows that the activation of phosphodiesterase does play a role in limiting the amount of stimulation by FSK. The effects of Mg^{2+}_i on phosphodiesterase are discussed in depth in the next section.

(3) Mg^{2+}_i requirements for stimulation of $I_{Ca,L}$ by phosphodiesterase inhibition

In order to determine the influence of phosphodiesterase on $I_{Ca,L}$, I used the non-specific phosphodiesterase inhibitor IBMX. The features from these experiments shown on Figures 15B and 16B are: (i) IBMX failed to stimulate the $I_{Ca,L}$ beyond the basal level when the cells were dialyzed with 1 (p=0.453) and 17 μM (p=0.076) Mg^{2+}_i;

(ii) at least 30 µM (p=0.012) Mg^{2+}_i was required to stimulate phosphodiesterase; (iii) higher levels of Mg^{2+}_i produced stronger and faster IBMX stimulatory responses; and (iv) the IBMX response did not decrease at higher Mg^{2+}_i levels.

Stimulation of the L-type calcium current by IBMX occurs by stimulating the cAMP-dependent phosphorylation of the Ca^{2+}-channel by indirectly elevating the level of cAMP through the inhibition of its breakdown. This experiment gives a good indication of the basal activity of both the adenylyl cyclase, and the phosphodiesterase. For example, in Figure 15B, when the cells were dialyzed with 1 and 17 µM Mg^{2+}_i, IBMX failed to stimulate the $I_{Ca,L}$ beyond the level observed under the basal condition. This result indicates that either the level of phosphodiesterase activity at these Mg^{2+}_i concentrations is negligible, or the level of adenylyl cyclase activity is zero. The second alternative pertaining to adenylyl cyclase activity can be dismissed due to the fact that the elevation of Mg^{2+}_i from 1 to 17 µM is accompanied by an increase in current density, and this increase requires cAMP-dependent channel phosphorylation. In other words, this result indicates that the increase in current when Mg^{2+}_i was elevated from 1 to 17 µM is caused by an increase in adenylyl cyclase activity. Therefore, it must be assumed that the level of phosphodiesterase activity is negligible when the Mg^{2+}_i level is ≤ 17 µM.

As reviewed in the introduction, about three different phosphodiesterases are found in the cardiomyocytes that exhibit higher affinities for cAMP than cGMP: PDE3 (Meacci et al., 1992); PDE4 (Percival et al., 1997); and PDE8 (Fisher et al., 1998). All of these phosphodiesterases need free Mg^{2+}_i for their catalytic activity. The Mg^{2+}_i

requirements differ for each phosphodiesterase, the EC_{50} for PDE3 is 200 μM

(MacPhee et al., 1988), PDE4 is 100 μM (Percival et al., 1997), and 400 μM for PDE8

(Fisher et al., 1998). In agreement with these studies, my experiments indicate a

requirement of ~30 μM Mg^{2+}_i, and the apparent EC_{50} would be between 30 and 100

μM. This interpretation is supported by Figure 16B, which shows that at least 30 μM of

Mg^{2+}_i was required to significantly stimulate the $I_{Ca,L}$ by IBMX, and the concentration

of half maximal stimulation seemed to be between 30 and 100 μM. This result shows

that under basal condition, not only is phosphodiesterase activated by 30 μM Mg^{2+}_i but

that the amount of activation is greater than that of the adenylyl cyclase. In fact, the

decrease in current density observed under basal conditions when Mg^{2+}_i levels are

above 17 μM reveals that the activation of phosphodiesterase by Mg^{2+}_i becomes

increasingly stronger than the activation of adenylyl cyclase (see Figure 5A). The

potency of the phosphodiesterase activity under basal conditions can be put into

perspective when it is analyzed in Figure 16B. This figure illustrates that in the absence

of phosphodiesterase activity, the level of adenylyl cyclase under basal condition is

increased by as much as ~200 % when the Mg^{2+}_i level is elevated from 1 μM to ≥ 100

μM; therefore, the activation of phosphodiesterase must be greater than ~200% at

similar Mg^{2+}_i levels to cause the amount of reduction in current density observed under

basal conditions.

(4) Summary of Mg^{2+}_i regulation of $I_{Ca,L}$ by phosphorylation

Although the influence of Mg^{2+}_i on the PKA and PP2C enzymes was not directly studied here, its impact cannot be ignored. I suggest that the regulatory influence of Mg^{2+}_i on PKA would most likely be minor. This is supported by the fact that the Mg^{2+}_i requirements for PKA activation is no greater than 1 μM as shown by the large stimulation at 1 μM by FSK; in addition, I hypothesize the limiting factor for PKA activation under physiological conditions would be the level of cAMP and not Mg^{2+}_i. The regulatory influence of Mg^{2+}_i on phosphatase, is hard to quantify since I was not able to study it directly. However, based on the fact that Mg^{2+}_i is known to stimulate PP2C (McGowan and Cohen, 1988), I must assume that a certain level of phosphatase activation must occur at the higher Mg^{2+}_i levels. In my experiments, the most probable effect from this phenomenon is shown on Figure 11. This figure shows that even with adenylyl cyclase stimulation and phosphodiesterase inhibition, an inhibitory process persists at >1mM Mg^{2+}_i. The activation of a phosphatase by high Mg^{2+}_i was also proposed by White and Hartzell in 1988 to explain their results. They observed that under β-adrenergic stimulation, a 50 % inhibition occurred when the Mg^{2+}_i was elevated from 0.3 mM to 3 mM. Therefore, I must assume that a certain level of phosphatase activation must occur at the higher Mg^{2+}_i levels, and the implication of this effect would be an underestimation of the stimulatory pathway.

All the data from my experiments led me to hypothesize that most of the effect of Mg^{2+}_i on the $I_{Ca,L}$ is focused on the net production of cAMP. The bimodal effect on the $I_{Ca,L}$ that I observed under basal conditions reflects a bimodal change in the cAMP level, which is caused primarily by the differences in Mg^{2+} concentration dependency of

the enzyme adenylyl cyclase, and phosphodiesterase. I propose the following mechanism to describe the data: at very low Mg^{2+}_i, in the nominal range (1 μM), $I_{Ca,L}$ is minimal because of very low adenylyl cyclase activity; as the Mg^{2+}_i level is increased to about 17 μM, the basal $I_{Ca,L}$ increases to its maximum level; the basal $I_{Ca,L}$ is largest at this Mg^{2+}_i concentration because it yields the highest net concentration of cAMP; there is enough Mg^{2+}_i to increase the function of the adenylyl cyclase, while at the same time insufficient to activate the phosphodiesterase. At higher levels of Mg^{2+}_i (≥30 μM), although the activity of adenylyl cyclase is enhanced, the function of the PDEs is also stimulated but to greater extent, resulting in a net reduction in the level of cAMP, diminishing the level cAMP-dependent phosphorylation, and causing a reduction in the $I_{Ca,L}$ amplitude.

SECTION D. Mg^{2+}_i EFFECTS ON Ca^{2+}-CHANNEL INACTIVATION:

The other salient feature of these results is the effect of Mg^{2+}_i on $I_{Ca,L}$ inactivation. The inactivation parameters τ_f and τ_s summarized on Figures 18 and 19 show: (i) inactivation is inhibited by Mg^{2+}_i; (ii) inactivation is independent of channel phosphorylation; and (iii) inactivation is independent of current density amplitude. In consideration of the most recent findings, I hypothesize that the Mg^{2+}_i inhibition of $I_{Ca,L}$ inactivation is related to Ca^{2+} dependent inactivation. These studies seem to support Ca^{2+}-induced inhibition results from Ca^{2+} binding to a channel-associated calmodulin (Zulke and Reuter 1998; Peterson et al., 1999; 2000). These researchers, demonstrated two very important factors that relate to the current study: (i) calmodulin-induced inactivation is only dependent on the Ca^{2+} entering the channel pore, and the $I_{Ca,L}$ amplitude has negligible effects on inactivation (Peterson et al., 1999 Figure 2c); and (ii) inactivation is dependent on a calmodulin that is constitutively linked to the α_{1c} subunit (Zulke and Reuter 1998; Peterson et al., 1999; 2000).

With respect to the first point, the results of the present study indicate that the rate of inactivation is independent of both the current amplitudes and cAMP-dependent phosphorylation. This is illustrated on Figures 18 and 19 which show no significant differences in the inactivation times between the different phosphorylated conditions when the Mg^{2+}_i concentrations were the same; in addition, the inactivation constants were not significantly different even though the current densities from the cAMP-pre-loaded cells were on average 10-times greater than the phosphorylation-inhibited

116

(K252a-treated) cells. The importance of these observations is their relationships to the mechanisms of Ca^{2+}-channel regulation. These results indicate that cAMP-dependent phosphorylation plays a major role in determining current amplitude, and has little impact on Ca^{2+} dependent inactivation.

Even though the amplitude of the $I_{Ca,L}$ did not affect the rate of inactivation, there was a clear trend towards longer τ_f and τ_s for all conditions (basal or drug stimulated) with increasing levels of Mg^{2+}_i. These results, as observed in Figure 18 and 19, strongly suggest that Mg^{2+}_i inhibits $I_{Ca,L}$ inactivation in a concentration dependent manner. I postulate that the Mg^{2+}_i inhibition of the Ca^{2+} dependent inactivation is caused by its influence on the calmodulin molecule. As proven by Zulke and Reuter (1998) and Peterson and colleagues (1999 and 2000), activation of the calmodulin that is constitutively linked to the α_{1c} subunit is an essential step towards $I_{Ca,L}$ inactivation. Peterson's group (1999 and 2000) proposed that channel inactivation occurs by activation of the tethered calmodulin by Ca^{2+} entry via the L-type Ca^{2+}-channel and the calmodulin's subsequent interaction with an IQ-like motif on the carboxyl tail of the α_{1c} (refer to Figure 22 for a simplified model of Ca^{2+} dependent inactivation). Thus, Ca^{2+}-activation of the calmodulin that is tethered to the channel is of primary importance. My findings suggest that Mg^{2+}_i might somehow prevent the activation of calmodulin. To support this concept, there are a number of studies that have shown that Mg^{2+} can inhibit the activation of calmodulin by acting as a competitive inhibitor of Ca^{2+} (Iida and Potter 1986; Ogawa and Tanokura, 1984; Ohki et al., 1996 and 1997). In addition to Mg^{2+}_i's effects as an antagonist to Ca^{2+}, Ohki et al., (1997) demonstrated that excess

$Mg^{2+}{}_i$ could lower the binding of activated calmodulin to its target peptides by as much as 40-fold. In consideration of these studies, I postulate that $Mg^{2+}{}_i$ progressively out-competes Ca^{2+} at the calmodulin molecule with increasing levels of $Mg^{2+}{}_i$, leading to a reduced Ca^{2+} dependent inactivation.

Figure 22: Simplified model of Ca^{2+} dependent inactivation of the L-type cardiac Ca^{2+}-channel. 1) Ca^{2+} entering the cells via the channel activates a calmodulin molecule that is tethered to the α_{1C} subunit. 2) Activation of the calmodulin by Ca^{2+} increases its affinity for the IQ-motif and binds on to it. 3) Binding of the IQ-motif to the calmodulin molecule causes the EF-hand motif to "open" resulting in a change in the channel structure causing it to inactivate. This simplified model is adopted from Peterson et al., (1999 and 2000). I hypothesize that $Mg^{2+}{}_i$ inhibits Ca^{2+} inactivation by inhibiting the activation of the calmodulin molecule by acting as a competitive antagonist at the Ca^{2+}-binding sites on the calmodulin molecule.
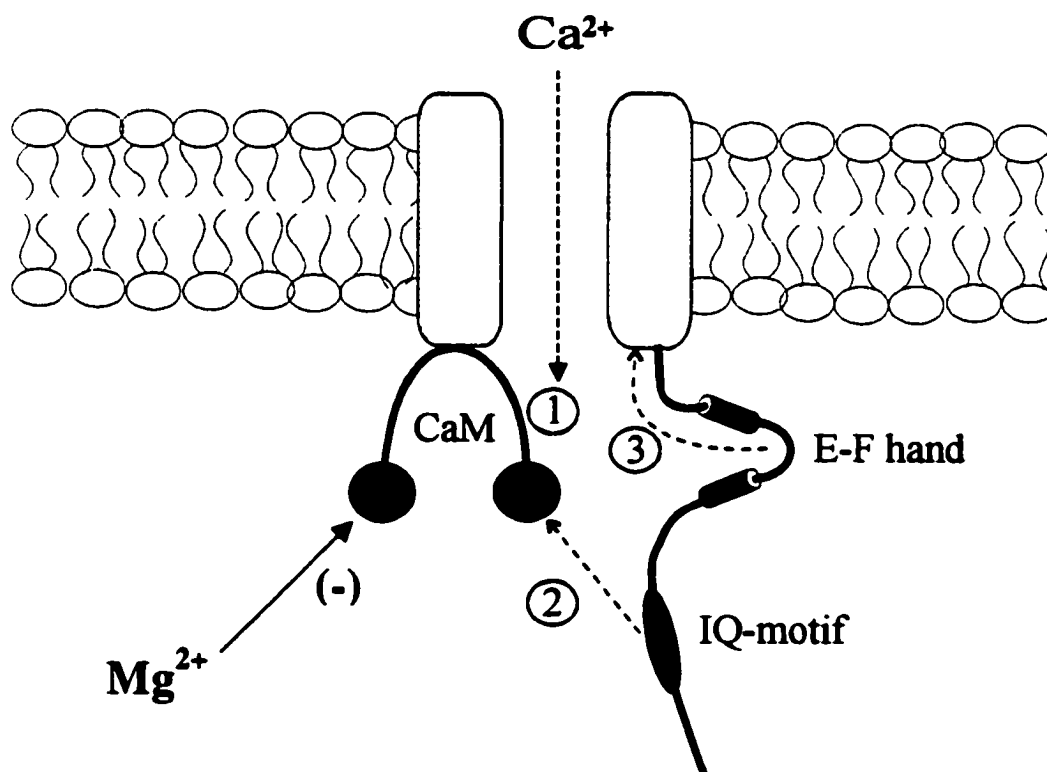
SECTION E. Mg^{2+}_i EFFECTS ON Ca^{2+}-INFLUX THROUGH

L-TYPE Ca^{2+}-CHANNEL:

In consideration of the present information, I propose that Mg^{2+} inhibits $I_{Ca,L}$ inactivation by acting as a competitive inhibitor of Ca^{2+} at the Ca^{2+}-binding site on the calmodulin which is associated with the α_{1C} subunit. Thus at higher levels of Mg^{2+}_i, a lower amount of Ca^{2+} dependent calmodulin would be stimulated leading to a reduction of the Ca^{2+} dependent inhibition. The intriguing aspect of this phenomenon is not its effect on $I_{Ca,L}$ amplitude, but rather its impact on the magnitude of the Ca^{2+} influx. As observed on Figure 17, especially for ISO and IBMX treated cells, there is a clear trend towards a higher influx of Ca^{2+} with increasing Mg^{2+}_i. When compared with the $I_{Ca,L}$ density in Figure 15 and inactivation time constants in Figures 18 and 19, I recognize that the total Ca^{2+} influx is highly dependent on the rate of channel inactivation and to a lesser extent the peak amplitude. For instance, under basal conditions, even though the $I_{Ca,L}$ amplitude at 5 mM Mg^{2+} is less than 50% of the amplitude at 17 μM, the total Ca^{2+} influx at 5 mM Mg^{2+} is not significantly different than at 17 μM Mg^{2+}_i (p=0.352).

119

SECTION F. RELEVANCE OF STUDY:

(1) Physiological relevance of Mg^{2+}_i's effect on cAMP dependent phosphorylation

The present study indicates that Mg^{2+}_i may be an important factor in the regulation of cAMP dependent stimulation. As demonstrated by the experiments involving isoproterenol, at least 17 μM of free Mg^{2+} was required to significantly stimulate the $I_{Ca,L}$ above the level observed under basal conditions, however perhaps more consequential is the observation that the degree of stimulation is acheived in a graded manner with higher levels of Mg^{2+}_i, throughout the physiological Mg^{2+}_i range. Similarly, the experiments with the phosphodiesterase inhibitor (IBMX) also exhibited a graded response with increasing Mg^{2+}_i in the physiological range. These results indicate that Mg^{2+}_i may act to determine the gain in the β-adrenergic pathway.

(2) Physiological relevance of Mg^{2+}_i's effect on inactivation

Physiologically, Mg^{2+}_i might play an important role in the calcium-induced calcium-release mechanism (CICR), and hence the activation of cardiac contraction. Dr. Eisner's work with CICR demonstrated that the L-type Ca^{2+}-current not only triggers the release of Ca^{2+} from the sarcoplasmic reticulum but also loads the cell with Ca^{2+} to balance the efflux produced by the systolic Ca^{2+} transient (Eisner et al., 1998;

120

Trafford et al., 2001). His work suggests that increasing the current amplitude alone would result in a purely transient increase of systolic Ca^{2+} and over time decrease the sarcoplasmic reticulum content (Trafford et al., 1998; 2000). This situation resembles the condition where the Mg^{2+}_i level is low in my experiments and is characterized by large Ca^{2+}-current amplitude and small Ca^{2+}-influx. In contrast, Eisner suggests that increasing the loading effect without elevating the amplitude would raise both the systolic Ca^{2+} and the sarcoplasmic reticulum content (Eisner et al., 1998). This situation is reflected by my condition where the Mg^{2+}_i level is greatest, characterized by smaller Ca^{2+} current amplitude and large Ca^{2+}-influx.

V. BIBLIOGRAPHY

Adams B., and Tanabe T., (1997) Structural regions of the cardiac Ca channel α_{1C} subunit involved in Ca-dependent inactivation. J Gen Physiol **110**: 379-389.

Agus ZS., Kelepouris E., Dukes I., and Morad M., (1989) Cytosolic magnesium modulates calcium channel activity in mammalian ventricular cells. Am J Physiol **256**: C452-C455.

Albillos A., Neher E., and Moser T., (2000) R-type Ca^{2+} channels are coupled to the rapid component of secretion in mouse adrenal slice chromaffin cells. J Neurosci **20(22)**: 8323-8330.

Amano T., Matsubara T., Watanabe J., Nakayama S., and Hotta N., (2000) Insulin modulation of intracellular free magnesium in heart: involvement of protein kinase C. Brit J Pharmacol **130**: 731-738.

Antoni FA., (2000) Molecular diversity of cyclic AMP signalling. Fronteirs Neuroendocrinology **21(2)**: 103-132.

Armstrong DL., (1989) Calcium channel regulation by calcineurin, a Ca^{2+}-activated phosphatase in mammalian brain. Trends Neurosci **12**: 117-122.

Backx PH., O'Rourke B., and Marban E., (1991) Flash photolysis of magnesium-DM-Nitrophen in heart cells. A novel approach to probe magnesium and ATP dependent regulation of calcium channels. Am J Hypertension **4**: 416S-421S.

Balke CW., and Wier WG., (1992) Modulation of L-type calcium channels by sodium ions. Proc Natl Acad Sci (USA) **89**: 4417-4421.

Bangalore R., Mehrke G., Gingrich K., Hofmann F., and Kass RS., (1996) Influence of L-type Ca channel α_{2d}-subunit. Am J Physiol **270**: H1521-1528.

Baumann, A., Grupe A., Ackerman A., and Pongs O., (1988) Structure of the voltage-dependent potassium channel is highly conserved from *Drosophila* to vertebrate central nervous system. EMBO J **7**: 2457-2463.

Baumann A., Krah-Jentgens I., Muller R., Muller-Holtkamp F., Seidel R., Keckskemethy N., Casal J., Ferrus A., and Pongs O., (1987) Molecular organization of the maternal effect region of the Shaker complex of *Drosophila*: characterization of an I_A channel transcpript with homology to vertebrate Na^+ channel. EMBO J **6**: 3419-3429.

Bean BP., (1984) Nitrendipine block of cardiac calcium channels: high-affinity binding to the inactivated state. Proc Natl Acad Sci (USA) **81**: 6388-6392.

Bean BP., Nowycky MC., and Tsien RW., (1984) β-adrenergic modulation of calcium channels in frog ventricular heart cells. Nature (Lond) **307**: 371-375.

Bean BP., (1985) Two kinds of calcium channels in canine atrial cells. Differences in kinetics, selectivity, and pharmacology. J Gen Physiol **86**: 1-30.

Beavo JA., and Reifsnyder DH., (1990) Primary sequence of cyclic nucleotide phosphodiesterase isoenzymes and the design of selective inhibitors. Trends in Pharmacol Sciences **11**: 150-155.

Beeler GW., and Reuter H., (1970) The relation between membrane potential, membrane currents, and activation contraction in ventricular myocardial fibres. J Physiol (Lond) **207**: 211-229.

Belardinelli L., Giles WR., and West A., (1988) Ionic mechanisms of adenosine actions in pacemakers cells from rabbit heart. J Physiol (Lond) **405**: 615-633.

Belles B., Hescheler J., Trautwein W., Blomgren K., and Karlsson JO., (1988) A possible role of the Ca-dependent protease calpain and its inhibitor calpastatin on the Ca current in guinea pig myocytes. Pfluegers Arch **412**: 554-556.

Belles B., Malécot CO., Hescheler J., and Trautwein W., (1988b) 'Rund-down' of the Ca current during long whole-cell recordings in guinea pig heart cells: role of phosphorylation and intracellular calcium. Pfluegers Arch **411**: 353-360.

Birnbaumer L, Pohl SL, and Rodbell M (1969) Adenyl cyclase in fat cells 1. Properties and the effects of adrenocorticotropin and fluoride. J Biol Chem **224**: 3468-3476.

Blatter LA., and McGuigan JAS., (1988) Estimation of the upper limit of the free magnesium concentration measured with Mg-sensitive microelectrodes in ferret ventricular muscle: (1) use of the Nicolsky-Eisenman equation and (2) in calibrating solutions of the appropriate concentration. Magnesium 7: 154-165.

Bloom TJ., and Beavo JA., (1996) Identification and tissue-specific expression of PDE7 phosphodiesterase splice variants. Proc Natl Acad Sci 93: 14188-14192.

Brandt DR., and Ross EM., (1985) GTPase activity of the stimulatory GTP-binding regulatory protein of adenylate cyclase, G_s-accumulation and turnover of enzyme-nucleotide intermediates. J Biol Chem 260: 266-272.

Brehm P., and Eckert R., (1978) An electrophysiological study of the regulation of ciliary beating frequency in Paramecium. J Physiol (Lond) 283: 557-68.

Brum G., Flockerzi V., Hofmann F., Osterrieder W., and Trautwein W., (1983) Injection of catalytic subunit of cAMP-dependent protein kinase into isolated cardiac myocytes. Pfluegers Arch 398: 147-154.

Brum G., Osterrieder W., and Trautwein W., (1984) β-adrenergic increase in the calcium conductance of cardiac myocytes studied with the patch clamp. Pfluegers Arch 401: 111-118.

Bünemann M., Gerhardstein BL., Gao T., and Hosey MM., (1999) Functional regulation of L-type calcium channels via protein kinase A-mediated phosphorylation of the β_2 subunit. J Biol Chem 274: 33841-33854.

Butcher RW., and Sutherland EW., (1962) Adenosine 3',5'-phosphate in biological materials. I. Purification and properties of cyclic 3'5'-nucleotide phosphodiesterase and use of this enzyme to characterize adenosine 3'5'-phosphate in human urine. J Biol Chem 237: 1244-1250.

Campbell DL., Giles WR., Hume JR., and Shibata EF., (1988) Inactivation of calcium current in bull-frog atrial myocytes. J Physiol (Lond) 403: 287-315.

Carmeliet E., Morad M., Van Der Heyden G., and Vereecke J., (1986) Electrophysiological effects of tetracaine in single guinea-pig ventricular myocytes. J. Physiol (Lond) **376:** 143-161.

Castellano A., Wei X., Birnbaumer L., and Perez-Reyes E., (1993a) Cloning and expression of a neuronal calcium channel beta subunit. J Biol Chem **268:** 12359-12366.

Castellano A., Wei X., Birnbaumer L., and Perez-Reyes E., (1993b) Cloning and expression of a third calcium channel β subunit. J Biol Chem **268:** 3450-3455.

Catterall WA., (1988) Structure and function of voltage-sensitive ion channels. Science **242:** 50-61.

Catterall WA., (1993)Structure and function of voltage-gated ion channels. Trends Neurosci **16:** 500-506.

Catterall WA., (2000) Structure and regulation of voltage-gated Ca^{2+} channels. Annu Rev Cell Dev Biol **16:** 521-555.

Cavalie A., Allen TJA., and Trautwein W., (1991) Role of GTP-binding protein in G_s in the β-adrenergic modulation of cardiac Ca channels. Pfluegers Arch **419:** 433-443.

Cavalie A., Pelzer D., and Trautwein W., (1983) Fast and slow gating behaviour in single calcium channels in cardiac cells. Relations to activation and inactivation of calcium-channel current. Pfluegers Arch **406:** 241-258.

Chad JE., and Eckert R., (1984) Calcium domains associated with individual channels can account for anomalous voltage relations of Ca-dependent responses. Biophys J **45:** 993-999.

Chad JE., and Eckert R., (1986) An enzymatic mechanism for calcium current inactiviation in dialysed Helix neurones. J Physiol (Lond) **378:** 31-51.

126

Cleemann L., and Morad M., (1991) Role of Ca^{2+} channel in cardiac excitation-contraction coupling in the rat: evidence from Ca^{2+} transients and contraction. J Physiol (Lond) 432: 283-312.

Colvin RA., Obio JA., and Allen RA., (1991) Calcium inhibition of cardiac adenylyl cyclase - evidence for two distinct sites of inhibition. Cell Calcium 12: 19-27.

Cooper DMF., Karpen JW., Fagan KA., and Mons NE., (1998) Ca^{2+}-sensitive adenylyl cyclases. Adv in Second Messenger and Phosphoprotein Res 32: 23-51.

Cooper DMF., Mons N., and Karpen JW., (1995) Adenylyl cyclases and the interaction between calcium and cAMP signaling. Nature (Lond) 374: 421-424.

Corey DP., and Stevens CF., (1983) Science and technology of patch-recording electrodes. In: Single Channel Recording, edited by Sakmann B., and Neher E., New York: Plenum Press p. 53-68.

Corkey BE., Duszynski J., Rich TL., Matschinsky B., and Williamson JR., (1986) Regulation of free and bound magnesium in rat hepatocytes and isolated mitochondria. J Biol Chem 261: 2567-2574.

Coronado R., Morrisette J., and Sukhareva M., (1994) Structure and function of ryanodine receptors. Am J Physiol 266: C1485-C1504.

Davare MA., Dong F., Rubin CS., Hell JW., (1999) The A-kinase anchor protein MAP2B and cAMP-dependent protein kinase are associated with class C L-type calcium channels in neurons. J Biol Chem 274: 30280-30287.

De Jongh KS., Warner C, Cattrall WA., (1990) Subunits of purified calcium channels. Alpha 2 and delta are encoded by the same gene. J Biol Chem 265: 14738-14741.

De Jongh K., Warner C., Colvin A., Catterall W., (1991) Characterization of the two size forms of the α1 subunit of skeletal muscle L-type calcium channels. Proc Natl Acad Sci (USA) 88: 107788-10782.

De Jongh KS., Murphy BJ., Colvin AA., Hell JW., Takahshi M., and Catterall WA., (1996) Specific phosphorylation of a site in the full length form of the α_1 subunit of the

cardiac L-type calcium channel by adenosine 3',5'-cyclic monophosphate-dependent protein kinase. Biochemistry **35**: 10392-10402.

De Leon M., Wang Y., Jones L., Perez-Reyes E., Wei X., Soong TW., Snutch TP., and Yue DT., (1995) Essential Ca^{2+}-binding motif for Ca^{2+}-sensitve inactivation of L-type Ca^{2+} channels. Science **270**: 1502-1506.

Droogmans G., and Nilius B., (1989) Kinetic properties of the cardiac T-type calcium channel in the guinea-pig. J Physiol (Lond) **419**: 627-650.

Drummond GI, and Duncan L (1970) Adenylate cyclase in cardiac tissue. J Biol Chem **245**: 976-983.

Eckert R., and Chad JE., (1984) Inactivation of Ca channels. Prog Biophys Mol Biol **44**: 215-267.

Eisner DA., Trafford AW., Diaz ME., Overend CL., and O'neill SC., (1998) The control of Ca release from the cardiac sarcoplasmic reticulum: regulation versus autoregulation. Cardiovasc Res **38**: 589-604.

Endo M., Tanaka M., and Ogawa Y., (1970) Calcium induced release of calcium from the sarcoplasmic reticulum of skinned skeletal muscle fibres. Nature (Lond) **228**: 34-36.

Fabiato A., (1985) Rapid ionic modification during the aequarin-detected calcium transient in skinned canine cardiac Purkinje cell. J Gen Physiol **85**: 189-246.

Fabiato A., (1989) Appraisal of the physiological relevance of two hypothesis for the mechanism of calcium release from the mammalian cardiac sarcoplasmic reticulum: calcium-induced release versus charge-coupled release. Mol Cell Biochem **89**: 135-140.

Fabiato A., and Fabiato F., (1977) Calcium release from the sarcoplasmic reticulum. Circ Res **40**: 119-129.

Ferrier GR., and Howlett SE., (1995) Contractions in guinea-pig ventricular myocytes triggered by a calcium-release mechanism separate from Na^+ and L-currents. J Physiol (Lond) **484**: 107-122.

Ferrier GR., and Howlett SE., (2001) Cardiac excitation-contraction coupling: role of membrane potential in regulation of contraction. Am J Physiol **280**: H1928-H10944.

Fischmeister R., and Hartzell HC., (1990) Regulation of calcium current by low-K_m cyclic AMP phosphodiesterases in cardiac cells. Mol Pharmacol **38**: 426-433.

Fischmeister R., and Shrier A., (1989) Interactive effects of isoprenaline, forskolin and acetylcholine on Ca^{2+} current in frog ventricular myocytes. J Physiol (Lond) **417**: 213-239.

Fisher DA, Smith JF, Pillar JS, St. Denis SH, and Cheng JB (1998) Isolation and characterization of PDE8A, a novel human cAMP-specific phosphodiesterase. Biochem Biophys Res Commun **246**: 570-577.

Flatman PW., (1984) Magnesium transport across cell membranes. J Memb Biol **80**:1-14.

Frace AM., Mery PF., Fischmeister R., and Hartzell HC., (1993) Rate-limiting steps in the β-adrenergic stimulation of cardiac calcium current. J Gen Physiol 101:337-353.

Gao T., Yatani A., Dell' Acqua ML., Sako H., Green SA., Drascal A., Scott SD., Hosey MM., (1997) cAMP-dependent regulation of cardiac L-type Ca^{2+} channels requires membrane targeting of PKA and phosphorylation of channel subunits. Neuron **19**: 185-196.

Gerhardstein BL., Gao T., Bünemann M., Puri TS., Adair A., Ma H., Hosey MM., (2000) Proteolytic processing of the C terminus of the $α_{1c}$ subunit of L-type calcium channels and the role of a proline-rich domain in membrane tethering of proteolytic fragments. J Biol Chem 275: 8556-8563.

Goldhaber JI., Parker JM., and Weiss JN., (1991) Mechanisms of excitation-contraction coupling failure during metabolic inhibition in guinea-pig ventricular myocytes. J Physiol (Lond) **443**: 371-386.

Gow IF., Latham T., Ellis D., and Flatman PW., (1995) Measurement of intracellular ionized magnesium concentration in myocytes isolated from the septomarginal band of sheep hearts. Magneisum Research 8: 223-232.

Gurnett CA., De Waard M., and Campbell KP., (1996) Dual function of the voltage-dependent Ca^{2+} channel α_{2d} subunit in current stimulation and subunit interaction. Neuron 16: 431-440.

Guy HR., and Conti F., (1990) Pursuing the structure and function of voltage-gated channels. Trends Neurosci 13: 201-206.

Hadley RW., and Hume JR., (1987) An intrinsic potential-dependent inactivation mechanism associated with calcium channels in guinea-pig myocytes. J Physiol (Lond) 389: 205-222.

Hamill OP., Marty A., Neher E., Sakmann B., and Sigworth FJ., (1981) Improved patch clamp techniques for high-resolution current recording from cells and cell-free membrane patches. Pflugers Arch 391: 85-100.

Han P., Zhu X., and Michaeli T., (1997) Alternative splicing of the high affinity cAMP-specific phosphodiesterase (PDE7A) mRNA in human skeletal muscle and heart. J Biol Chem 272: 16152-16157.

Handy RD., Gow IF., Ellis D., and Flatman PW., (1996) Na-dependent regulation of intracellular free magnesium concentration in isolated rat ventricular myocytes. J Mol Cell Cardiol 28: 1641-1651.

Hartzell HC., and Budnitz D., (1992) Differences in effects of forskolin and an analog on calcium currents in cardiac myocytes suggest intra- and extracellular sites of action. Mol Pharmacol 41: 880-888.

Hartzell HC., and Fischmeister R., (1987) Effect of forskolin and acetylcholine on calcium current in single isolated cardiac myocytes. Mol Pharmacol 32: 639-645.

Hartzell HC., and White RE., (1989) Effects of magnesium on inactivation of the voltage-gated calcium current in cardiac myocytes. J Gen Physiol **94:** 745-767.

Hartzell HC., Mery PF., Fischmeister R., and Szabo G., (1991) Sympathetic regulation of cardiac calcium current is due exclusively to cAMP-dependent phosphorylation. Nature (Lond) **351:** 573-576.

Haase H., Karczewski P., Beckert R., and Krause EG., (1993) Phosphorylation of the L-type calcium channel beta subunit is involved in beta-adrenergic signal transduction in canine myocardium. FEBS Lett **335:** 217-22.

Hell JW., Yokoyama CT., Wong ST., Warner C., Snutch TP., and Catterall WA., (1993) Differential phosphorylation of two size forms of the neuronal class C L-type calcium channel α_1 subunit. J Biol Chem **268:** 19451-19457.

Hell JW., Yokoyama CT., Breeze LJ., Chavkin C., and Catterall WA., (1995) Phosphorylation of presynaptic and postsynaptic calcium channels by cAMP-dependent protein kinase in hippocampal neurons. EMBO J **14:** 3036-3044.

Hell JW., Westenbroek RE., Breeze LJ., Wang KKW., Chavkin C., and Catterall WA., (1996) N-methyl-D-aspartate receptor-induced proteolytic conversion postsynaptic class C L-type calcium channels in hippocampal neurons. Proc Natl Acad Sci USA **93:** 3362-3367.

Hescheler J., Kameyama M., Trautwein W., Mieskes G., and Soling H.D., (1987) Regulation of the cardiac calcium channel by protein phosphatases. Eur J Biochem **165:** 261-266.

Hess P., and Tsein RW., (1984) Mechanism of ion permeation through calcium channels. Nature (Lond) **309:** 453-456.

Higashijima T., Ferguson KM., Sternweis PC., Smigel MD., and Gilman AG., (1987) Effects of Mg^{2+} and the $\beta\gamma$-subunit complex on the interaction of guanine nucleotides with G proteins. J Biol Chem **262:** 2762-766.

Hille B., (1994) Modulation of ion-channel function by G-protein-coupled receptors. Trends Neurosci **17:** 531-536.

Hirano Y., Fozzard HA., and January CT., (1989) Characteristics of L- and T-type Ca^{2+} currents in canine Purkinje cells. Am J Physiol **256**: H1478-H1492.

Hobi IA., and Levi AJ., (1999) Coming full circle: membrane potential, sarcolemmal calcium influx and excitation-contraction coupling in heart muscle. Cardiovasc Res **44**: 477-487.

Hoffmann F., Flockerzi V., Nastainczyk W., Ruth P., and Schneider T., (1990) The molecular structure and regulation of muscular calcium channels. Curr Top Cell Regul **31**: 223-239.

Horackova M., and Vassort G., (1976) Calcium conductance in relation to contractility in frog myocardium. J Physiol (Lond) **259**: 597-616.

Howlett SE., Zhu JQ., and Ferrier GR., (1998) Contribution of a voltage-sensitive calcium release mechanism to contraction in cardiac ventricular myocytes. Am J Physiol **274**: H155-H170.

Hullin R., Singer-Lahat D., Freichell M., Biel M., Dascal N., Hofmann F., and Flockerzi V., (1992) Calcium channel beta subunit heterogeneity: functional expression of cloned cDNA from heart, aorta and brain. EMBO J **11**: 885-890.

Imoto Y., Yatani A., Reeves JP., Codina J., Birnbauer L., and Brown AM., (1988) α-Subunit of G_s directly activates cardiac calcium channels in lipid bilayers. Am J Physiol **255**: 722-728.

Imredy JP., and Yue DT., (1992) Submicroscopic Ca^{2+} diffusion mediates inhibitory coupling between individual Ca^{2+} channels. Neuron **9**: 197-207.

Imredy JP., and Yue DT., (1994) Mechanism of Ca^{2+}-sensitive inactivation of L-type Ca^{2+} channels. Neuron **12**: 1301-1318.

Irisawa H., and Kokubun S., (1983) Modulation by intracellular ATP and cyclic AMP of the slow inward current in isolated single ventricular cells of the guinea-pig. J Physiol (Lond) **338**: 321-337.

Isenberg G., and Klockner U., (1980) Glycocalyx is not required for slow inward calcium current in isolated rat heart myocytes. Nature (Lond) **284**: 358-360.

Isenberg G., and Klockner U., (1982) Calcium currents of isolated bovine ventricular myocytes are fast and of large amplitude. Pfluegers Arch **395**: 30-41.

Jay SD., Ellis SB., McCue AF., Williams ME., Vedvick TS., Harpold MM., and Campbell FP., (1990) Primary structure of the gamma subunit of the DHP-sensitive calcium channel from skeletal muscle. Science **248**: 490-492.

Jay SD., Sharp AH., Kahl SD., Vedvick TS., Harpold MM., and Campbell KP., (1991) Structural characterization of the dihydropyridine-sensitive calcium channel alpha 2-subunit and the associated delta peptides. J Biol Chem **266**: 3287-3293.

Josephson IR., Sanchez-Chapula J., and Brown AM., (1984) A comparison of calcium currents in rat and guinea pig single ventricular cells. Circ Res **54**: 144-156.

Kameyama M., Hofmann F., and Trautwein W., (1985) On the mechanism of β-adrenergic regulation of the Ca channel in the guinea-pig heart. Pfluegers Arch **405**: 285-293.

Kameyama M., Hescheler J., Hofmann F., and Trautwein W., (1986) Modulation of Ca current during the phosphorylation cycle in the guinea pig heart. Pfluegers Arch **407**: 123-128.

Kameyama M., Kameyama A., Nakayama T., and Kaibara M., (1988) Tissue extract recovers cardiac calcium channels form rundown. Pfluegers Arch **412**: 328-330.

Kaspar SP., and Pelzer DJ., (1995) Modulation by stimulation rate of basal and cAMP-elevated Ca^{2+} channel current in guinea pig ventricular cardiomyocytes. J Gen Physiol **106**: 175-201.

Kass RS., and Sanguinetti MC., (1984) Inactivation of calcium channel current in the calf cardiac Purkinje fibre. Evidence for voltage- and calcium mediated mechanisms. J Gen Physiol **84**: 705-726.

Katada T., and Oinuma M., (1986) Two guanine nucleotide-binding proteins in rat brain serving as the specific substrate of islet-activating protein, pertussis toxin. J Biol Chem 261: 8182-8191.

Katzka DA., and Morad M., (1989) Properties of calcium channel in guinea-pig gastric myocytes. J Physiol (Lond) 413: 175-197.

Kayano T., Noda M., Flockerzi V., Takahashi H., and Numa S., (1988) Primary structure of rat brain sodium channel III deduced from the cDNA sequence. FEBS Lett 228: 187-194.

Keizer J., and Maki LW., (1992) Conditional probability analysis for a domain model of Ca^{2+}-inactivation of Ca^{2+} channels. Biophys J 63: 291-295.

Kepplinger JF., Forstner G., Kahr H., Leitner K., Pammer P., Groschner K., Soldatov NM., and Romanin C., (2000) Molecular determinant for run-down of L-type Ca^{2+} channels localized in the carboxyl terminus of the α_{1C} subunit. J Physiol (Lond) 529: 119-130.

Keung EC., and Karliner JS., (1990) Complex regulation of calcium current in cardiac cells. Dependence on a pertussis toxin-sensitive substrate, adenosine triphosphate, and an α_1-adrenoceptor. J Clin Invest 85: 950-954.

Lacerda AE., Kim HS., Ruth P., Perez-Reyes E., Flockerzi V., Hofmann F., Birnbaumer L., and Brown AM., (1991) Normalization of current kinetics by integration between the α_1 and β subunits of the skeletal muscle dihydropyridine-sensitive Ca^{2+} channel. Nature (Lond) 352: 527-530.

Laver DR., Baynes TM., and Dulhunty AF., (1997) Magnesium inhibition of ryanodine-receptor calcium channels: evidence for two independent mechanisms. J Membr Biol 156: 213-29.

Lee KS., and Tsien RW., (1982) Reversal of current through calcium channels in dialysed single heart cells. Nature (Lond) 297: 498-501.

Lee KS., and Tsien RW., (1984) High selectivity of calcium channels in single dialysed heart cells of the guinea pig. J Physiol (Lond) 354: 253-272.

Lew WYW., Hryshko LV., and Bers DM., (1991) Dihydropyridine receptors are primarily functional L-type calcium channels in rabbit ventricular myocytes. Circ Res **69**: 1139-1145.

Li HY., and Quamme GA., (1997) Caffeine decreases intracellular free Mg^{2+} in isolated adult rat ventricular myocytes. Biochim Biophys Acta **1355**: 61-68.

Liu J., Lai ZF., Wang XD., Tokutomi N., and Nishi K., (1998) Inhibition of sodium current by chloride channel blocker 4,4'-diisothiocyanatostilbene-2,2'-disulfonic acid (DIDS) in guinea pig cardiac ventricular cells. J Cardiovasc Pharmacol **31**: 558-567.

Londos C., and Preston MS., (1977) Activation of the hepatic adenylate cyclase system by divalent cations. J Biol Chem **252**: 5957-5961.

Lui W., Pasek DA., and Meissner G., (1998) Modulation of Ca^{2+}-gated cardiac muscle Ca^{2+}-release channel (ryanodine receptor) by mono and divalent ions. Am J Phyiol **274**: C120-C128.

Mackiewicz U., Emanuel K., and Lewartowski B., (1999) Voltage sensors in cardiac myocytes. J Mol Cell Cardiol **31**: A105.

McDonald TF., (1982) The slow inward calcium current in the heart. Annu Rev Physiol **44**: 425-434.

McDonald TF., Cavalie A., Trautwein W., and Pelzer D., (1986) Voltage-dependent properties of macroscopic and elementary calcium channel currents in guinea pig ventricular myocytes. Pfluegers Arch **406**: 437-448.

McDonald TF., Pelzer S., Trautwein W., and Pelzer DJ., (1994) Regulation and modulation of calcium channels in cardiac, skeletal, and smooth muscle cells. Am J Physiol **74**: 365-507.

McGowan CH., and Cohen P., (1988) Protein phosphatase-2C from rabbit skeletal muscle and liver: Mg^{2+}-dependent enzymes. In Methods in Enzymology (Corbin JD., and Johnson RA., eds.) Academic Press, London pp. 416-426.

MacPhee CH., Riefsnyder DH., Moore TA., Lerea KM., and Beavo JA., (1988) Phosphorylation results in activation of a cAMP phosphodiesterase in human platelets. J Biol Chem 263: 10353-10358.

Meacci E., Taira M., Moos MJ., Smith CJ., Movsesian MA., Degerman E., Belfarge P., and Manganiello V., (1992) Molecular cloning and expression of human myocardial cGMP-inhibited cAMP phosphodiesterase. Proc Natl Acad Sci 89: 3721-3725.

Mitra R., and Morad M., (1986) Two types of calcium channels in guinea pig ventricular myocytes. Proc Natl Acad Sci (USA) 83: 5340-5344.

Murphy E., Freudenrich CC., Levy LA., London RE., and Lieberman M., (1989) Monitoring cytosolic free magnesium in cultured chicken heart cells by use of the fluorescent indicator Furaptra. Proc Natl Acad Sci (USA) 86: 2981-2984.

Narayanan N., and Sulakhe PV., (1977) 5'-Guanylylimidodiphosphate-activated adenylate cyclase of cardiac sarcolemma displays higher affinity for magnesium ions. Mol Pharmacol 13: 1033-1047.

Narayana N., Wei JW., and Sulakhe PV., (1979) Differences in the cation sensitivity of adenylate cyclase from heart and skeletal muscle: modification by guanyl nucleotides and isoproterenol. Arch Biochem Biophys 197: 18-29.

Nargeot J., Nerbonne JM., Engles J., and Lester HA., (1983) Time course of the increase in the myocardial slow inward current after photochemically generated concentration jump of intracellular cAMP. Proc Natl Acad Sci (USA) 80: 2395-2399.

Negretti N., O'Neil SC., and Eisner DFA., (1993) The relative contribution of different intracellular and sarcolemmal systems to relaxation in rat ventricular myocytes. Cardiovasc Res 27: 1826-1830.

New W., and Trautwein W., (1972). Inward membrane currents in mammalian myocardium. Pfluegers Arch **334**: 24-28.

Nilius B., and Benndorf K., (1986) Joint voltage and calcium dependent inactivation of Ca channels in frog atrial myocardium. Biomed Biochim Acta **45**: 795-811.

Nilius B., Hess P., Lansman JB., and Tsien RW., (1985) A novel type of cardiac calcium channel in ventricular cells. Nature (Lond) **316**: 443-446.

Nilius B., Hess P., Lansman JB., and Tsien RW., (1986) Two kinds of Ca channels in isolated ventricular cells from guinea pig heart. Prog Zool **33**: 75-82.

Noma A., and Shibasaki T., (1985) Membrane current through adenosine-triphosphate-regulated potassium channels in guinea-pig ventricular cells. J Physiol (Lond) **363**: 463-480.

Ochi RM., and Trautwein W., (1971) The dependence of cardiac contraction on depolarization and slow inward current. Pfluegers Arch **323**: 187-203.

Ochi R., and Kawashima Y., (1990) Modulation of slow gating process of calcium channels by isoprenaline in guinea-pig ventricular cells. J Physiol (Lond) **424**: 187-204.

Omburo GA., Brikus T., Ghazaleh FA., and Colman RW., (1995) Divalent metal cation requirement and possible classification of cGMP-inhibited phosphodiesterase as a metallohydrolase. Arch Biochem Biophys **323**: 1-5.

Ono K., and Fozzard HA., (1992) Phosphorylation restores activity of L-type calcium channels after rundown in inside-out patches from rabbit cardiac cells. J Physiol (Lond) **454**: 673-688.

Ono K., and Trautwein W., (1991) Potentiation by cyclic GMP of β-adrenergic effect on Ca^{2+} current in guinea-pig ventricular cells. J Physiol (Lond) **443**: 387-404.

O'Rourke B., Backx PH., and Marban E., (1992) Phosphorylation-independent modulation of L-type calcium channels by magnesium-nucleotide complexes. Science **257**: 245-247.

Osaka T., and Joyner RW., (1992) Developmental changes in the β-adrenergic modulation of calcium currents in rabbit ventricular cells. Circ Res **70**: 104-115.

Osterrieder W., Brum G., Hescheler J., Trautwein W., Flockerzi V., and Hofmann F., (1982) Injection of subunits of cyclic AMP-dependent protein kinase into cardiac myocytes modulates Ca^{2+} current. Nature (Lond) **298**: 576-578.

Pelzer D., Cavalie A., McDonald TF., and Trautwein W., (1986) Macroscopic and elementary currents through cardiac calcium channels. Prog Zool **33**: 83-98.

Pelzer D., Pelzer S., and McDonald TF., (1990) Properties and regulation of calcium channels in muscle cells. Rev Physiol Biochem Pharmacol **114**: 107-207.

Pelzer S., Shuba YM., Asai T., Codina J., Birnbaumer L., McDonald TF., and Pelzer DJ., (1990) Membrane delimited stimulation of heart cell calcium current by β-adrenergic signal-transducing G_s protein. Am J Physiol **259**: H264-H267.

Pelzer S., McDonald TF., and Pelzer D., (1991) Cyclic AMP-independent component of stimulatory isoprenaline action on calcium channels in mammalian heart cells. Nature (Lond) **354**: 363.

Pelzer S., Shuba YM., and Pelzer DJ., (1993) A fast, Rp-cAMP-S-resistant, GDP-β-S-sensitive component of stimulatory isoprenaline action accelerates the response of calcium channel current to elevation of cAMP in isolated guinea-pig ventricular myocytes (Abstract). J Physiol (Lond) **459**: 228P.

Perez-Reyes E., Castellano A., Kim HS., et al. (1992) Cloning and expression of a cardiac/brain beta subunit of the L-type calcium channel. J Biol Chem **267**: 1792-1797.

Percival MD, Yeh B, and Falgueyret J (1997) Zinc dependent activation of cAMP-specific phosphodiesterase (PDE4A). Biochem Biophys Res Commun **241**: 175-180.

Peterson BZ., DeMaria CD., and Yue DT., (1999) Calmodulin is the Ca^{2+} sensor for Ca^{2+}-dependent inactivation of L-type calcium channels. Neuron **22**: 549-558.

Peterson BZ., Lee JS., Mulle JG., Wang Y., de Leon M., and Yue DT., (2000) Critical determinants of Ca^{2+}-dependent inactivation within an EF-hand motif of L-type Ca^{2+} channels. Biophys J **78**: 1906-1920.

Pitcher JA., Inglese J., Higgins JB., Arriza JL., Casey PJ., Kim C, Benovic JL., Kwatra MM., Caron MG., and Lefkowitz RJ., (1992) Role of beta gamma subunits of G proteins in targeting the beta-adrenergic kinase to membrane-bound receptors. **257**: 1264-1267.

Pohl SL., Birnbaumer L., and Rodbell M., (1971) The glucagon-sensitve adenylyl cyclase system in plasma membranes of rat liver. J Biol Chem **246**: 1849-1856.

Puri TS., Gerhardstein BL., Zhao XL., Ladner MB., and Hosey MM., (1997) Differential effects of subunit interactions on protein kinase A-and C-mediated phosphorylation of L-type calcium channels. Biochemistry **36**: 9605-9615.

Pusch M., Neher E., (1988) Rate of diffusional exchange between small cells and a measuring patch pipette. Pflugers Arch **411**: 204-211.

Rall TW, and Sutherland EW (1958) Formation of a cyclic adenine ribonucleotide by tissue particles. J Biol Chem **232**: 1065-1076.

Rahn T., Riderstrale M., Tornqvist H., Frederikkson G., Manganiello VC., Belfrage V., and Degerman E., (1994) Essential role of phosphatidylinositol 3-kinase in insulin-induced activation and phosphorylation of the cGMP-inhibited cAMP phosphodiesterase in rat adipocytes - studies using the selective inhibitor wortmannin. FEBS Lett **350:** 314-318.

Reuter H., and Scholz H., (1977) The regulation of the calcium conductance of cardiac muscle by adrenaline. J Physiol (Lond) **264:** 49-62.

Reuter H., (1979) Properties of two inward membrane currents in the heart. Annu Rev Physiol **41:** 413-424.

Reuter H., Stevens CF., Tsien RW., and Yellen LG., (1982) Properties of single calcium channels in cardiac cell culture. Nature (Lond) **297:** 501-504.

Richard S., Charnet P., and Nerbonne JM., (1993) Interconversion between distinct gating pathways of the high threshold calcium channel in rat ventricular myocytes. J Physiol (Lond) **462:** 197-228.

Rodan SB., Golub EE., Egan JJ., and Rodan GA., (1980) Comparison of bone and osteosarcoma adenylate cyclase - effects of Mg^{2+}, Ca^{2+}, ATP^{4-} and $HATP^{3-}$ in the assay mixture. Biochemistry J **185:** 629-637.

Rodbell M (1992) The role of GTP-binding proteins in signal transduction: from the sublimely simple to the conceptually complex. Current topics in cellular regulation **32:**1-47.

Rodbell M., (1996) G-proteins: out of the cytoskeletal closet. Mount Sinai J Medicine **63:** 381-386.

Romani A., and Scarpa A., (1990) Hormonal control of Mg^{2+} transport in the heart. Nature (Lond) **346:** 841-844.

Romani A., Marfella C., and Scarpa A., (1992) Regulation of Mg^{2+} uptake in isolated rat myocytes and hepatocytes by protein kinase C. FEBS Lett **296:** 135-140.

Romani A., Marfella C., and Scarpa A., (1993) Regulation of magnesium uptake and release in the heart and in isolated ventricular myocytes. Circ Res **72:** 1139-1148.

Romanin C., and Grösswagen P., and Schindler H., (1991) Calpastatin and nucleotides stabilize cardiac calcium channel activity in excised patches. Pfluegers Arch **418:** 86-92.

Rose WC., Balke CW., Wier WG., and Marban E., (1992) Macroscopic and unitary properties of physiological ion flux through L-type Ca^{2+} channels in guinea-pig heart cells. J Physiol (Lond) **456:** 267-284.

Ross EM., Maguire ME., Sturgill TW., Biltonen RL., and Gilman AG., (1977) Relationship between the β-adrenergic receptor and adenylate cyclase - studies of ligand binding and enzyme activity in purified membranes of S49 lymphoma cells. J Biol Chem **252:** 5761-5775.

Scamps F., Rybin V., Puceat M., Tkachuk V., and Vassort G., (1992) A G_s protein couples P_2-puriinergic stimulation to cardiac Ca channels without cyclic AMP production. J Gen Physiol **100:** 675-701.

Seamon KB., and Daly JW., (1983) Forskolin, cyclic AMP and cellular physiology. Trends Pharmacol Sci **4:** 120-123.

Seamon KB., and Daly JW., (1986) Forskolin: its biological and chemical properties. Adv Cyclic Nucleotide Protein Phosphorylation Res **20:** 1-150.

Sette C., Vicini E., and Conti M., (1994) The rat PDE3/IVd phosphodiesterase gene codes for mulitple proteins differentially activated by cAMP-dependent protein kinase. J Biol Chem **269:** 18271-18274.

Sette C., and Conti M., (1996) Phosphorylation and activation of a cAMP-specific phosphodiesterase by the cAMP-dependent protein kinase. J Biol Chem 271: 16526-16534.

Seydl K., Karlsson JO., Dominik A., Gruber H., and Romanin C., (1995) Action of calpastatin in prevention of cardiac L-type Ca^{2+} channel run down cannot be mimicked by synthetic calpain inhibitors. Pflugers Arch 429: 503-510.

Sherman A., Keizer J., and Rinzel J., (1990) Domain model for Ca^{2+}-inactivation of Ca^{2+} channels at low channel density. Biophys J 58: 985-995.

Shuba YM., Hesslinger B., Trautwein W., McDonald TF., and Pelzer DJ., (1990) Whole-cell calcium current in guinea-pig ventricular myocytes dialysed with guanine nucleotides. J Physiol (Lond) 424: 205-228.

Singer D., Biel M., Lotan I., Flockerzi V., Hofmann F., and Dascal N., (1991) The roles of the subunits in the function of the calcium channels. Science 253: 1553-1557.

Shistik E., Ivanina T., Puri T., Hosey M., and Dascal N., (1995) Ca^{2+} current enhancement by alpha 2/delta and beta subunits in Xenopus oocytes: contribution of changes in channel gating and alpha 1 protein level. J Physiol (Lond) 489: 55-62.

Schoenmakers TJ., Visser GJ., Flik G., and Theuvenet AP., (1992) Chelator: an improved method for computing metal ion concentrations in physiological solutions. Biotechniques 12: 870-874, 876-879.

Shuba YM., Hesslinger B., Trautwein W., McDonald TF., and Pelzer D., (1990a) A dual-pipette technique that permits rapid internal dialysis and membrane potential measurement in voltage-clamped cardiomyocytes. Pfleugers Arch 415: 767-773.

Shuba YM., Hesslinger B., Trautwein W., McDonald TF., and Pelzer D., (1990b) Whole-cell calcium current in guinea-pig ventricular myocytes dialysed with guanine nucleotides. J Physiol (Lond) 424: 205-228.

Shuba YM., McDonald TF., Trautwein W., Pelzer S., and Pelzer D., (1991) Direct up-regulating effects of G_s on the whole-cell L-type Ca current in cardiac cells. Gen Physiol Biophys 10: 105-110.

Silverman HS., Di Lisa F., Hui RC., Miyata H., Sollott SJ., Hansford RG., Lakatta EG., and Stern MD., (1994) Regulation of intracellular free Mg^{2+} and contraction in single adult mammalian cardiac myocytes. Am J Physiol 266: C222-C233.

Soldatov NM., Zuhlke RD., Bouron A., and Reuter H., (1997) Molecular structures involved in L-type calcium channel inactivation. J Biol Chem 272: 3560-3566.

Sperelakis N., and Schneider J., (1976) A metabolic control mechanism for calcium ion influx that may protect the ventricular myocardial cell. Am J Cardiol 37: 1079-1085.

Standen NB., and Stanfield PR., (1982) A binding-site model for calcium channel inactivation that depends of calcium entry. Proc R Soc Lond B Biol Sci 217: 101-110.

Steer ML., and Levitszki A., (1975a) The control of adenylate cyclase by calcium in erythrocyte ghosts. J Biol Chem 250: 2080-2084.

Steer ML., and Levitski A., (1975b) The interaction of catecholamines, Ca^{2+} and adenylate cyclase in the intact turkey erythrocyte. Arch Biochem Biophys 167:371-376.

Steinberg SF., Chow YK., and Bilezikian., (1986) Regulation of heart membrane adenylate cyclase by magnesium and manganese. J Pharmacol Exp Therap 237: 764-772.

Strada SJ., Martin MW., and Thompson WJ., (1984) General properties of multiple molecular forms of cyclic nucleotide phosphodiesterase in the nervous system. Adv Cyclic Nucleotide Protein Phosphorylation Res 16: 13-29.

Sun G., and Budde RJA., (1997) Requirement for an additional divalent metal cation to activate protein tyrosine kinases. Biochemistry 36: 2139-2146.

Tanabe T., Takeshima H., Mikami A., Flockerzi V., Takahashi H., Kanagawa K., Kojima M., Matsuo H., Hirose T., and Numa, S., (1987) Primary structure of the

receptor for calcium channel blockers from skeletal muscle. Nature (Lond) **328:** 313-318.

Tanabe, T., Beam KG., Adams BA., Niidome T., and Numa S., (1990a) Regions of the skeletal muscle dihydropyridine receptor critical for excitation-contraction coupling. Nature (Lond) **346:** 567-569.

Tanabe, T., Mikami A., Numa S., and Beam KG., (1990b) Cardiac-type excitation-contraction coupling in dysgenic skeletal muscle injected with cardiac dihydropyridine receptor cDNA. Nature (Lond) **344:** 451-453.

Tang WJ., and Hurley., J (1998) Catalytic mechansim and regulation of mammalian adenyl cyclases. Mol Pharmacol **54:** 231-240.

Tiaho F., Nargeot J., and Richard S., (1991) Voltage-dependent regulation of L-type cardiac Ca channels by isoproterenol. Pfluegers Arch **419:** 596-602.

Trafford AW., Diaz ME., and Eisner DA., (1998) Stimulation of Ca-induced Ca release only t ransiently increases the systolic Ca transient: measurement of Ca fluxes and sarcoplasmic reticulum Ca. Cardiovasc Res **37:** 710-717.

Trafford AW., Diaz ME., Sibbring GC., and Eisner DA., (2000) Modulation of CICR has no maintained effect on systolic Ca^{2+}: simultaneous measurements of sarcoplasmic reticulum and sarcolemmal Ca^{2+} fluxes in rat ventricular myocytes. J Physiol (Lond) **522:** 259-270.

Trafford AW., Diaz ME., and Eisner DA., (2001) Coordinated control of cell Ca^{2+} loading and triggered release from the sarcoplasmic reticulum underlies the rapid inotropic response to increased L-type Ca^{2+} current. Circ Res **88:** 195-201.

Trautwein W., Cavalie A., Allen TJA., Shuba YM., Pelzer S., and Pelzer D., (1990) Direct and indirect regulation of cardiac L-type calcium channels by β-adrenoreceptor agonists. In: The biology and medicine of signal transduction, edited by Nishizuka Y., Endo M., and Tanaka C., New York: Raven p. 45-50.

Trautwein W., and Hescheler J., (1990) Regulation of cardiac L-type calcium current by phosphorylation and G proteins. Annu Rev Physiol **52:** 257-274.

Trautwein W., Kameyama M., Hescheler J., and Hofmann F., (1986) Cardiac calcium channels and their transmitter modulation. Prog Zool **33**: 163-182.

Trautwein W., and Pelzer D., (1988) Kinetics and β-adrenergic modulation of cardiac Ca^{2+} channels. In: The Calcium Channel: Structure, Function and Implications, edited by Morad M., Nayler W., Kazda S., and Schram M., Berlin: Springer-Verlag, p. 39-53.

Tseng GN., Robinson RB., and Hoffman BF., (1987) Passive properties and membrane currents of canine ventricular myocytes. J Gen Physiol **90**: 671-701.

Tsien RW., (1973) Adrenaline-like effects of intracellular ionophoresis of cyclic AMP in cardiac Purkinje fibres. Nature New Biol **245**: 120-121.

Tsien RW., (1983) Calcium channels in excitable cell membranes. Annu Rev Physiol **45**: 341-358.

Tsien RW., Bean BP., Hess P., Lansman JB., Nilius B., and Nowycky MC., (1986) Mechanisms of calcium channel modulation by β-adrenergic agents and dihydropyridine calcium agonists. J Mol Cell Cardiol **18**: 691-710.

Vajna R., Klockner U., Pereverzev A., Weiergraber M., Chen X., Miljanich G., Klugbauer N., Hescheler J., Perez-Reyes E., and Schneider T., (2001) Functional coupling between 'R-type' Ca^{2+} channels and insulin secretion in the insulinoma cell line INS-1. Eur J Biochem **268**: 1066-1075.

Walker D., and De Waard M., (1998) Subunit interaction sites in voltage-dependent Ca^{2+} channels: role in channel function. Trends Neurosci **21**: 148-154.

Walsh KB., Begenisich TB., and Kass RS., (1989) β-Adrenergic modulation of cardiac ion channels. Differential temperature sensitivity of potassium and calcium currents. J Gen Physiol **93**: 841-854.

Walsh, KB., and Long KJ., (1992) Inhibition of heart calcium and chloride currents by sodium iodide. Specific attenuation in cAMP-dependent protein kinase-mediated regulation. J Gen Physiol **100**: 847-865.

Watanabe J., Nakayama S., Matsubara T., and Hotta N., (1998) Regulation of intracellular free Mg^{2+} concentration in isolated rat hearts via β-adrenergic and muscarinic receptors. J Mol Cell Cardiol 30(10): 2307-2318.

Wei X., Pan S., Lang W., Kim H., Schneider T., Perez-Reyes E., and Birnbaumer L., (1995) Molecular determinants of cardia Ca^{2+} channel pharmacology: subunit requirement for the high affinity and allosteric regulation of dihydropyridine binding. J Biol Chem 270: 27106-27111.

White RE., and Hartzell HC., (1988) Effects of intracellular free magnesium on calcium current in isolated cardiac myocytes. Science 239: 778-780.

Wier WG., and Balke CW., (1999) Ca^{2+} release mechanisms, Ca^{2+} sparks, and local control of excitation-contraction coupling in normal heart muscle. Circ Res 85: 770-776.

Xu L., Mann G., and Meissner G., (1996) Regulation of cardiac Ca^{2+} release channel (ryanodine receptor) by Ca^{2+}, H^+, Mg^{2+}, and adenine nucleotides under normal and simulated ischemic conditions. Circ Res 79: 1100-1109.

Yamaoka K., and Seyama I., (1996a) Regulation of Ca channel by intracellular Ca^{2+} and Mg^{2+} in frog ventricular cells. Pfluegers Arch 431: 305-317.

Yamaoka K., and Seyama I., (1996b) Modulation of Ca^{2+} channels by intracellular Mg^{2+} ions and GTP in frog ventricular myocytes. Pfluegers Arch 432: 433-438.

Yamaoka K., and Seyama I., (1998) Phosphorylation modulates L-type Ca channels in frog ventricular myocytes by changes in sensitivity to Mg^{2+} block. Pfluegers Arch 435: 329-337.

Yatani A., Codina J., Imoto Y., Reeves JP., Birnbaumer L., and Brown AM., (1987) A G-protein directly regulates mammalian cardiac calcium channels. Science 238: 1288-1292.

Yatani A., Imoto Y., Codina J., Hamilton SL., Brown AM., and Birnbaumer L., (1988) The stimulatory G protein of adenylyl cyclase, G_s, also stimulates dihydropyridine-sensitive Ca^{2+} channels. J Biol Chem **263**: 9887-9895.

Yatani A., and Brown AM., (1989) Rapid β-adrenergic modulation of cardiac calcium channel currents by a fast G protein pathway. Science **245**: 71-74.

Yoshida A., Takahashi M., Nishimura S., Takeshima H., and Kokubun S., (1992) Cyclic AMP-dependent phosphorylation and regulation of the cardiac dihydropyridine-sensitive Ca channel. FEBS Lett **309**: 343-349.

You Y., Pelzer DJ., and Pelzer S., (1995) Trypsin and Forskolin decrease the sensitivity of L-type calcium current to inhibition by cytoplasmic free calcium in guinea pig heart muscle cells. Biophys J **69**: 1838-1846.

You Y., Pelzer DJ., and Pelzer S., (1997) Modulation of L-type Ca^{2+} current by fast and slow Ca^{2+} buffering in guinea-pig ventricular cardiomyocytes. Biophys J **72**: 175-187.

Yuan W., and Bers DM., (1994) Ca-dependent facilitation of cardiac Ca current is due to Ca-calmodulin-dependent protein kinase. Am J Physiol **267**: H982-H993.

Yuan W., and Bers DM., (1995) Protein kinase inhibitor H-89 reverses forskolin stimulation of cardiac L-type calcium current. Am J Physiol **268**: C651-C659.

Yue DT., Herzig S., and Marban E., (1990) β-adrenergic stimulation of calcium channels occurs by potentiation of high-activity gating modes. Proc Natl Acad Sci (USA) **87**: 753-757.

Zimmermann G., Zhou D., and Taussig R., (1998) Mutations uncover a role for two magnesium ions in the catalytic mechanism of adenylyl cyclase. J Biol Chem **273**: 19650-19655.

Zuhlke RD., and Reuter H., (1998) Ca^{2+}-sensitive inactivation of L-type Ca^{2+} channels depends on multiple cytoplasmic amino acid sequences of the α_{1c} subunit. Proc Natl Acad Sci (USA) **95**: 3287-3294.

Zuhlke RD., Pitt GS., Deisseroth K., Tsien RW., Reuter H., (1999) Calmodulin supports both inactivation and facilitation of L-type calcium channels. Nature (Lond) **399:** 159-162.

Zygmunt AC., and Maylie J (1990) Stimulation-dependent facilitation of the high threshold calcium current in guinea-pig ventricular myocytes. J Physiol (Lond) **428:** 653-671.